# IDENTIFICATION OF BIOMARKER RESPONSES IN HUMANS UNDER EXPERIMENTALLY INDUCED ZINC DEPLETION

By

MOON-SUHN RYU

A DISSERTATION PRESENTED TO THE GRADUATE SCHOOL
OF THE UNIVERSITY OF FLORIDA IN PARTIAL FULFILLMENT
OF THE REQUIREMENTS FOR THE DEGREE OF
DOCTOR OF PHILOSOPHY

UNIVERSITY OF FLORIDA

2011

To my parents, Ji-Chul Ryu and Soon-Young Park, and my grandmother, Jung-Seo Seo

ACKNOWLEDGMENTS

The achievements from the past years in my life as a doctoral student would not exist without the presence of the support and love from my family far way in South Korea. I thank my parents for their love and belief in me which have been the greatest motivation for me to pursue accomplishments and success with my best efforts. I also render my gratefulness to my younger sister, Jin-Suhn Ryu, for being the best supporter in all aspects of my life. Additionally, I thank everyone with whom I shared the moments in the lab, especially, Dr. Juan P. Liuzzi, Dr. Louis A. Lichten, Dr. Liang Guo, Dr. Shou-mei Chang, Tolunay Beker Aydemir, for their invaluable advices and help. The excitement from our findings was always the greatest motivation for me to stay in progress. I also thank Gregory Guthrie, Alyssa Maki, Luisa Rios and Vanessa Da Silva for their cheer and support, particularly, during the last year of my doctoral research. I thank Meena Shankar and the staff members at the General Clinical Research Center for their advices and assistance during the phases of study design and implementation of the dietary regimen. Finally, I fully render my gratefulness to my supervisory committee members, Dr. Robert J. Cousins, Dr. Bobbi Langkamp-Henken, Dr. James F. Collins and Dr. Nancy D. Denslow, for being the best mentors and role-models for my career in the field of nutrition and molecular biology. Their advice has been the key for the development of my insights in research, and will last long in my minds. Especially, I thank Dr. Robert J. Cousins for allowing me to substantiate my thoughts and ideas by research, and for encouraging me to continue my journey in the field of discovery by science. I will truly miss the times under his guidance at the University of Florida, and will continue my best with pride of being a previous member of the Cousins lab.

TABLE OF CONTENTS

page

LIST OF TABLES

LIST OF FIGURES

## LIST OF ABBREVIATIONS

| | |
|---|---|
| AAS | Atomic Absorption Spectrophotometry |
| ANOVA | Analysis of Variance |
| AP | Affinity Purified Antibody |
| AP-2α | Activator Protein-2 Alpha |
| CAMP | Cyclic Adenosine Monophosphate |
| CBC | Complete Blood Count |
| CDNA | Complementary Deoxyribonucleic Acid |
| CGMP | Cyclic Guanosine Monophosphate |
| CHCM | Cell Hemoglobin Concentration Mean |
| CRNA | Complementary Ribonucleic Acid |
| CT | Threshold Cycle |
| d | Days |
| DE | Differentially Expressed |
| DNA | Deoxyribonucleic Acid |
| EDTA | Ethylenediaminetetraacetic Acid |
| EKLF | Erythroid Krüppel-Like Factor |
| ELISA | Enzyme-Linked Immunosorbent Assay |
| ELK-1 | ETS-Like Gene-1 |
| EPO | Erythropoietin |
| ETF | Epidermal Growth Factor Receptor-Specific Transcription Factor |
| EXPANDER | Expression Analyzer and Displayer |
| FC | Fold-Change |
| FDR | False Discovery Rate |
| GAPDH | Glyceraldehyde 3-Phosphate Dehydrogenase |

| | |
|---|---|
| GCRC | General Clinical Research Center |
| GO | Gene Ontology |
| GRP | Globin Transcript-Reduced PAXgene Ribonucleic Acid |
| ICP-OES | Inductively Coupled Plasma Optical Emission Spectrophotometry |
| IFN | Interferon |
| IgG | Immunoglobulin G |
| IL | Interleukin |
| IPA | Ingenuity Pathway Analysis |
| IRB | Institutional Review Board |
| kDa | Kilodalton |
| KLF4 | Krüppel-Like Factor 4 |
| LC-MS/MS | Liquid Chromatography Coupled with Tandem Mass Spectrometry |
| LiCl | Lithium Chloride |
| LPS | Lipopolysaccharides |
| MCHC | Mean Corpuscular Hemoglobin Concentration |
| min | Minute |
| miRNA | Micro-Ribonucleic Acid |
| MRE | Metal Response Element |
| mRNA | Messenger Ribonucleic Acid |
| MT | Metallothionein |
| MTF-1 | Metal-Regulatory Transcription Factor 1 |
| MW | Molecular Weight |
| NDSR | Nutrition Data System for Research |
| NF | Nuclear Factor |
| PAX | PAXgene Whole Blood Ribonucleic Acid |

| | |
|---|---|
| PBMC | Peripheral Blood Mononuclear Cells |
| PCT | Probability of Conserved Targeting |
| PDE | Phosphodiesterase |
| PHA | Phytohemagglutinin |
| PKA | Cyclic AMP-Dependent Protein Kinase |
| PKC | Protein Kinase C |
| Pre-miRNA | Precursor MicroRNA |
| PRIMA | Promoter Integration in Microarray Analysis |
| Pri-miRNA | Primary MicroRNA |
| QPCR | Quantitative Real-Time Polymerase Chain Reaction |
| RDA | Recommended Daily Allowance |
| RISC | RNA-Induced Silencing Complex |
| RNA | Ribonucleic Acid |
| RRNA | Ribosomal Ribonucleic Acid |
| RT | Reverse Transcription |
| SD | Standard Deviation |
| SEM | Standard Error of the Means |
| SLC | Solute Carrier |
| TANGO | Tool for Analysis of Gene Ontology Enrichments |
| TEF | TEA Domain Family Member 2 |
| TNF | Tumor Necrosis Factor |
| UTR | Untranslated Region |
| VEGF | Vascular Endothelial Growth Factor |
| vol | Volume |
| wt | Weight |

| | |
|---|---|
| ZIP | Zrt-/Irt-Like Protein |
| ZnA | Zinc-Adequate |
| ZnD | Zinc-Depleted |
| ZnT | Zinc Transporter |

Abstract of Dissertation Presented to the Graduate School
of the University of Florida in Partial Fulfillment of the
Requirements for the Degree of Doctor of Philosophy

# IDENTIFICATION OF BIOMARKER RESPONSES IN HUMANS UNDER EXPERIMENTALLY INDUCED ZINC DEPLETION

By

Moon-Suhn Ryu

August 2011

Chair: Robert J. Cousins
Major: Nutritional Sciences

Zinc, an essential micronutrient, functions as a catalytic, structural and regulatory component for numerous metabolic processes. The estimated prevalence of zinc deficiency worldwide remains substantially high at 31%. The lack of a reliable biomarker limits the identification of individuals requiring zinc interventions, and thus a specific and sensitive assessment tool for such condition is greatly needed.

To identify candidate markers holding the potential to indicate zinc status, a 24-d observational study comprised of acclimation, zinc depletion and repletion phases was conducted with healthy male subjects. Serum zinc levels were monitored throughout the 24-d period. On day 0, 6 and 10 of zinc depletion, buccal swabs and whole blood were collected for various molecular assays. Decreased serum zinc concentrations confirmed the zinc-depleted status of each participant along with a reduction in buccal MT transcript levels. Abundance of MT, ZnT1, ZnT4 and ZnT5 mRNA levels in peripheral blood mononuclear cells (PBMC) and ZnT1 and Zip3 transcripts in purified reticulocytes significantly decreased by dietary zinc depletion. The reduction of ZnT1 mRNA levels was measurable in whole blood RNA. Additionally, the presence of ZnT1 and Zip10 in the plasma membrane of erythrocytes, of which differential expression by

zinc deficiency has been shown in mice, was confirmed. Increase in membrane dematin levels was observed in erythrocytes collected after zinc depletion. Microarray analysis with globin RNA-depleted whole blood RNA revealed 328 genes responsive to acute dietary zinc depletion. Bioinformatic analysis identified enriched pathways associated with cell cycle and immunity by the up-regulated and down-regulated genes, respectively. Depression in immunostimulated TNFα release by dietary zinc depletion confirmed the functional significance of zinc in immune responses. Furthermore, responses of serum miRNA to dietary zinc levels were measured.

Based on a comprehensive analysis of specimens from zinc-depleted human subjects, gene transcripts and proteins holding the potential of being zinc biomarkers were identified. These results also implicated impaired host defense and predisposition to cancer development as expected outcomes of dietary zinc deficiency. This trial was registered at clinicaltrials.gov as NCT01221129.

# CHAPTER 1
# INTRODUCTION

## Zinc Biology

Zinc, an essential micronutrient ubiquitously distributed in the human body, is required for numerous metabolic processes in the biological system as a catalytic, structural and regulatory component (1). The absence of redox chemistry of zinc, which is in contrast to the properties of copper and iron, allows this trace element to be involved in numerous physiologic events without introducing the risk of oxidative damage. Such events include cell growth and differentiation, DNA and RNA synthesis, bone formation, cell-mediated immune responses and gene expression.

Zinc mediates enzymatic reactions at the catalytic site and/or serves as a key element for the maintenance of structural integrity of various enzymes. The activity of metalloenzymes such as carbonic anhydrase, alkaline phosphatase and carboxypeptidase A has been shown but not consistantly to decrease under dietary zinc deficiency, which implicates the critical role of zinc for the function of these enzymes (1, 2). Configurational changes of zinc-finger transcription factors produced by zinc binding allow for the DNA binding activity of these proteins. One of the most extensively studied regulatory roles of zinc involves control of the activity of a zinc-sensing transcription, metal-regulatory transcription factor 1 (MTF-1) (3-7). Upon interaction with cytosolic zinc, MTF-1 translocates to the nucleus and functions as a transregulator of genes with metal response elements (MRE) at their promoter region. Such genes include metallothionein (MT) and ZnT1, for both of which expression is up-regulated by an increase in zinc availability.

## Regulation of Zinc Homeostasis

The human body holds the capability to maintain the homeostasis of zinc by regulatory mechanisms involving differential expression of zinc transporters by zinc-deficient or excessive conditions (8, 9). The zinc transporter family, residing in intracellular membranes or the plasma membranes of cells, is composed of 24 genes which can be categorized as 10 SLC30A (Zinc Transporter; ZnT) and 14 SLC39A (Zrt-/Irt-like protein; Zip) subfamilies. The ZnT transporters mostly mediate the down-regulation of zinc availability in the cytosolic region of cells by exporting and retaining zinc to extracellular and vesicular compartments, respectively. Conversely, Zip transporters function as a zinc channel that provides zinc into the cytosolic region of cells by delivering zinc molecules in an opposite manner to that of ZnT. The molecular mechanism of homeostatic regulation of zinc in response to zinc restriction or excess involves the differential expression or localization of these transporters as described below.

### Whole Body Zinc

Based on observations from cell-based, animal and human studies, the small intestine and pancreas play the major role in the maintenance of body zinc homeostasis by the regulation of absorption and excretion rates under zinc deficiency and excess conditions (9). The underlying mechanism involves the zinc-responsive expression and cellular translocation, i.e., transcriptional and post-translational regulation, respectively, of the zinc transporters present in enterocytes or pancreatic acinar cells. Under conditions which reduce the availability of zinc such as low dietary zinc levels or the presence of zinc chelators, intestinal zinc transport system responds to dietary zinc

restriction towards the direction for enhanced zinc absorption while that of the pancreas is modulated to minimize the loss of zinc via its secretory pathway.

Zip4, Zip5 and ZnT1 are the major zinc transporters involved in the trafficking of dietary zinc through the intestinal epithelium (9). While apical Zip4 and basolateral ZnT1 mediate the transport of dietary zinc from the intestinal lumen to the bloodstream, basolateral Zip5 functions as a route of zinc removal from the circulation to intestinal cells. When the intestinal cells are exposed to a zinc-restricted condition due to low zinc intake or presence of zinc chelators, an increase in Zip4 gene expression by the induction of Krüppel-like factor 4 (KLF4) expression and the DNA-binding activity of this transactivator to the promoter region of Zip4 occur (10). Under such conditions, the basolateral importer Zip5 is internalized and degraded, which results in reduced transfer of zinc from the circulation to intestinal cells (11). Conversely, down-regulation of Zip4 transcription along with the internalization of its protein product has been shown as the regulatory mechanism for reducing the zinc uptake rate by intestinal cells when the dietary zinc bioavailability is in excess. The level of ZnT1, which mediates zinc transport across the basolateral membrane from intestinal cells to blood, is refractory to the bioavailability of dietary zinc (12).

Pancreatic acinar cells play a significant role in the regulation of fecal zinc excretion, which is the primary route of endogenous zinc loss (9). The relevant mechanism of zinc excretion involves zinc transporters Zip5, ZnT1 and ZnT2 that respond to zinc, which enables the regulation of the zinc loss rate by the host's zinc status. Acinar cells mediate the excretion of zinc via the uptake of zinc from the circulation by basolateral Zip5 (11, 13) and the efflux through ZnT1 at the apical plasma

membrane or by a secretory pathway involving vesicular ZnT2 activity (7, 12). Under zinc restricted conditions, the route of zinc excretion across acinar cells is compromised via a decrease in basolateral Zip5 levels and reduction in apical ZnT1 and secretory vesicular ZnT2 levels. The regulatory mechanism of pancreatic Zip5 expression mimics that of the intestinal Zip5, i.e., posttranslational regulation by internalization and subsequent degradation in low zinc status (11). Recently, MTF-1 has been shown to be the key regulator of both pancreatic acinar zinc exporters involved in the efflux of zinc to the intestinal lumen, ZnT1 and ZnT2, by its zinc-responsive binding activity to MRE present in the promoter region of each respective gene (7). Consequently, zinc excess, which induces the nuclear translocation of MTF-1, enhances both ZnT1 and ZnT2 gene expression and eventually facilitates the zinc efflux rate by up-regulating ZnT1 and ZnT2 activities.

**Cellular Zinc**

Independent of the regulatory mechanism of whole body zinc, each cell or tissue has molecular mechanisms for the adaptation to low or excessive zinc conditions. In general, when cells are exposed to a zinc restricted environment, up-regulation of Zip transporters along with down-regulation of the ZnT exporters occurs as a means to maximize the retention of cytosolic zinc content (8, 9). Typical examples include the increase in Zip10 and the decrease in ZnT1 expression levels on the plasma membrane of erythrocytes, which may contribute to the enhanced cellular zinc uptake rate in mice fed a low zinc diet (14). Additionally, the decrease in hepatic Zip10, at both transcript and protein levels (6), and increase in ZnT1 protein levels by oral dosing of zinc (15) reflect the critical role of these zinc transporters in the regulatory mechanism of cellular zinc homeostasis. However, it is of note that not all transporters have been shown to be

responsive to zinc status and the magnitude or mode of zinc responsiveness can differ by the type of cell or tissue in which the gene is expressed (8). For instance, while the production of Zip4 transcripts in the small intestine is markedly induced by dietary zinc depletion in mice, no changes in the transcript level occurs in the pancreas (12). Furthermore, hepatic Zip4 transcript levels reflect dietary zinc deficiency in a manner opposite to that in enterocytes, i.e., down-regulation during deficiency (6). Thus, even though it is a general consensus that differential expression of zinc transporters exerts the adaptive mechanism of cells to modulated zinc conditions, cell-type specificity of zinc-responsiveness of each zinc transporter is of importance as well.

## Dietary Zinc Deficiency

The current recommended daily allowance (RDA) of dietary zinc intake for the adult male and female are 11 and 8 mg/d, respectively (1). RDA for females under pregnancy or lactation are set at higher levels (i.e., 11 and 12 mg/d) due to the loss of zinc by fetal accumulation and zinc secretion by milk. Since the first report in the early 1960s, human dietary zinc deficiency has been associated with various clinical manifestations including impaired growth, diarrhea, dermatitis, neurological and immunological defects, and cancer development (2, 16-18). Conversely, protective effects of adequate zinc intake on the risk of various clinical outcomes, such as type 2 diabetes (19, 20), and its essential role in immunity (21, 22), have been reported by epidemiologic, *in vitro* and nutritional biochemistry studies. Even though the importance of adequate zinc intake has been known for around half a century, the global prevalence of zinc deficiency, predicted by food-based estimates, remains as high as 31% (23). Additionally, the disability-adjusted life years attributable to zinc deficiency

have been estimated to be above 28 million, of which cases are mostly associated with diarrhea, pneumonia and malaria deaths (23).

In contrast to iron of which the majority is stored and recycled via the liver and reticuloendothelial system, there is no reserve or recycling mechanism for zinc (1). Thus, adequate uniform dietary zinc intake is essential for the human body to acquire and maintain the systemic pool size of zinc in an appropriate range. The significance of dietary zinc absorption has been characterized by the deficient zinc status of patients suffering from acrodermatitis enteropathica (AE) which is due to mutations in a zinc transporter gene, Zip4 (24, 25). This protein mediates zinc transport through the apical membrane of the intestinal cell. The severe zinc deficiency produced by this autosomal recessive disorder includes symptoms as dermatological lesions, diarrhea, lack of weight gain, and impairment in immune and reproductive systems (26, 27). It is of note that these symptoms can be corrected by supplemental zinc, through which absorption occurs by paracellular transport or via other lower affinity zinc transporters functioning in the intestinal epithelium (28).

Extensive consumption of diets with high contents of phytic acid (Inositol hexaphosphate) may lead to dietary zinc deficiency even in cases when adequate zinc is present in the diet. The tenacious zinc binding nature of phytic acid binding leads to formation of an insoluble zinc-phytate complex which decreases the bioavailability of ingested zinc in the small intestine (29). Thus, the molar ratio between phytate and zinc may serve as a useful index of zinc bioavailability. At a phytate to zinc molar ratio of 10, the solubility of zinc has been shown to be reduced by 98% *in vitro* and the detrimental effect of phytate on zinc absorption has been observed by a significant decrease in

plasma zinc concentrations of rats (30). A decrease in zinc absorption resulting in a negative zinc balance has been reported in human males fed a diet with a phytate/zinc molar ratio of 15 (29). Recently, a mathematic model for the estimation of quantitative effects of dietary phytate on the bioavailability of zinc was developed based on previous dietary studies reporting the phytate content of diet and measures of the fractional zinc absorbed (31). Based on this model, the absorption of zinc in the absence of phytates is estimated to be approximately 4.5 mg/d when the amount of dietary zinc meets the current RDA for males (32). By the presence of 1000 mg/d of phytic acid, the estimated physiological requirement becomes 2-fold that of a phytate-free diet. This implies the necessity of sufficient zinc intake by individuals on a diet with high phytate contents, such as vegetarians.

**Biomarker Studies of Dietary Zinc Deficiency**

Serum (or plasma) zinc concentration is currently the only biomolecular tool recommended by the World Health Organization (WHO) for the community-based assessment of dietary zinc status in epidemiological nutrition studies (33). As supported by numerous dietary human studies, serum zinc concentrations can successfully reflect the ingested levels of zinc in a dose-dependent manner (34-37). The currently suggested lower cut-off values for healthy male and female adults under morning fasting state are 74 and 70 μg/dL, respectively (38). However, due to its lack of specificity, the use of this indicator is generally limited to experimental conditions of which subjects are in a healthy state and under well-controlled conditions preventing other variables that can affect serum zinc measures. For instance, a decrease in serum zinc levels can be caused by inflammation and infection which are prevalent conditions in most sites where nutrient status assessment is needed (33). In other words, serum

zinc concentration remains inadequate for the diagnosis of dietary zinc deficiency in individuals, and the identification of an alternative reliable laboratory biomarker of zinc status remains as an essential task for the field of zinc nutrition.

**Blood MT and Zinc Transporters**

Data from a considerable amount of research with *in vitro* and *in vivo* models suggest that gene products related to zinc metabolism can reflect the host's dietary zinc status. MT transcript and protein levels, respectively, respond to the cellular zinc availability by a transcriptional and posttranslational regulatory mechanism, and thus hold the potential as biomarkers of zinc deficiency. Under the zinc-depleted condition, gene expression of MT decreases due to reduction in translocation of its transactivator, MTF-1, to the nucleus (3). Both marginal and supplemental intakes of zinc have been shown to decrease and increase blood MT transcript levels in humans, respectively (39-41). Posttranslational regulation of MT by zinc depletion involves the conformational change by metal release which leads an increase in its susceptibility to proteolysis. In accordance to this, the MT protein level in human erythrocytes was shown to decrease after subjects were fed a zinc-restricted diet (42, 43). Additionally, erythrocyte lysates at the zinc-depleted state exhibited higher degradation capabilities for MT protein *in vitro* (42).

In addition to MT, zinc transporter transcript levels in blood cells have been shown to respond to supplemental zinc. Higher levels of ZnT1 transcripts along with lower abundance in Zip3 mRNA were measured in whole blood RNA isolated from dried blood spots of male adult under zinc supplementation (41). Additionally, down-regulation in Zip1 mRNA of peripheral leukocytes has been reported as a consequence of dietary zinc supplementation to elderly women (44). However, due to the absence of

experimental confirmation of the effects of dietary zinc depletion on these zinc transporters in humans, the potential of these transporters to identify dietary zinc depletion remains unclear.

**Cellular Zinc Concentrations**

Extensive research on the properties of cellular zinc content of these cells have been conducted for the evaluation of their potential of being assessment tools of zinc status. Comprehensive analysis of the effects of dietary zinc depletion on the zinc concentration of blood cells indicate these parameters lack the ability to serve as indices of zinc deficiency (45). No significant changes in erythrocyte, neutrophil or platelet zinc content were identified while effects of the experimental zinc treatment (0.6 mg/d, 1 week; 4 mg/d, 6 weeks) on other biological indices such as plasma zinc concentrations were present. However, the effect of dietary zinc depletion on erythrocyte zinc remains controversial. When healthy male subjects were fed a low zinc diet (0.55 mg/d, 12 days) a significant decrease in erythrocyte zinc was produced regardless of the amount of zinc ingested during the preceding phase of the study (43). The discrepancy between these two studies may be due to the dietary zinc content of the diet provided during the depletion period. It is also of importance to note that citric acid, which causes osmotic redistribution of fluid between plasma and cells and thus modulates plasma or cellular metabolite concentrations (46), was used in the first study while the latter used heparin for anticoagulation. Another population-based study characterizing zinc parameters with heparinized blood from elderly subjects showed lower erythrocyte zinc content in subjects with zinc scores (= frequency x quantity x zinc content calculated by a food frequency questionnaire) below 134 (47). Increase in the red cell zinc content was observed after zinc supplementation as well. Thus, further

validation studies focused on the selection of anticoagulants are required to determine whether the erythrocyte zinc concentration is a valid index of zinc deficiency.

The effects of dietary zinc depletion and supplementation on white blood cells remain controversial due to inconsistent results. Increases in lymphocyte and granulocyte zinc by prolonged zinc supplementation (3 years) have been observed in individuals with sickle cell disease (48). Additionally, dietary zinc restriction resulted in a decrease in both lymphocyte and granulocyte zinc concentrations of healthy male adults (49). However, no effects of dietary zinc content on mononuclear white cells and neutrophils in postmenopausal women were identified after consumption of a zinc restricted diet for 6 months (50).

The practicality of using isolated blood cells for zinc measures is limited due to the technical complexity of sample processing. Fractionation of leukocytes from whole blood requires extensive exposure of the cells to exogenous conditions which may influence the cellular zinc trafficking and retention *ex vivo*. Additionally, recent research has shown the effects of immune responses on zinc transporter expression of T-cells (51) and dendritic cells (51, 52), which imply redistribution of the cellular zinc contents during inflammation and infection. Thus, as for the case of serum zinc concentrations, the responsiveness of cellular zinc of the white blood cells may not be specific to dietary zinc deficiency.

**Other Potential Zinc Indices**

Zinc is essential for the activity of various enzymes and, thus, it has been hypothesized that these metalloenzymes may reflect the host's zinc status. The enzymatic activity of serum alkaline phosphatase, which requires zinc as a catalytic component, has been shown to be affected by dietary zinc deficiency in rats (53, 54).

Data from human studies partially support this observation with a decrease in the metalloenzyme activity by low zinc status indicated by serum zinc concentrations (55, 56). However, the sensitivity of this index to identify zinc deficiency is questionable due to the lack of responses in experimental models with humans under mild dietary zinc restriction (34). Additionally, because of its responsiveness to absolute zinc deficiency caused by inflammation (57), other complementary means for the discrimination of zinc deficiency by low intake levels from other cases leading to a decrease in serum zinc is required. The validity of other metalloenzymes, e.g. α-D-mannosidase (34, 45), 5' nucleotidase (8, 34, 58) and superoxide dismutase (59, 60), as indicators of dietary zinc deficiency has been investigated with animal and human models as well. However, according to the inconsistency in the results, there is no consensus for any zinc-dependent enzyme as a biomarker for dietary zinc deficiency as yet.

One of the most broadly studied properties of zinc is its regulatory function in immune and inflammatory responses. The recently discovered essentiality of zinc transporters for the activation of immune cells, such as Zip8 and Zip6 for T cells and dendritic cells, respectively, imply the critical role of zinc in immunity (51, 52). In accordance to this, increases in zinc availability has been shown to result in induction of interleukin 1 beta (IL-1β) and tumor necrosis factor-alpha (TNFα) release by PBMC *in vitro* (61, 62). It is of note that none of the other metals sharing structural similarity with zinc (i.e., calcium, magnesium, cobalt, nickel and mercury) were able to significantly induce the release of these cytokines by PBMC (62). Modulation in serum cytokine profiles by experimental depletion of dietary zinc in human suggests immunoregulatory properties of zinc *in vivo* (63). Association of IL-2 levels with serum zinc concentrations

(64) and its responsiveness to dietary zinc supplementation in elderly subjects (65) implicate the properties of this cytokine as a diagnostic tool for dietary zinc deficiency. Additionally, dietary zinc supplementation to healthy male adults enhances the capability of immune cells to be activated in response to immunostimulation (41). Thus, functional analyses focusing on immune responses of blood cells may serve as means for identifying dietary zinc depletion, particularly when responses to low zinc are opposite to those produced by infection or inflammation.

Another biological function of zinc is its involvement in metabolic processes related to cancer development. Overexpression or repression of certain zinc transporters has been identified as characteristics of various cancers and their modulated expression levels have been associated with the metastatic stage of each cancer type (8, 9). These imply the therapeutic properties of zinc as well as the feasibility to apply approaches for cancer biomarker research onto the identification of diagnostic tools of dietary zinc deficiency. Recently, multiple zinc-responsive defense mechanisms against oxidative stress and DNA damage have been identified by using a zinc-deficient animal model (66) or human prostate epithelial cells (67). Additionally, DNA integrity, measured by comet assays, was lower in PBMCs collected after the host human subjects were fed a diet leading to mild dietary zinc deficiency than in those collected at the baseline (68). The effect of zinc-depletion was reversed by dietary zinc supplementation. Thus, such a technique would be applicable to the identification of subclinical zinc deficiency in healthy individuals that have been confirmed to be free from cancer development (which may be assessed by other cancer-specific diagnostic tools).

## Advances in Techniques for Transcriptome Analysis

The initial phase of biomarker research includes the identification of biomolecules that differentially respond to the clinical or nutritional condition of interest. Human genome project and consecutive and continuous updates to the genome database provide the list of genes expressed in human cells. Novel approaches allow comprehensive analysis of whole transcriptome for a simultaneous detection of multiple responsive gene products in a cost-effective and high-throughput manner.

### Microarray Analysis

DNA microarray technology has been considered as the gold-standard approach for a comprehensive analysis of the whole gene expression pattern (69). The technology is based on the detection of transcripts mediated by their hybridization to gene-specific probes placed on glass plates, beads or nitrocellulose etc., and the validity of this approach has been investigated extensively, e.g., by the Microarray Quality Control project (70). The principle of detecting differentially expressed genes within the transcriptome depends on the number of fluorescent dyes used during visualization. Single-channel microarray allows comparisons among transcript profiles of more than two samples. Signal intensities of transcripts in each RNA sample are produced by a single dye and are measured individually. Thus, appropriate means of normalization prior to comparison is required to minimize the variables that may have been introduced during the sample processing and measurement steps. In contrast to the single-dye approach, the dual-channel microarray system is suitable for comparison between two samples. Each sample is labeled with different detection dyes and combined prior to hybridization to the microarray chip. Simultaneous assessment of signals produced by each dye labeling the treatment and control sample enables the

identification of affected transcripts by detecting higher or lower intensities originating from the dye labeling of treatment samples.

Even though the use of this technique led to success in identification of numerous genes responding to experimental treatments under laboratory environments, the application to clinical settings has been limited due to its high-cost and labor-intensive nature. A recently introduced bead-based platform by Illumina has been suggested to hold advantages over other platforms with regards of its practicality for the use in clinical fields due to its relatively lower cost per sample and its multiplexing feature, which allows simultaneous scanning of up to 12 samples (71-73). Other key features of the beadchip system versus the classical Affymetrix platform include a lower requirement of starting material (50 ng vs. 5 µg total RNA) and its higher stringency (50-mer vs. 25-mer probes) in detection. Recent research for the development of a standardized protocol for blood-based biomarker discovery supports the use of beadchip arrays due to its outperformance over other microarray platforms (6).

**RNA Sequencing (RNA-Seq)**

The currently most advanced technique for transcriptome profiling is based on direct sequencing of RNA molecules present in the sample of interest, and holds multiple advantages over the hybridization-based approaches for gene expression analysis (i.e., DNA microarray) (74). The principle steps of deep sequencing technology are 1) generation of fragmented cDNA with adaptor ligation, 2) next-generation sequencing, and 3) mapping by sequence alignment. Due to its nature of direct sequencing, RNA-Seq allows absolute quantitation of individual transcripts enabling direct comparison among multiple samples in the absence of any references or standards. Other novel features include identification of polymorphisms within the

coding sequence of each gene that may lead clinical manifestations due to defective protein products. In other words, RNA-seq allows the characterization of transcriptome in posttranscriptional perspectives in addition to that at the transcription level. However, due to its novelty and active stage of development, substantial costs are yet required which limits its practicality to laboratory experiments with small sample sizes.

**Sampling and Processing of Biospecimens for Transcriptome Profiling**

Two of the most noninvasive collection means of biological sampling from human, and thus widely used approach for clinical diagnosis, are blood draws and buccal swabs (75). However, limitations in the use of these samples for transcript analysis exist due to the requirement of extensive care during the processing steps after sampling. In the absence of RNA stabilization methods, the transcriptome profile of blood cells can be modulated by multiple technical factors such as the processing or storage temperature and time of exposure to the respective temperature (76, 77). Additionally, high content of RNase in saliva limit the use of buccal swabs as a source of RNA samples (78, 79). In other words, immediate lab processing and a cold-chain system for storage, processing and transportation have been considered as prerequisites for reliable transcript measures with minimal *ex vivo* effects, i.e., preservation of the *in vivo* transcriptome profile.

Sites at which nutrient status assessment would be conducted, e.g., communities of a developing country, mostly lack the availability of certain facilities that are required for immediate processing or sample stabilization (75). Particularly for cases of multiple-center clinical practices, the time lag between sample collection and processing may vary, and thus contribute to the variable of transcript measures. Thus, optimal methods for biomarker studies would be those that allow maximum stability of the target molecule

of interest for an extensive period of time under ambient temperature. The PAXgene Blood RNA system developed by PreAnalytiX allows the preservation of blood samples for up to 3 days at room temperature or 5 days at 2~8°C without compromising RNA integrity (76). By direct collection of blood into tubes with PAXgene reagent, the transcriptome profile of whole blood is immediately stabilized, and thus minimal *ex vivo* effects are introduce after blood collection. Another recently developed technique for nucleic acid stabilization is based on a filter paper composed of microfibers that denature proteins, including nucleases (80). Even though the major application of this platform is for preservation of DNA contents in plant or mammalian samples, it has been successfully implemented as templates of dried blood spots that can be used for whole blood RNA assays (40, 41).

It is of note that globin mRNA, highly abundant in whole blood RNA (>70%), has been shown to mask the presence of transcripts, particularly those at low abundance, during gene expression analysis (71-73, 81). In order to avoid the effects of globin RNA on transcriptome analysis, fractionation of PBMC from whole blood may be conducted in cases of experiments carried out in laboratories (77). However, this approach may not be practical for field applications due to the requirement of immediate processing and the use a refrigerated centrifuge machine. Alternatively, strategies to reduce globin transcript levels in whole blood RNA have been developed (82), and validation studies of the combination of PAXgene reagent and globin RNA methods strongly support the practicality of this approach for biomarker studies (71-73).

## Study Aims

Based on the essentiality of zinc and the absence of a reliable biomarker for its status assessment, it is of importance to characterize biomolecules that are affected by

dietary zinc depletion in humans. The major aim of this study was to identify differential responses of RNA and proteins that occur when the dietary intake of zinc is acutely reduced below the dietary requirement for a period of ten days. Biospecimens were collected in a noninvasive manner and novel techniques for high-throughput analysis with cost-effectiveness were selected to allow the application of the findings to the field where nutrient assessment is conducted.

# CHAPTER 2
# MATERIALS AND METHODS

## Human Subjects

Male subjects 21-35 years of age, weighing at least 50 kg, were recruited to participate (Table 2-1). Exclusion criteria for the dietary regimen included; current cigarette smoking, alcohol abuse, routine consumption of medications, chronic use of denture cream or dietary supplements containing zinc, and history of any chronic disease or allergic reaction (Appendix A). Upon enrollment, the zinc contents in the habitual diet of each subject were determined by a 24-h diet recall followed by calculations with the Nutrition Data System for Research (NDSR) and blood was collected for serum zinc measures. The study was reviewed and approved by the University of Florida Institutional Review Board and the General Clinical Research Center (GCRC) at the University of Florida, and was registered at clinicaltrials.gov as NCT01221129. All subjects were asked for a written informed consent prior to enrollment.

## Acute Dietary Zinc Depletion

The study design was a 24-day observational study comprised of three phases of dietary treatment, and each subject served as one's own control. In order to establish a defined baseline condition (acclimation) prior to dietary zinc depletion, subjects consumed meals composed of a basal mixed diet (2-d cycle menu; Table 3-1), providing 2,700 kcal and ~11 mg Zn/d, and adequate amount of zinc-free energy supplement for additional calories required for body weight maintenance. After 7 days of acclimation, the subjects consumed a strawberry flavored (Hershey's) egg-white based liquid formula which provided <0.5 mg Zn/d for 10 days. The caloric and mineral

contents of the liquid formula (Table 2-3) were similar to those used in previous dietary zinc studies. It is of note that additional care was taken for the current study to minimize the difference in the daily intake levels of each mineral between the two phases with the exception of zinc. This was confirmed by analyses using inductively coupled plasma optical emission spectrophotometry (ICP-OES) at Michigan State University (Table 2-4). Four pieces of starburst fruitchews (< 2.50 ug zinc/g by ICP-OES; Mars, Inc) and a supplemental energy shake, used in phase 1, were provided for energy adjustment. To minimize the bioavailability of zinc, 1.4 g/d of sodium phytate from rice (Sigma) was supplemented to the formula. Carboxymethyl cellulose (2 g/d; TIC Gums) was added to prevent bowel discomfort that could be caused by the liquid diet (83). Supplemental biotin (2 mg/d) was provided to ensure sufficient biotin absorption under the presence of excessive avidin originating from egg white. A multivitamin supplement (CVS) was given as a source of other vitamins. Distilled water (Zephyhills), Diet Pepsi and Sierra Mist (Pepsico), of which zinc contents were undetectable by flame atomic absorption spectrophotometry (AAS), were provided throughout the first two phases. Upon completion of the second phase (on day 17), subjects returned to their self-selected diet and 15 mg Zn/d (Jarrow) was provided for the repletion of their zinc status. On the last day of participation, an anonymous questionnaire of compliance was provided to each subject in order to identify any major deviations from the protocol (Appendix B). Serum zinc concentrations were also monitored throughout the study to assess whether the dietary effect was present.

**Sample Collection**

All samples were collected at the GCRC by an on-site nurse under overnight fasting status of each subject. On day 7, 13 and 17, two buccal swabs and 33.5 mL of

whole blood were collected. Each buccal mucosa sample was immediately transferred to a Whatman FTA filter paper sampling card to stabilize its RNA contents. All samples, except for 3 mL of whole blood used for complete blood counting (CBC) at Shands Hospital at the University of Florida, were transported to the Food Science and Human Nutrition Department for further processing. A Styrofoam chamber with an internal temperature of 5~10°C, maintained with wet ice sealed in leak-proof plastic bags, was used for the transportation of whole blood samples collected in PAXgene tubes and EDTA-treated tubes. Other samples were transported under room temperature. Additional blood draws (5 mL) were conducted on the first day and at day 10, day15, day 20 and day 24 for serum samples. Overall scheme of the sample handling and processing work-flow is shown in Figure 2-1, and described in details below.

**Preparation of Buccal RNA**

Buccal RNA samples were prepared by using the protocol previously developed for whole blood RNA extraction from dried blood spots. FTA paper cards (Whatman) with buccal samples were air-dried for 3~4 h at room temperature and stored at -20°C until processed. To isolate RNA, filter papers with the buccal samples were cut into small parts using sterile surgical scissors, and were incubated in 1.5 mL of TRI reagent (Ambion) at room temperature for 15 min. Samples were agitated every 5 min during this period. After centrifugation at 12,000 x g x 30 min, 4°C, the lysate was transferred to a new microcentrifuge tube for RNA isolation. When residual filter paper was observed in the RNA solution, samples were treated with 1 mL of TRI reagent and the phenol-chloroform extraction step was repeated. All samples were further purified by the sodium acetate-isopropanol precipitation, and the final RNA solution was stored at -80°C until analyzed.

## Processing of Blood Samples

Sera were isolated from 5 mL of whole blood collected in red-top serum tubes (BD Vacutainer). Blood was allowed to clot at room temperature for 60 min after collection, and placed on ice for no longer that 2 h until processed. Clotted blood was centrifuged at 2,000 x g x 10 min, 4°C, and serum was collected in 500-µL aliquots. One aliquot was treated with 1% (vol/vol) protease inhibitor cocktail (Pierce) and stored at -80°C. Untreated samples were stored in 4°C and -80°C until processed for AAS.

PBMC and circulating erythroid cells (erythrocytes and reticulocytes) were fractionated from whole blood collected in Vacutainer tubes pretreated with $K_3$ EDTA. For PBMC isolation, 9 mL of whole blood was placed on an equal vol of Histopaque 1077 (Sigma) and centrifuged at 400 x g x 30 min at room temperature. The PBMC layer was collected and washed with PBS at 250 x g x 10 min, twice, and the RBC pellet diluted with 1 vol of PBS was stored at 4°C until processed for reticulocyte RNA preparation. After counting the cells, half of the recovered PBMC was treated with 1 mL of TRI reagent for RNA isolation while the other was cryopreserved as previously described (47). Briefly, cells were placed in heat-inactivated FBS supplemented with 10% DMSO and were stored in a Nalgene freezing containers overnight at -80°C, and transferred to liquid nitrogen for extensive storage.

Remnant erythroid cells from the PBMC isolation procedure (with 9 mL of whole blood) were processed for reticulocyte RNA preparation. To achieve a pure population of erythroid cells, leukocyte depletion was carried out by using cellulose columns (84). Enriched RBCs were suspended in 1 vol of HEPES buffer (154 mM NaCl, 10 mM HEPES, 1 g/L BSA) and filtered through a cellulose column composed of α-cellulose (Sigma) and Sigmacell Type 50 microcrystalline cellulose (Sigma) in a 1:1 (wt:wt) ratio.

After RBC preparations were loaded into the cellulose column, 2 vol of HEPES buffer was applied for the elution of RBC. After being collected from the eluate by 2,000 x g x 5 min at 4°C, the cells were washed two times with equal vol of ice-cold PBS at 200 x g for 10 min to eliminate platelets. Purified RBCs packed by centrifugation at 2,000 x g x 5 min at 4°C were treated with 20 mL of TRI reagent for reticulocyte RNA isolation and purification by the phenol-chloroform extraction and sodium acetate-isopropanol precipitation, respectively.

Plasma membrane of RBC (ghost cells) was prepared from 6 mL of whole blood, collected in a $K_3$ EDTA-treated Vacutainer. After leukocytes and platelets were removed as described above, packed RBCs were suspended in an equal vol of ice-cold PBS. After 3 washes with PBS, the RBCs were lysed by 5 vol of ice-cold hypotonic buffer [5 mM $Na_2HPO_4$ (pH 7.4)] containing protease inhibitor cocktail (Pierce) and the membranes were collected by centrifugation at 12,000 x g x 10 min, 4°C, until the supernatant and pellet were clarified. After a final wash at 20,000 x g, membrane pellets were solubilized in 5 mM Tris-HCl, 0.5% Triton X-100 with protease inhibitors, and stored at -80°C.

**Measures of Serum Zinc Concentrations**

Serum zinc concentrations were determined by AAS on the day of sample collection. Sera were diluted 1/4 with Milli-Q water, of which zinc content was undetectable by AAS, prior to each analysis. To monitor the consistency among each respective measure, a reference zinc solution was prepared at a concentration of 0.6 mg Zn/L with zinc sulfate and was subject to AAS along with the diluted serum samples. After the completion of participation of each subject, measures from each collection day were confirmed by repeating AAS with all samples collected throughout the study period.

## Isolation and Processing of Blood Cell RNA

With the exception of RNA from whole blood collected in PAXgene tubes, all blood RNA samples were prepared by phenol-chloroform extraction using either TRI reagent or TRI reagent BD, and treated with Turbo DNA-free reagents (Ambion) to remove residual DNA contamination. For RNA isolated from samples of whole blood assays, additional RNA precipitation using 2.5 M lithium chloride (LiCl) was conducted to minimize the inhibitory effects of heparin on reverse transcription and PCR reactions (85). Stabilized whole blood RNA was prepared from 7.5 mL of blood collected in PAXgene blood collection tubes (BD) by the manual procedure described in the manufacturer's protocol. Briefly, whole blood lysates treated with proteinase K were homogenized and RNA was isolated by using silica-gel membrane columns (Qiagen). Samples were treated with DNase I (Qiagen) prior to elution.

A genome-wide gene expression analysis for the detection of transcripts responsive to dietary zinc depletion was conducted with stabilized whole blood RNA from PAXgene samples. Globin RNA depletion from the whole blood RNA was done by using GLOBINclear (Ambion). Globin transcripts in PAXgene RNA (3 µg) was hybridized to biotinylated oligonucleotides and captured by streptavidin magnetic beads. The supernatant was further purified by a poly-T-oligos conjugated to magnetic beads prior to downstream processing for microarray analysis. All RNA samples were stored at -80°C until further processed. Integrity and quality of RNA were assessed by using 2100 Bioanalyzer (Agilent) and Nanodrop 1000 (Thermo Scientific), respectively.

## RNA Amplification, Hybridization, and Microarray Analysis

The Illumina BeadChip platform (HumanHT-12 v4) was selected for the assessment of global effect of dietary zinc depletion on the blood transcriptome, due to

its high-throughput and cost-effective nature. PAXgene whole blood RNA depleted of globin transcripts (200 ng of total RNA) was amplified by the Illumina TotalPrep RNA Amplification Kit (Ambion) for the array analysis. After reverse transcription using T7 Oligo(dT) primers and second strand cDNA synthesis, biotinylated cRNA was synthesized by *in vitro* transcription with T7 RNA polymerase and biotin-UTP. The yield and quality of cRNA were assessed with the NanoDrop spectrophotometer and Agilent 2100 bioanalyzer, respectively. For the detection of differential gene expression, labeled cRNA (750 ng) was loaded to beadchips, hybridized for 14~20 h at 58°C, and stained with Cy3-streptavidin. Fluorescence signals from Cy3 were detected by a BeadArray Reader (Illumina Beadstation 500GX) and signal intensities were exported by using GenomeStudio software (Illumina). The hybridization and scanning processes were conducted at the Gene Expression core at the Interdisciplinary Center for Biotechnology Research, University of Florida.

**Microarray Data Analysis**

Probes with detection *P*-values lower than 0.05 in all samples were excluded from the dataset prior to analyses. Raw data were quantile normalized and log-transformed for statistical analyses. Differentially expressed (DE) genes were determined by comparisons between baseline and post-zinc-depletion levels using BRB-ArrayTools developed by Dr. Richard Simon and BRB-ArrayTools Development Team (permutation = 10,000). Genes differentially affected by acute zinc depletion were determined by a pairwise comparison at $P < 0.005$. For the visualization of gene expression patterns by using a heat-map, intensity values were standardized by subtracting the mean value of each gene across all arrays and division by the standard deviation of each respective gene (resulting in mean = 0, standard deviation = 1). After unsupervised clustering by

expression patterns using the k-means algorithm (k = 2), computational analyses based on gene ontology and putative transcription factor motifs were conducted to identify the highly associated functional aspects of the DE genes by using EXpression Analyzer and DisplayER (EXPANDER) 5.2 software (86). Ingenuity Pathway Analysis (IPA) with the list of DE genes was conducted to identify biological networks between the responsive genes and to predict the associated functions, diseases and disorders to the modulated gene expression by dietary zinc depletion.

**Real-Time Quantitative PCR**

Transcript abundance of genes known to be directly involved in the regulation of cellular zinc homeostasis, i.e., zinc transporters (ZnT1, ZnT2, ZnT4, ZnT5, ZnT6, ZnT7, Zip1, Zip2, Zip4, Zip5, Zip8, Zip10, and Zip14) and MT, were measured by assays designed and validated previously (9). Primers and probe sets for the detection of Zip6 (forward, 5'-AGGCTGGCATGACCGTTAAG-3'; reverse, 5'-AAAATTCCTGTTGCCATTCCA-3'; probe, 5'-FAM-CCTTTATAATGCATTGTCAGCCATGCTGG-BHQ1-3') and GAPDH transcripts (forward, 5'-GAAGGTGAAGGTCGGAGTC-3'; reverse, 5'-GAAGATGGTGATGGGATTTC-3'; probe, 5'-FAM-CAAGCTTCCCGTTCTCAGCC-BHQ1-3') were designed by using PRIMER EXPRESS 3.0 software (Applied Biosystem) and validated by Primer3plus. Quantitation of CDC20, TXNDC5, MZB1 and IGJ transcripts were conducted using TaqMan gene expression assays from Applied Biosystems. Real-time quantitative reverse transcriptase polymerase chain reaction (qPCR) assays were done with cDNA, generated by using high capacity cDNA reverse transcription kit (Applied Biosystems), and the TaqMan fast universal PCR master mix (Applied Biosystems). For assays with the RNA samples from the whole blood cytokine assay, Taqman one-step RT-PCR

master mix reagents were used in order to minimize the residual contents of heparin that was present in the reaction mixture. Glyceraldehyde 3-phosphate dehydrogenase (GAPDH) mRNA and 18S rRNA levels were measured as internal controls, and amplification and detection were performed with the StepOnePlus real-time PCR system (Applied Biosystems).

**Western Analysis of RBC Zinc Transporters**

We have previously reported the presence of ZnT1, Zip8 and Zip10 in murine erythrocytes (14). A decrease and increase in RBC ZnT1 and Zip10, respectively, was observed when mice were fed a low-zinc diet. The presence of these transporters in human RBC was confirmed by western analysis using affinity-purified rabbit polyclonal antibodies. All primary antibodies, besides that for the detection of dematin (Abcam ab89161), were designed for previous studies (14, 15, 51). Specificity of signals produced by each in-house made antibody was determined by preabsorption with respective antigenic peptides specific to the target proteins of interest. Glycosylation status of each protein was evaluated by incubation of protein samples with PNGase-F at 37°C for 2 h prior to western analysis. Erythrocyte proteins (total of 20 μg) were separated by 7.5~10% sodium dodecyl sulfate polyacrylamide gel electrophoresis (SDS-PAGE) and were transferred to nitrocellulose membranes. Efficient transfer and equal loading were visualized by Ponceau staining. Membranes were blocked by Tris-buffered saline (TBS-T) containing 5% skim-milk for 1 h, and primary antibodies were added at a final concentration of 1~2 μg/mL. After incubation with the primary antibody for 1~2 h, blots were washed with TBS-T and then treated with anti-IgG antibody conjugated to horseradish peroxidase (1:2,000~1:10,000 of antibody in 5% blocking solution) for 1 h. Signals indicating abundance of the protein were visualized by using

an enhanced chemiluminescent substrate SuperSignal WestPico (Pierce) and autoradiographic films. Blots were incubated in Restore PLUS Western Blot stripping buffer (Thermo Scientific) for 15 min when reprobing with subsequent primary antibody was needed.

**Immunoprecipitation and Mass Spectrometry**

Erythrocyte membrane fraction was immunoprecipitated by using anti-human Zip8 polyclonal antibodies to enrich the abundance of proteins targeted by the respective antibody. Briefly, 1 mg of protein was incubated in 1 vol of RIPA buffer containing 4 μg of antibody at 4°C, overnight, and purified by using protein A/G agarose conjugates (Pierce). After extensive wash steps, protein bound to the agarose beads were eluted by 10 min incubation at 100°C with Laemmli buffer. Immunoprecipitated proteins were loaded on wells of a 7.5% polyacrylamide gel for the separation by electrophoresis. After the gel was divided into two halves, each was subject to gel staining and western analysis, respectively. Proteins were stained by incubation in Coomassie Blue staining solution (0.1% Coomassie Brilliant Blue R-250, 10% acetic acid, 50% methanol and 40% water) for 1 h at room temperature, and background stains were removed by a destaining solution composed of 10% acetic acid, 50% methanol and 40% water. Stained gel was stored in the destaining solution diluted 1/4 with water until processed for mass spectrometry. Western analysis was conducted for the identification of IgG-oriented bands and the protein producing a non-specific band by the anti-human Zip8 primary antibody. Thereafter, the western image was matched with the stained gel to determine the position of the non-specific band in the gel, which was excised with methanol-treated blades for liquid chromatography coupled with tandem mass spectrometry (LC-MS/MS) using a hybrid quadrupole/time-of-flight mass spectrometer

(QSTAR Elite, Applied Biosystems). Protein digestion and LC-MS/ MS were conducted at the proteomics core at the Interdisciplinary Center for Biotechnology Research, University of Florida. The nature of identified peptides was determined with Mascot version 2.2.2 (Matrix Science) and the IPI human database. Scaffold (Proteome Software Inc.) was used to validate MS/MS-based peptide identifications.

**Whole Blood Cytokine Assay**

Whole blood collected in heparin Vacutainers (5 mL) was used to determine the effects of dietary zinc on the production of cytokines by LPS or PHA stimulation. *In vitro* induction of cytokine release were conducted with 20% of whole blood in phenol-free RPMI-1640 medium supplemented with 2 mM L-glutamine, 100 kU penicillin/L and 100 mg streptomycin/L, with or without LPS (1 mg/L) or PHA (10 mg/L) treatment. Cells were incubated in 24-well ultra-low-attachment plates (Corning) at 37°C in 5% CO2 for up to 24 h. For measures of cytokine release, cell-free supernatant was collected by centrifugation at 600 x g x 5 min, 4°C, and stored with protease inhibitor cocktail at -80°C. Whole blood cell pellets were treated with TRI reagent BD (Molecular Research Center) supplemented with acetic acid, and stored at -80°C for RNA isolation.

**Enzyme-Linked Immunosorbent Assay**

*In vitro* zinc treatment has been shown to increase IL-1β, TNFα, and interferon-gamma (IFN-γ) expression levels of PBMC. A previous study from our lab has shown the effects of dietary zinc supplementation on the IL-1β, TNFα, and IFNγ gene expression of immune cells activated *in vitro* (41). To test whether dietary zinc depletion causes a modulation in LPS- or PHA-induced cytokine production, cytokine levels in pooled cell-free medium collected from the whole blood culture were measured by using a multi-analyte ELISA array kit for inflammatory cytokines (IL-1 α, IL-1 β, IL-2,

IL-4, IL-6, IL-8, IL-10, IL-12, IL-17α, IFNγ, TNFα, GM-CSF; SA Biosciences). The effects on IL-1β, TNFα, and IFNγ were further assessed with individual samples by using single analyte ELISArray kits from SA Biosciences. Briefly, protease inhibitor-treated cell-free medium were added to each well of a pre-coated capture antibody microplate loaded with assay buffer. With extensive washes in between each step, captured cytokines were probed with relevant detection antibodies and avidin-horse radish peroxidase (HRP). After subsequent treatments with the development and stop solution, absorbance at 450 nm was measured by a multi-mode microplate reader (SpectraMax M5; Molecular Devices) for quantification.

**Isolation and Quantitation of Serum MicroRNA**

Serum was treated with 5 volumes of QIAzol (Qiagen) for the denaturation of protein contents and subsequent isolation of RNA. Due to the absence of a known housekeeping microRNA (miRNA) in human serum, 25 fmol of synthetic cel-miR-39 (5'-UCACCGGGUGUAAAUCAGCUUG-3') was added as a means of normalization (87). After adding 1 volume of chloroform, aqueous and organic phases were separated by centrifugation at 12,000 x g x 15 min at 4°C. The aqueous phase was treated with 1.5 volumes of 100% ethanol and loaded to a miRNeasy Mini column for RNA extraction. After extensive washes, purified RNA was eluted from the column membrane with 50 µL of nuclease-free water and stored at -80°C until analyzed.

The human serum miRNA PCR array from SABiosciences was used for the identification of circulating miRNA responsive to dietary zinc levels. Serum RNA was isolated from 400 µL of pooled sera at the initial screening step. Day 7, 17 and 24 samples were selected as those representing baseline, zinc-depleted and zinc-repleted conditions, respectively. Serum RNA was polyadenylated and converted to cDNA by

using $RT^2$ miRNA First Strand kit (SABiosciences) containing universal reverse transcription (RT) primers targeting poly-A-tails. After a 1/4-dilution with nuclease-free water, RT products were distributed across the miRNA qPCR arrays with SYBR Green qPCR reagents (SABiosciences) for amplification and quantitation. Melt-curve analyses with amplified products were conducted to determine the specificity of each primer set. Criteria for determining the zinc-responsive miRNA were; 1) single melting temperature, 2) fold-change > 1.5 by dietary zinc depletion, 3) threshold cycle (Ct) < 35, and 4) response to zinc-repletion in a direction opposite to that of zinc-depletion. Zinc-responsiveness of selected miRNA, identified in pooled samples, was confirmed with RNA from 200 µL of individual serum samples collected at day 7, 13, 17, 20 and 24 by using the miScript PCR system (Qiagen). Reverse transcription products of miRNA were diluted by equal volume of nuclease-free water, and 2 µL of the diluted cDNA was used as templates for SYBRgreen-based qPCR assays at a total reaction volume of 10 µL. All values of miRNA qPCR experiments were normalized to the abundance of their respective cel-miR-39, of which values were constant across all RNA preparations.

**Statistical Analysis**

Based on measures from previous dietary zinc studies with humans (41, 42), a complete dataset from 9 subjects is adequate to detect a within-subject difference in transcript levels of zinc-responsive gene with 80% power at $P < 0.05$ two-sided. Values from samples of Day 7 (baseline) served as the control for comparisons. Student's t-test or repeated measures of ANOVA followed by a Student-Newman-Keuls multiple comparisons test were conducted for pairwise comparisons. Linear association between transcript levels and serum zinc concentrations was determined by the linear regression method. All statistical analyses were conducted using the InStat 3 software

(GraphPad). The level of significance was set at $P < 0.05$ for all analyses except for those of microarray data.

Table 2-1. Subject characteristics at screening phase (n = 9)

| Subject | Age (years) | Height (cm) | BWt (kg) | Caloric Needs (kcal/d) | Serum Zn (ug/dL) | 24 h Recall (mg Zn/day) |
|---|---|---|---|---|---|---|
| 1 | 31 | 179.5 | 86.3 | 2,950 | 96 | 20.6 |
| 2 | 26 | 163.0 | 62.4 | 2,854 | 114 | 8.8 |
| 3 | 29 | 178.6 | 88.5 | 3,201 | 87 | 8.6 |
| 4 | 25 | 177.4 | 66.8 | 2,760 | 111 | 10.5 |
| 5 | 25 | 179.1 | 96.6 | 3,161 | 96 | 11.3 |
| 6 | 23 | 182.5 | 72.7 | 2,819 | 99 | 17.9 |
| 7 | 22 | 165.0 | 85.1 | 3,236 | 72 | 28.4 |
| 8 | 22 | 171.5 | 64.7 | 3,000 | 84 | 12.6 |
| 9 | 24 | 176.1 | 87.8 | 3,091 | 104 | 21.2 |
| Mean | 25 | 174.7 | 79.0 | 3008 | 95.9 | 15.5 |
| (SD) | (3) | (6.8) | (12.4) | (175) | (13.3) | (6.8) |

Table 2-2. The 2-day cycle menu of the acclimation phase

| Meal | Menu 1 | Menu 2 |
|---|---|---|
| Breakfast (8:00 AM) | English muffin (63 g) | Grape-nuts cereal (56 g) |
| | Margarine (11 g) | Milk (135 g) |
| | Jelly (15 g) | Low-fat yogurt (238 g) |
| | Low-fat yogurt (146 g) | |
| | Apple juice (215 g) | |
| Lunch (12:00 PM) | Roast beef (120 g) | Chicken breast (203 g) |
| | White bread (63 g) | Gravy (23 g) |
| | Mayonnaise (12 g) | Corn (89 g) |
| | Canned peach (126 g) | Margarine (9 g) |
| | Pudding (126 g) | Canned peach (176 g) |
| | Cool whip (6 g) | Cookies(38 g) |
| Snack (3:00 PM) | Power bar (39 g) | Short bread(47 g) |
| | Canned pear (170 g) | Peanut butter (20 g) |
| | Jell-O (196 g) | Crackers (15 g) |
| Dinner (5:00 PM) | Chicken breast (139 g) | Turkey breast (155 g) |
| | Peas (120 g) | Gravy (27 g) |
| | Margarine (7 g) | Carrots (108 g) |
| | Icecream (107 g) | Margarine (11 g) |
| | Wafers (31 g) | White bread (34 g) |
| | Apple juice 200 g) | Ice cream (114 g) |
| Snack (8:00 PM) | Almonds (30 g) | Raisins (51 g) |
| | Sherbet (104 g) | Power bar (64 g) |
| | Lemonade (200 g) | Jell-O (166 g) |

Table 2-3. Dietary components of the liquid diet for the zinc depletion phase[1,2]

| Component | Mineral content | Amount per kg diet |
|---|---|---|
| Egg white | | 129 g |
| Cornstarch | | 300 g |
| Maltose-dextrin | | 300 g |
| Sucrose | | 60 g |
| Corn oil | | 151 g |
| Cellulose | | 10 g |
| Mineral mixture | Sodium chloride | 9.8 g Na |
| | Calcium carbonate | 10.0 g Ca |
| | Potassium phosphate, monobasic [a] | 3.8 g P [a+b] |
| | Potassium phosphate, dibasic [b] | 12.0 g K [a+b+c] |
| | Potassium chloride [c] | |
| | Magnesium carbonate·$5H_2O$ | 1.28 g Mg |
| | Ferric citrate·$6H_2O$ | 57.6 mg Fe |
| | Copper sulfate·$5H_2O$ | 7.6 mg Cu |
| | Potassium Iodate | 0.50 mg I |
| | Manganese chloride | 11.4 mg Mn |
| | Glucose | 16.8 g |

[1] Vitamins and extra biotin were provided as separate supplements.
[2] Sufficient energy intakes were ensured by supplemental mineral-free energy shakes.

Table 2-4. Mineral contents of the acclimation and zinc repletion diets measured by inductively coupled plasma optical emission spectrophotometry (ICP-OES)

| Minerals per day | Acclimation phase | Depletion phase |
|---|---|---|
| g Calcium | 1.134 | 2.994 |
| g Phosphorus | 2.048 | 1.390 |
| g Magnesium | 0.343 | 0.509 |
| g Potassium | 3.259 | 4.417 |
| g Sodium | 3.208 | 5.038 |
| g Sulfur | 1.302 | 1.319 |
| mg Copper | 1.818 | 1.539 |
| mg Iron | 25.014 | 25.988 |
| **mg Zinc** | **10.415** | **0.296** |
| mg Manganese | 3.533 | 3.828 |
| mg Molybdenum | ND[1] | ND[1] |
| mg Cobalt | ND[1] | ND[1] |

[1] Not detected: Measures were below the detection limit of ICP-OES.

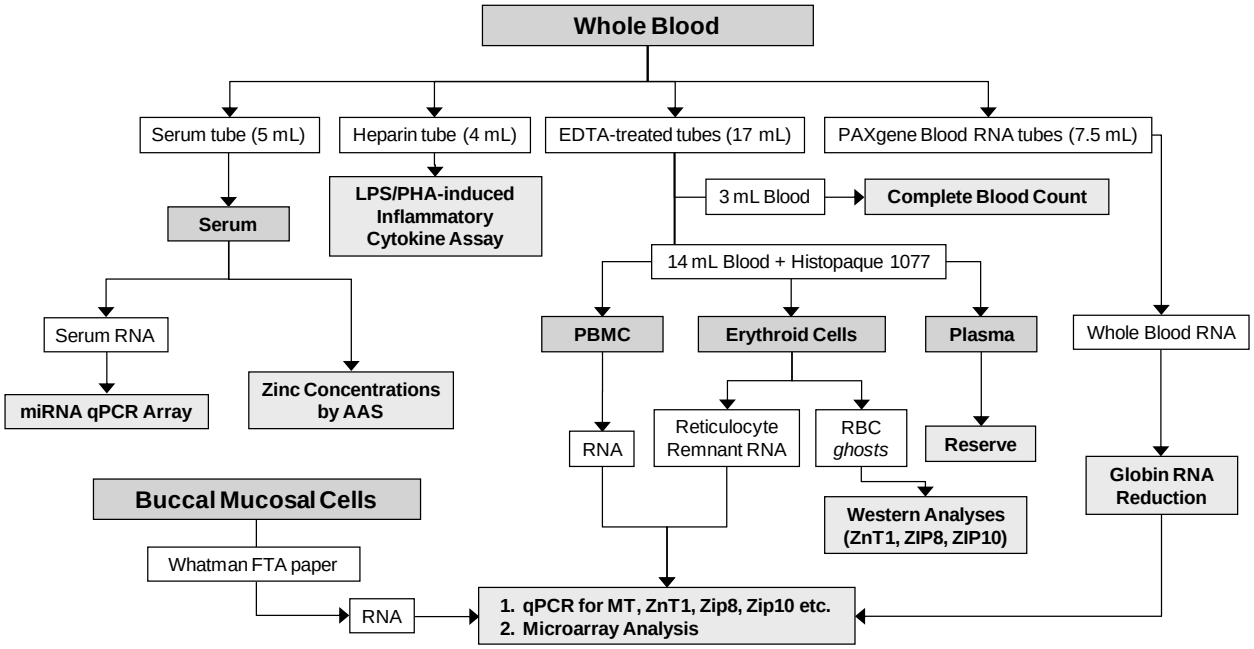


Figure 2-1. Schematic diagram of sample collection and handling processes. Relevant materials and methods were selected based on their practicality for being used in the field for nutrient assessment. Availability of methods for sample stabilization allowed the completion of the entire processing by a single researcher.

# CHAPTER 3
# IDENTIFICATION OF ZINC-RESPONSIVE GENE TRANSCRIPTS IN BUCCAL AND BLOOD CELLS

## Introductory Remarks

Zinc, as a catalytic, structural and regulatory component, is involved in various physiological events in the human body (1). Documented outcomes of inadequate zinc ingestion include growth retardation, diarrhea, dermatitis, hypogonadism, visceromegaly, hematological abnormalities and impaired immunity (2, 16). Recent evidence of the protective role of zinc against DNA oxidation (66, 68), which may result in predisposition to cancer development, indicates the detrimental long-term effect of low zinc consumption. Therapeutic properties of supplemental zinc against infectious diseases (23) and diabetes mellitus (19) substantiate the values of this nutrient for the maintenance of human health. Even though the biological and biochemical properties of zinc has been intensively explored since the first characterization of its essentiality (18), a reliable diagnostic tool to assess the dietary zinc status of individual humans or populations is in absence. Dietary zinc deficiency, with a predicted worldwide prevalence of 31% (23), has been estimated to be responsible for approximately 450,000 global deaths in children under 5 years of age (88). Consequently, development of a biomarker defining zinc status is needed, particularly, for the identification of individuals or communities which may benefit from zinc interventions.

Serum or plasma zinc concentrations are widely used for the assessment of zinc status in experimental animal and human models. However, due to its lack of specificity, e.g., responsiveness to stress, starvation or immunological conditions, its capability to serve as a diagnostic tool for zinc deficiency is limited. Past research has shown that both metallothionein gene expression and specific zinc transporter genes in blood

leukocyte subsets are directly proportional to dietary zinc intake (40, 41). Additionally, specific zinc transporter genes in monocytes, T-cells, and granulocytes have been shown to be also zinc-responsive. ZnT1 and Zip3 transcript levels of whole blood corresponded to dietary zinc supplementation in human subjects with an increase and decrease, respectively (41). Transcripts for specific cytokines produced when these cells are activated *in vitro* were also zinc-responsive over a 16-day dietary protocol that included 10 days of zinc supplementation at 15 mg/day or a placebo (41). These findings reflecting the regulatory role of zinc in gene expression have provided the hypothesis that these specific transcript changes can be used for the identification of zinc deficiency.

Transcriptome profiling using cDNA array analysis and qPCR technology enables the identification of genes most sensitive to a biological variable of interest, and thus have been considered as the gold-standard approaches for developing gene transcript-based diagnostic methods (69). Information related to the zinc effect on whole genome expression of human cells is limited to those from *in vitro* treatments (44, 89, 90). Our previous microarray experiments with monocytic/macrophage THP-1 cells under zinc-deprived and -excess conditions identified several hundreds of zinc-responsive genes (89). Functional grouping of the differentially expressed genes indicated the regulatory role of zinc in immune/cytokine function and signal transduction. Another study on various cell-lines each representing T-cells, B-cells and monocytes, identified a list of differentially expressed genes coordinately associated with immunity and cellular survival (90). Although these clearly indicate the presence of zinc effects on the whole

genome expression of blood cells, assessment of the *in vivo* effect via a dietary study is required to fully understand the physiological role of zinc in human biology.

In a manner to pursue this, a human dietary study of experimentally induced acute zinc depletion was conducted and transcriptome analyses of whole blood were undertaken using oligonucleotide microarrays. Transcripts holding the potential of being an assessment tool of dietary zinc status were identified by quantitative measures of buccal and blood RNA as well. Specific aims of this part of study include;

1) Evaluation of the effects of acute dietary zinc depletion on MT and zinc transporter transcript levels in buccal epithelial cells.
2) Evaluation of the effects of acute dietary zinc depletion on levels of zinc transporter and MT transcripts in leukocytes and reticulocytes.
3) Identification of genes responding to dietary zinc restriction through transcriptome profiling of whole blood RNA by cDNA microarray analysis.

## Results

### Experimental Zinc-Depletion in Human Subjects

The experimental model of acute dietary zinc depletion used in this study was developed based on previously standardized methods successfully implemented by others (34, 37, 42, 43). Analytic measures by OES-ICP confirmed the zinc contents of the acclimation diets as 10.4 mg zinc per daily serving, which is approximate to the current RDA of zinc for adult males (Figure 3-1). The low zinc (0.3 mg/d by OES-ICP) and high phytate contents (1.4 g/d) of the depletion diet yields a phytate to zinc molar ratio of 462, indicating low bioavailability of zinc. In accordance to these aspects of the diet, subjects had a significant decrease in their serum zinc concentrations after 8 and 10 d after consuming the zinc-depleted diet, and this was reversed by subsequent zinc

supplementation (Figure 3-2). It is of note that the inter-subject variability of serum zinc levels decreased by the end of the acclimation phase. All participants had a serum zinc concentration above the suggested lower cutoff value for males, 74 μg/dL (38), at the baseline state. No hematological effects of dietary zinc depletion were observed by complete blood counts (Table 3-1) of which values were all residing within their respective suggested normal ranges.

**Effects of Zinc-Depletion on Zinc-Related Transcript Levels**

A panel of gene expression assays targeting zinc-related gene products was used for the quantitation of respective mRNA levels in the biological samples collected. Buccal RNA samples were selected as an optimal approach of sampling due to its noninvasiveness, and the yield of RNA isolated from FTA filter papers were 989 ± 492 ng per oral swab. Among the zinc-related transcripts in buccal RNA, only those of MT and ZnT1 were stably detected by qPCR (Figure 3-3A). Criteria for determining the reliability of these assays include; 1) low analytical variation, 2) amplification curve parallel to that produced from reference RNA, and 3) Ct values below 35. Human Reference RNA composed of total RNA from various cancer cell-lines (Stratagene) was used as a positive control of amplification. A significant decrease in MT mRNA abundance was observed in samples collected after 10 d of dietary zinc depletion, while no effect was present in the ZnT1 transcript levels (Figure 3-3B).

Cell-type-specific detection and responsiveness to dietary zinc of MT and zinc transporter transcript levels were observed by qPCR with PBMC and reticulocyte RNA. MT, ZnT1, ZnT4 and ZnT5 mRNA levels significantly decreased in PBMC (Figure 3-4) while reduction in ZnT1 and Zip3 transcripts of purified reticulocytes (Figure 3-5) occurred by acute dietary zinc depletion. Among the differentially expressed zinc

transporter transcripts, ZnT1 and Zip3 were the most significantly affected ones (with lowest *P*-value) in PBMC and reticulocytes, respectively. Linear regression analysis revealed a significant correlation between serum zinc concentrations and PBMC ZnT1 transcript abundance with a correlation coefficient (*R*) of 0.6900 and a *P*-value of 0.0015. However, the R between serum zinc concentrations and reticulocyte Zip3 levels was not significantly different from 1 ($P = 0.0778$) indicating the absence of association between these two indices in this study. The reduction of ZnT1 mRNA levels, observed by both PBMC and reticulocyte RNA, was measurable in whole blood RNA as well. As with the PBMC ZnT1, a significant correlation of serum zinc concentrations with whole blood ZnT1 mRNA levels was observed ($R = 0.5558$, $P = 0.0026$).

**Whole Blood RNA Processing and Quality Assessment for Microarray Analysis**

Because of the requirement of high quality RNA for reliable microarray results, stringent quality assessment was conducted throughout the sample preprocessing steps, i.e., from RNA isolation to hybridization to the array chips. Whole blood RNA isolated by using the PAXgene system was highly intact as indicated by RNA integrity numbers (RIN) above 8 (Figure 3-8). A260/A230 and A260/A280 ratios were above 2.00 in all samples implying the high purity of RNA in each preparation. The yield of RNA after globin transcript depletion was approximately 75% of the starting material (Figure 3-9A), and the purity of these products were confirmed by A260/A230 and A260/A280 ratios at 2.12~2.31 and 2.19~2.30, respectively. There were no differences in the cRNA recovery between RNA prepared from whole blood collected at day 7 (baseline) and day 17 (ZnD) after biotinylation and amplification (Figure 3-9B). When the post-amplification yield between RNA samples that were untreated (PAX) and treated for globin RNA reduction (GRP) was compared, higher recovery was observed

in PAX samples (Figure 3-9C) which is due to the presence of redundant globin RNA. The amplification efficiency indicated by folds of the starting amount are comparable to reference values provided by the manufacturer, which are 148 and 61 for PAX and GRP, respectively (Figure 3-9D). Electropherogram profiles of the amplified PAX RNA and GRP RNA confirm the successful removal of globin transcripts from the processed whole blood RNA (Figure 3-10). The prominent peak produced by the highly abundant globin RNA content was only present in the PAX samples after RNA amplification.

**Global Effect of Zinc-Depletion on Whole Blood Transcriptome**

The Illumina bead-array chip was selected for the transcriptome analysis due to its multiplexing feature and lower per-sample-cost when compared to platforms from Affymetrix and Agilent (71, 72). Prior to the data preprocessing, microarray data quality control was conducted by using control metrics generated by the GenomStudio software. Values of each control parameter corresponded to the reference values provided by Illumina in all arrays and, thus, verified the validity of gene expression data obtained (Figure 3-11). Quantile normalization, producing a best-fit slope near 1 between the distribution of signals from each probe by pooled GRP samples from day 7 and 17, was selected for the downstream data analyses (Figure 3-12). Lists of differentially expressed genes were determined by using various combinations of *P*-value and fold-change as filtering thresholds (Table 3-2). It is of note that fewer genes were considered as differentially expressed by unpaired comparisons than by paired t-tests, which indicates the presence of inter-subject variability in the genes of which expression before and after the acute dietary zinc depletion.

The list of differentially expressed genes determined by a pairwise comparison at $P < 0.005$ (328 genes) were further analyzed by bioinformatic tools for characterization

and the identification of biological events associated with dietary zinc depletion. Among the genes identified, 192 had higher expression levels (Table C-1) while 136 showed less expression (Table C-2) after the consumption of a low-zinc diet. Unsupervised average-linkage hierarchical clustering of these genes with Pearson correlation metric identified two major clusters each composed of 192 and 136 genes showing trends of overexpression and repression by zinc depletion, respectively (Figure 3-13A). While no clustering by baseline and post-zinc depletion conditions was observed when hierarchical clustering of the individual samples was conducted with all genes (Figure 3-13B), a partial separation between the baseline and post-zinc depletion condition was identified by using the 328 differentially expressed genes for clustering (Figure 3-13C).

To determine the effect of globin RNA reduction on the detection of differentially expressed genes, average signals produced by pooled PAX and GRP samples from day 7, 13 and 17 were compared. Based on a detection *P*-value of 0.05 as a upper cutoff threshold, a total of 6,861 genes were considered absent when the RNA samples were not processed for globin RNA reduction (Figure 3-14A). Among those masked genes, 51 were among the 328 genes determined to be differentially expressed by dietary zinc intake levels. As indicated in Figure 3-14B, the relative signal intensities of these gene transcripts were higher when RNA samples were processed for globin RNA reduction, implying the importance of the removal of this highly abundant RNA prior to whole blood transcriptome analyses. By using the data obtained from the pooled samples, the temporal expression pattern of the 328 differentially expressed genes were determined as well. A gradual increase and decrease throughout the 10-day

depletion period was observed by the up-regulated and down-regulated genes, respectively (Figure 3-15).

Advances in bioinformatic tools allowing the integration of transcriptome profiles into molecular and network databases enable the prediction of physiological effects attributed to the differential gene expression by changes in clinical or nutritional conditions. By using the EXPANDER and IPA software packages, functional analyses were conducted to discover the implications of differential expression of genes caused by dietary zinc depletion. Gene ontology enrichment analysis of gene clusters categorized based on their expression pattern as analyzed with the k-means algorithm (Figure 3-16), by using the Tool for Analysis of GO enrichment (TANGO) of EXPANDER (86), identified overrepresentation of functional categories associated with cell cycle regulation and ATP binding by the up-regulated genes (Table 3-3). Promoter Integration in Microarray Analysis (PRIMA) predictions based on the cis-regulatory elements of the responsive genes identified NF-Y, AP-2α and ETF as the transcription factors mediating dietary zinc effects on the up-regulated genes, and Elk-1 and TEF as those involved in the repression of the down-regulated genes (Table 3-4).

Further characterization of all 328 differentially expressed genes using the Ingenuity Pathway Analysis (IPA) confirmed the TANGO results by identifying enrichment in functional categories related to cell proliferation (Table 3-5). It is of note that cancer was identified as the top disease and disorder associated with the differential gene expression caused by the dietary restriction regimen. While the enriched functional categories identified using the list of up-regulated genes for IPA functional analysis corresponded to those by all responsive genes (Table 3-6), genes

down-regulated by acute dietary zinc depletion were shown to be associated with biological events related to cell death, cell-mediated immune response, and cellular development and function (Table 3-7). To further unravel the physiological and mechanistic implications of our microarray data, molecular networks composed of connections between functionally related genes were generated by analyzing the list of differentially expressed genes with IPA. In accordance to the results from functional analyses above, the top two networks identified by all differentially expressed genes were composed of molecular interactions related to cell cycle and cellular growth, respectively (Figure 3-17). Overrepresented functional networks by the up-regulated and down-regulated genes, respectively, imply enhancement in cell proliferative events and repression in cell death, cell-mediated immunity and cellular development as physiological outcomes of inadequate zinc intake (Figure 3-18).

**Gene Transcripts with Potential of being Biomarkers of Zinc Deficiency**

Pairwise comparisons between before and after treatment values of each individual are suitable for the identification of indices responsive to the treatment. However, in order to identify molecular responses with potentials of being a biomarker, inter-individual variability should be taken into account. As shown in Figure 3-19, a clear discrimination between baseline and post-zinc depletion conditions was produced by hierarchical clustering with the 203 differentially expressed genes determined by paired t-test ($P < 0.005$). After filtering by fold-changes above 2, a total of 8 well-characterized genes among the 14 filtered genes, including LOC649923, LOC651751, IGJ, CDC20, MZB1, TXNDC5, IGLL1, CD38, LOC642113, LOC647506, LOC652493, GLDC, LOC647450 and TNFRSF17, were determined as candidate molecules for the status assessment of dietary zinc intake levels (Table 3-8). qPCR of IGJ, CDC20,

MZB1 and TXNDC5 mRNAs confirmed the responsiveness of these gene transcripts to acute dietary zinc depletion identified by microarray analysis (Figure 3-20).

## Discussion

Zinc transporter and MT expression were the primary targets of interest due to their direct involvement in zinc trafficking and homeostatic regulation and likelihood to respond to lower zinc availability by dietary restriction (8, 9). It was of importance to implement noninvasive means for biopsy collection for future applications to human patients in the field of nutrient assessment (75). Thus, we selected buccal swabs and blood draws as the sources of RNA for the current study.

The method we utilized for RNA isolation from oral epithelial cells was developed based on swabbing approach commonly used for DNA-based diagnosis and profiling in clinical and forensic settings. The major concern of this technique was the high contents of RNase in saliva which may lead impairment of RNA quality during and after the collection process (78, 79). By using Whatman FTA filter papers originally designed for the stabilization of nucleic acid isolated from plant specimens and which has also been used for RNA preparation from whole blood (preprocessed as dried blood spots) (41, 80), we attempted to eliminate the *ex vivo* effects on RNA integrity. Amplification curves indicated successful acquirement of RNA sufficient for the detection of buccal MT and ZnT1 transcripts by qPCR. A marked decrease in transcript levels of MT, the prototypical zinc-regulated gene, by low zinc ingestion was measured in oral epithelium, indicating its potential of being a zinc biomarker.

Quantitative real-time PCR identifies the presence of transcripts by amplifying a short region of its template cDNA, i.e., amplicon, which is generally composed of less than 100 nucleotides. Thus, the reliability of qPCR results depends on the integrity of

the amplicon site. Consequently, our results do not exclude the presence of partial RNA fragmentation due to RNase activity. The expression of some zinc transporter transcripts may be present in the buccal mucosa *in vivo* although they were not detected during our screening step. Further optimization in the experimental approach for buccal RNA preparation may allow us to identify other zinc homeostatic genes responsive to the host's zinc status.

Previous findings of the effects of zinc supplementation on the blood zinc transporter expression in humans (41) led us to the characterization of such indices of individuals under dietary zinc restriction. The distinction between the differentially expressed transporter genes in PBMC and reticulocyte RNA indicate the cell-type-specific regulation of these genes (8). Only ZnT1, which is known to be ubiquitously expressed on the plasma membrane of various cell types and tissues (8), was commonly affected by the acute zinc depletion regimen in these blood cells. This zinc-responsiveness of ZnT1 was also detected in whole blood RNA by using qPCR. However, the differential expression was not identified by our microarray experiments, indicating the low sensitivity, particularly for transcripts at low abundance and minimal fold-change responses, of microarray technology. The mode of ZnT1 response to dietary zinc depletion agrees with its role in cellular zinc export (8). The data of the present study also corresponds to our previous observation of ZnT1 responding in an opposite mode to supplemental zinc (41), indicating its property to reflect the levels of dietary zinc bioavailability in both zinc-deprived and -excess conditions.

Serum zinc concentrations were measured as an evaluation tool of compliance and the effectiveness of our dietary zinc depletion protocol. Lower variation in the

serum zinc levels after acclimation indicates the equilibrated zinc status of each individual at the baseline level. Its significant decrease by zinc depletion and its reversal by repletion, respectively, imply the value of this index to be indicative of dietary zinc ingestion levels. However, due to its responsiveness to other conditions such as acute infection or starvation (1, 33), the use of this serum zinc measures may be limited to healthy individuals under well-controlled experimental settings.

We identified significant association serum zinc measures with ZnT1 levels in PBMC and whole blood samples. This further validates the potential of this zinc transporter transcript to function as a diagnostic tool for dietary zinc deficiency. A recent study reported the lack of association between PBMC ZnT1 transcript abundance and serum zinc levels of human subjects (91). It is of note that this was based on measures from individuals under self-selected diets, mostly providing daily zinc above the estimated average requirement. Additionally, as indicated by the absence of correlation between plasma zinc concentrations and the estimated dietary intake levels (determined by food record or food frequency questionnaire), the plasma levels were not successfully reflecting the dietary zinc status of each individual. Another notable difference of this study from the present study is the use of values from a sample group composed of both females and males, and thus possible gender effects on plasma zinc or ZnT1 expression may have confounded the statistics. Data of the present study were produced from men only. These imply the correlation between serum zinc concentrations and blood ZnT1 transcripts may be present only when 1) a defined group representing zinc deficiency is included, 2) variables affecting serum zinc

(besides of dietary zinc level) are minimal, and 3) the study population is composed of a single gender.

Among the transporters assessed with the blood cells, reticulocyte Zip3 was the only importer transcript affected after the 10-day dietary zinc depletion phase, however in an opposite direction to the general response mode of Zip genes to zinc deprived conditions, i.e., up-regulation (8). It is of note that the presence of Zip3 was not detected in the plasma membrane fraction of mature erythrocytes (14), which implies the intracellular localization of this protein in differentiating erythoid progenitor cells. Decrease in its expression by low zinc availability suggests its function mediating zinc removal from a cellular compartment at conditions of higher zinc availability. Recently, a cellular zinc exporter ZnT2 has been characterized to function as a mitochondrial zinc importer (92). This leads to the speculation of Zip3 functioning as a zinc exporter for the mitochondrion, of which zinc content needs to be tightly regulated for optimal hemoglobin synthesis during the terminal erythroid differentiation (93, 94). Thus, relevant mechanistic studies for the characterization of erythroid Zip3 function are required.

The global effects of zinc on the transcriptome of blood cells have been previously characterized by us and others (44, 89, 90). We identified total of 1,045 zinc-responsive genes in a human acute monocytic leukemia cell line, THP-1, under zinc excess or depleted condition *in vitro* (89). Among those, expression levels of 283 genes were significantly altered by both zinc-excess and -deprived conditions, of which 104 and 86 genes responded to zinc levels in a positive and negative mode, respectively. The organ-specific effect of zinc on the transcriptome was identified by microarray analyses

of Jurkat, Raji and THP-1 cell lines representing the T-cell, B-cell and monocyte population, respectively, under different zinc conditions (90). Even though the expression of only 7 genes was generally modulated by zinc in all cell types, the functional networks identified by the zinc-responsive genes in each cell type were commonly related to inflammatory response and cellular survival.

In the present study, we identified whole blood genes having modulated expression levels after acute dietary zinc depletion using an extensively validated platform originally designed for cancer biomarker research (71). A combination of PAXgene reagent and globin RNA reduction allows the preservation of *in vivo* transcriptome profile and an increase in detection sensitivity of gene transcripts at low abundance (71, 72). The capability to minimize *ex vivo* effects on the original gene expression profile is essential for transcriptome analyses, particularly, when immediate sample processing is impossible (75). The negative effect of globin RNA, representing ~70% of the total whole blood RNA, on transcript detection was clearly observed by comparisons between pre- and post-globin RNA reduction samples from the current study. Additionally, among the 328 genes differentially expressed by zinc depletion, fifty one were determined as absent due to the masking effect of globin RNA. These data further support the importance of globin transcript removal from whole blood RNA prior to microarray-based biomarker discovery (81, 82).

As an approach to predict physiological outcome attributed to the overexpression and repression of the differentially regulated genes by low zinc intake, we implemented functional enrichment analyses in a fashion similar to that of Haase H et al. (90). The overrepresentation of genes involved in cell cycle and cell-mediated immune response

identified by the up- and down-regulated genes in the whole blood RNA, respectively, remarkably aligns with the finding from the *in vitro* study of zinc status with a combination of various immune cell models (90). Such observations indicate that whole blood transcriptome is compatible for the identification of biological zinc effects on its subsets, i.e., monocytes and lymphocytes, which coordinately function and interact during circulation *in vivo*.

The functional implications of the differentially expressed genes we identified correspond to the well-characterized clinical outcomes of prolonged zinc deficiency, i.e., impaired immunity (95-97) and predisposition to cancer development (98, 99). Of considerable interest is the appearance of vascular endothelial growth factor (VEGF) in the functional networks enriched by the overexpressed genes. VEGF has been considered to be a therapeutic target for anti-cancer treatment due to its pro-tumorigenic feature (100, 101). Recently, intracellular zinc deprivation has been shown to result in increased production of VEGF by prostate cancer cells (102). No change of VEGF gene expression in the blood cell population was identified by our microarray experiments, indicating that modulated production or secretion of this growth factor, holding both autocrine and paracrine functions, may have occurred in a different organ during zinc depletion. Low serum zinc has been characterized in patients of various types of cancer (103-105). Impairment in repair systems for DNA damage has been suggested as the underlying mechanism of higher risks of cancer by zinc deficiency (98). Here, we propose another possible regulatory factor, VEGF, as a mediator of an effect of zinc on tumor development and cancer progression.

Nuclear factor kappa B (NFκB) was identified in the functional network composed of down-regulated genes, indicating its impaired function under acute dietary zinc depletion. The immunosuppressive effect of suboptimal zinc conditions has been associated with impaired DNA binding activity of this transcription factor (63). Relevant mechanisms include the zinc dependence of the transactivation capability of NFκB indicated by lower affinity to its binding motif under zinc deprivation (106-108). Glucocorticoid, another key regulator of immunity, and its nuclear receptors can decrease NFκB activity by up-regulating its inhibitor IκB or by competitively binding to coactivators of NFκB-induced gene expression (109). Increased plasma corticosterone has been found in zinc-deficient mice (110). However, the contribution of this hormonal change to immune dysfunction by low zinc intake was determined to be minimal because the zinc effect was yet present in adrenalectomized animals (111). These imply that low zinc ingestion leads to a modulation in host defense by affecting gene expression associated with immune response via a direct effect on NFκB activity. Functional assays confirming the dietary zinc effect on cytokine production will be further described in the following chapter.

Transcription factors potentially mediating the zinc-responsive regulation were determined by computational analysis identifying the enriched cis-regulatory elements present in the differentially expressed gene promoters. The results suggest modulated activity of transcription factors, NF-Y, AP-2α, ETF, Elk-1 and TEF, during zinc depletion. A recent promoter analysis of miRNA identified c-Myb, NF-Y, Sp-1, MTF-1 and AP-2α as master-regulators of their gene expression (112). The inclusion of NF-Y, AP-2α and the zinc-sensing transcription factor MTF-1 suggests a putative role of zinc on miRNA

gene regulation. Even though probes against miRNA were present, we could not test this hypothesis by our microarray experiments as the PAXgene system used was incompatible for small RNA isolation. Alternatively, circulating miRNA in serum samples were assessed and relevant information will be described in Chapter 5.

Comparisons between before and after treatment values paired by subjects enable the removal of inter-person variability, and thus are suitable for the identification of indices responsive to the treatment. However, a reliable diagnostic tool requires low variance among individuals at a healthy status. The lower numbers of differentially expressed genes determined by unpaired testing indicate high variation among the baseline levels of those identified by pairwise comparison. Thus, the genes suggested as potential biomarkers were suggested by statistically affected genes based on unpaired t-tests. By applying a stringent filtering criterion, we identified eight well-characterized gene transcripts as candidate indices of dietary zinc deprivation. All of these were up-regulated by the dietary zinc restriction protocol. Whether other clinical or nutritional conditions affect each of these gene transcripts cannot be determined by the current study, and thus requires further exploration. However, a simultaneous measurement of these highly responsive genes as a signature profile may sufficiently serve as a diagnostic approach for dietary zinc deficiency.

Based on our knowledge, this is the first study to conduct whole genome expression analysis and measure zinc transporter transcripts in human subjects under experimental zinc restriction. The two major purposes of the current study was to identify mRNAs that hold the potential to reflect the host's zinc intake levels, and to evaluate the physiological effects of short-term zinc depletion based on whole gene

expression profiling. Our data suggest genes involved in the regulation of zinc homeostasis, cell proliferation and immune response as biomolecules applicable to the diagnosis of zinc deficiency. The microarray data presented provide target molecules for future research for the understanding of molecular mechanism of zinc effects on immune response and cancer development.

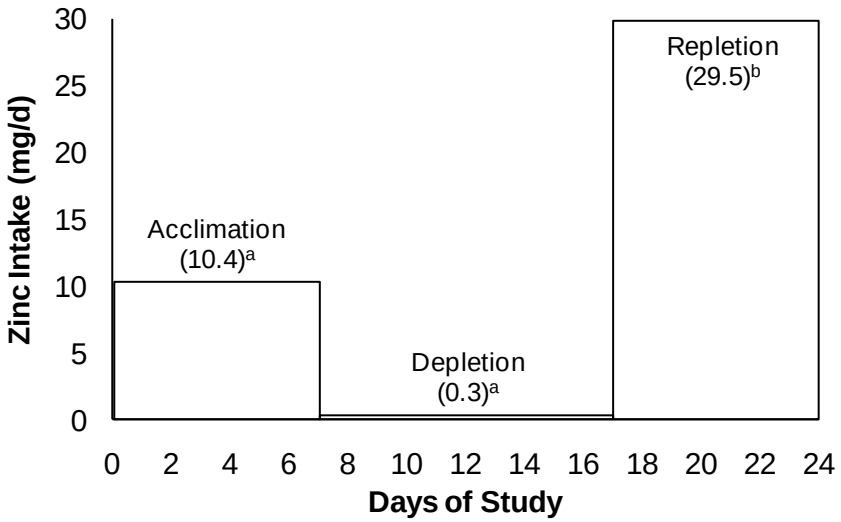


Figure 3-1. Dietary regimen for acute dietary zinc depletion. Supplemental phytate (1.4 g/d) was added to the diet during the depletion to limit the bioavailability of zinc. [a]Analytical measures of zinc content by inductively coupled plasma optical emission spectrophotometry with sample diets. [b]Estimated zinc content based on calculations by adding the zinc content of the supplement used (15 mg) and the average zinc level of self-selected diets from 24-h diet recalls (14.5 mg).

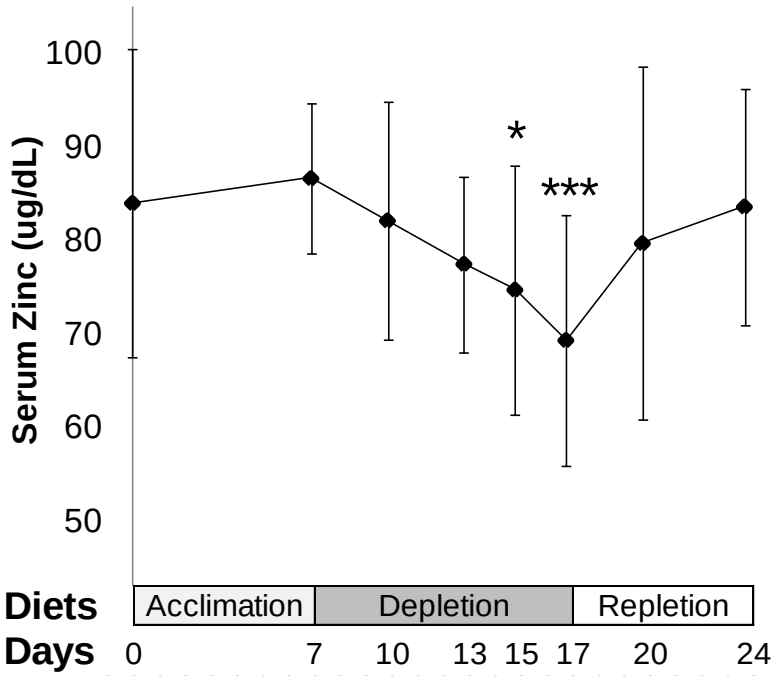


Figure 3-2. Measures of serum zinc concentrations indicating the effectiveness of the experimental diet for dietary zinc depletion. Serum was diluted with 3 volumes of Milli-Q water and zinc content was measured by atomic absorption spectrophotometry. Values are expressed as mean ± standard deviation (SD), and those significantly different compared to baseline (Day 7) levels are noted by *, $P < 0.05$; ***, $P < 0.001$ (n = 9 subjects).

Table 3-1. Hematological parameters measured during dietary zinc depletion

| Measures | Normal Range | Days of Depletion 0 | | 6 | | 10 | |
|---|---|---|---|---|---|---|---|
| | | Mean | (SD) | Mean | (SD) | Mean | (SD) |
| WBC (thousand/mm$^3$) | 4.0~10.0 | 5.78 | (1.43) | 5.8 | (1.39) | 5.97 | (1.50) |
| Hemoblobin (g/dL) | 13.0~16.5 | 15.9 | (0.98) | 15.44 | (1.09) | 15.41 | (1.11) |
| Hematocrit (%) | 39.0~49.0 | 44.83 | (2.49) | 44.08 | (3.02) | 43.18 | (2.97) |
| Platelet Count (thousand/mm$^3$) | 150~450 | 282.9 | (29.4) | 266.7 | (32.7) | 249.9 | (37.9) |
| RBC (million/mm$^3$) | 4.5~5.9 | 5.379 | (0.46) | 5.279 | (0.49) | 5.179 | (0.45) |
| Mean Cell Volume (micron$^3$) | 78.0~100.0 | 83.64 | (5.09) | 83.84 | (5.12) | 83.56 | (5.15) |
| Mean Cell Hemoglobin (pg) | 26.0~34.0 | 29.64 | (2.01) | 29.35 | (1.68) | 29.8 | (1.62) |
| MCHC (g/dL)[1] | 31~37 | 35.41 | (0.77) | 35.03 | (0.68) | 35.7 | (1.15) |
| CHCM (g/dL)[2] | 32.0~38.0 | 36.34 | (1.21) | 35.59 | (1.06) | 36.38 | (1.49) |
| RBC Distance Width (%) | 11.0~14.0 | 12.96 | (1.20) | 13.15 | (1.19) | 12.79 | (1.22) |
| Mean Platelet Volume (fL) | 6.0~10.0 | 7.91 | (0.41) | 8.07 | (0.83) | 8.84 | (0.64) |

[1] MCHC, mean corpuscular hemoglobin concentration.
[2] CHCM, cell hemoglobin concentration mean.

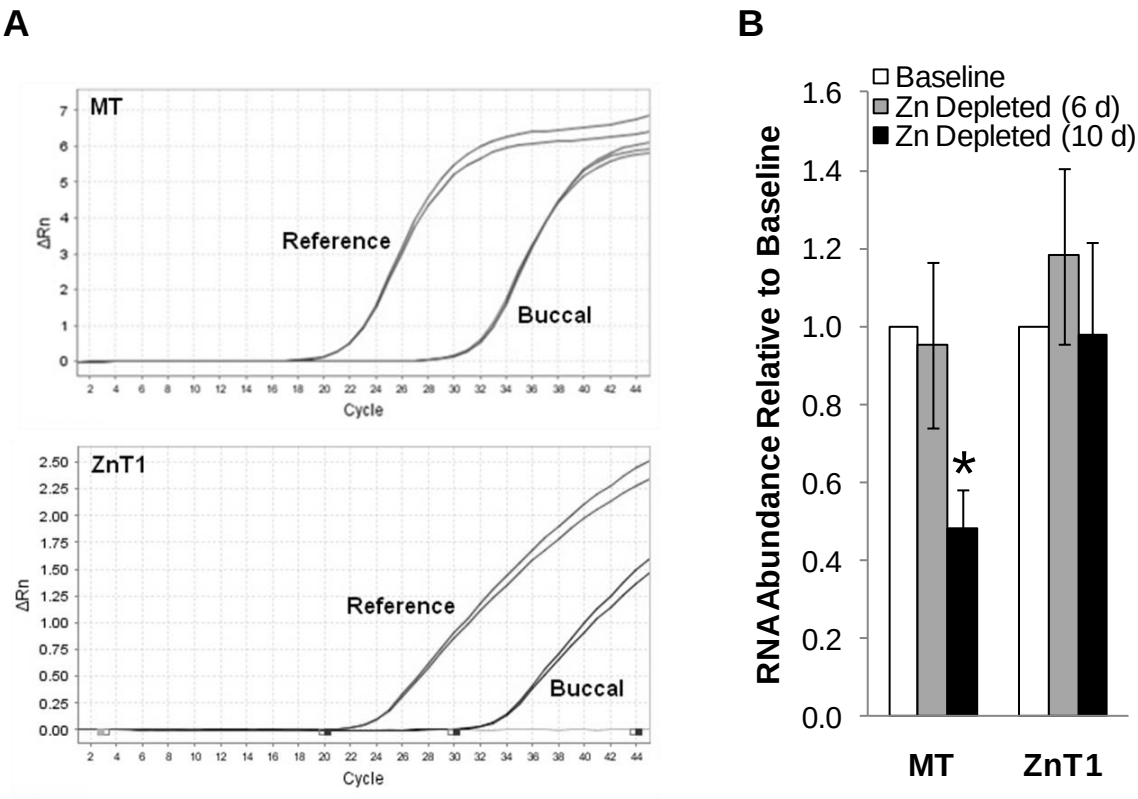


Figure 3-3. Effects of acute dietary zinc depletion on buccal MT and ZnT1 transcript abundance. (A) Amplification curve of MT and ZnT1 transcripts in human reference RNA (Stratagene) and buccal RNA produced by qPCR. These were the only zinc-related gene transcripts being stably detected, i.e., with 1) low variation, 2) amplification curves parallel to those from human reference RNA, and 3) Ct values lower than 35, in buccal RNA. (B) Relative MT and ZnT1 mRNA abundance during dietary zinc depletion. Values were normalized to 18S rRNA levels and baseline levels for each individual were set at 1. Data are expressed as mean ± standard error of the means (SEM). * indicates significant difference to baseline levels at $P < 0.05$ (n = 9 subjects).

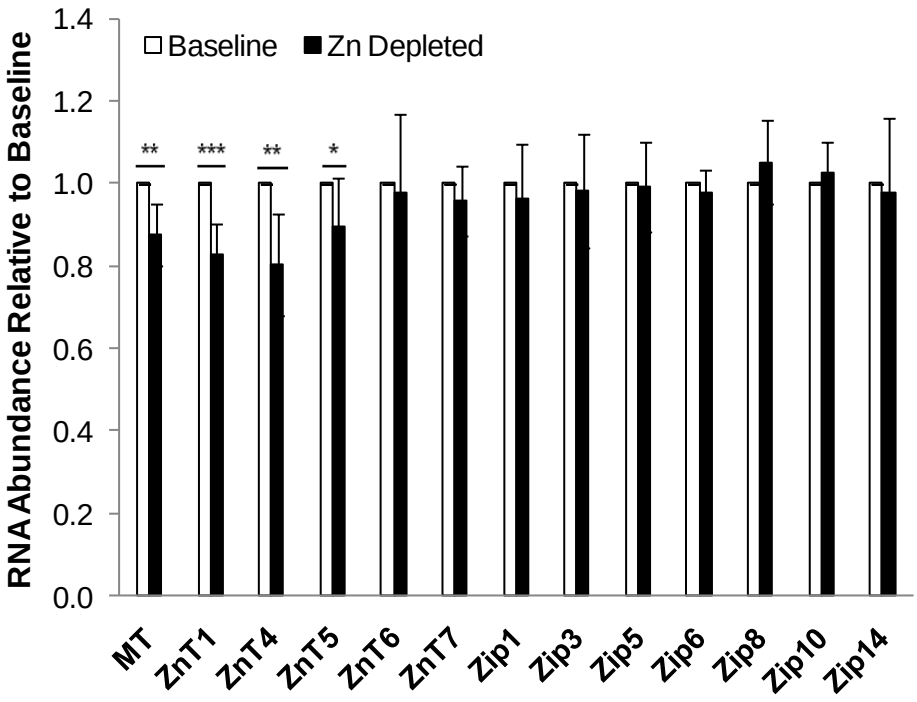


Figure 3-4. Effects of acute dietary zinc depletion on zinc-related gene transcripts in peripheral blood mononuclear cells (PBMC). Values were normalized to GAPDH mRNA levels and baseline levels for each individual were set at 1. Data are expressed as mean ± SD. Values significantly different to respective baseline levels are *, $P < 0.05$; **, $P < 0.01$; ***, $P < 0.001$ (n = 9 subjects).

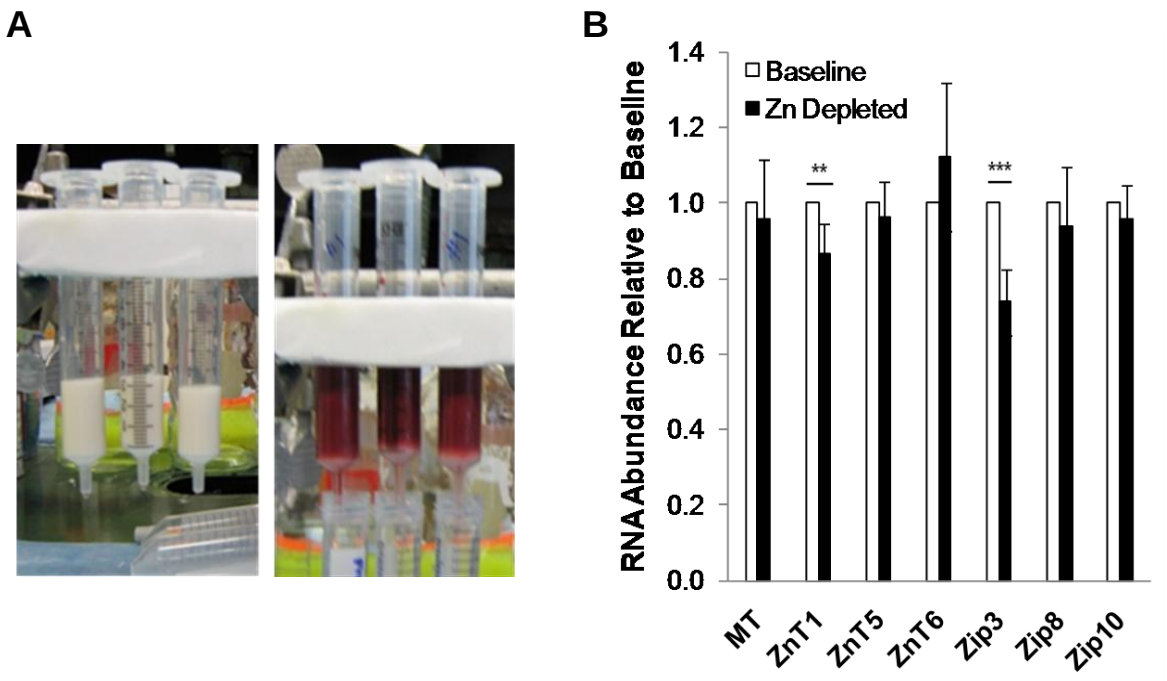


Figure 3-5. Effects of acute dietary zinc depletion on zinc-related gene transcripts in circulating reticulocytes. (A) Cellulose columns made in-house were used for the purification of erythroid cells by leukocyte depletion. (B) Relative MT and zinc transporter mRNA abundance before and after dietary zinc restriction. Values were normalized to GAPDH mRNA levels and baseline levels for each individual were set at 1. Data are expressed as mean ± SD. Values significantly different to respective baseline levels are **, $P < 0.01$; ***, $P < 0.001$ (n = 9 subjects).

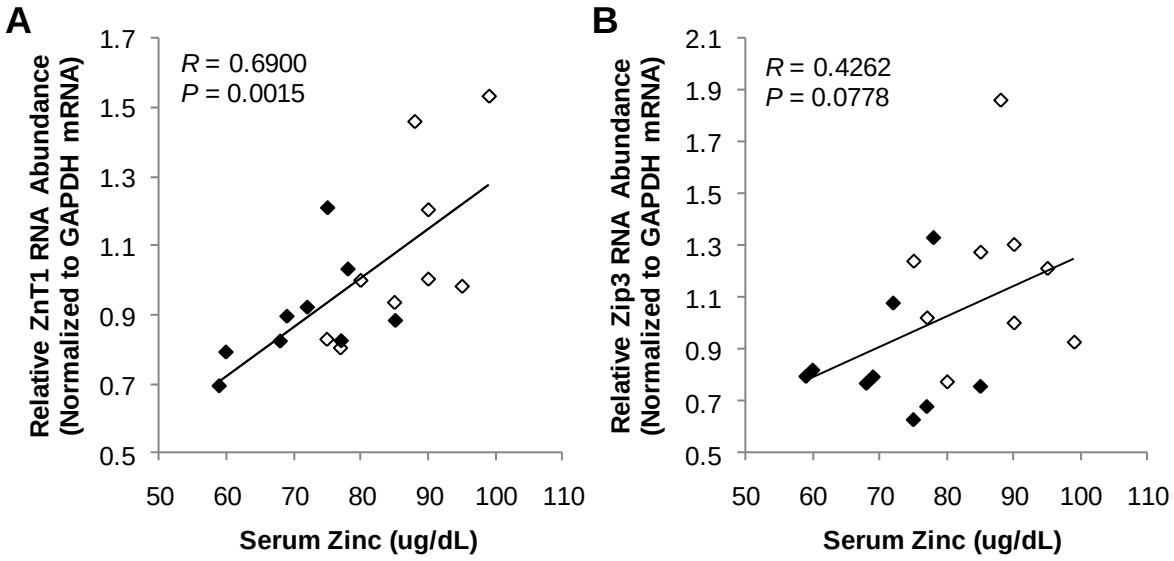


Figure 3-6. Association between serum zinc concentrations and transcript abundance of the zinc transporters most significantly responsive to dietary zinc depletion. (A) PBMC ZnT1 and (B) reticulocyte Zip3 transcript abundance were normalized to their respective GAPDH mRNA levels. Correlation with serum zinc levels was determined by correlation coefficients (*R*) determined by linear regression analyses. White, baseline levels; black, measures after 10 d of zinc depletion.

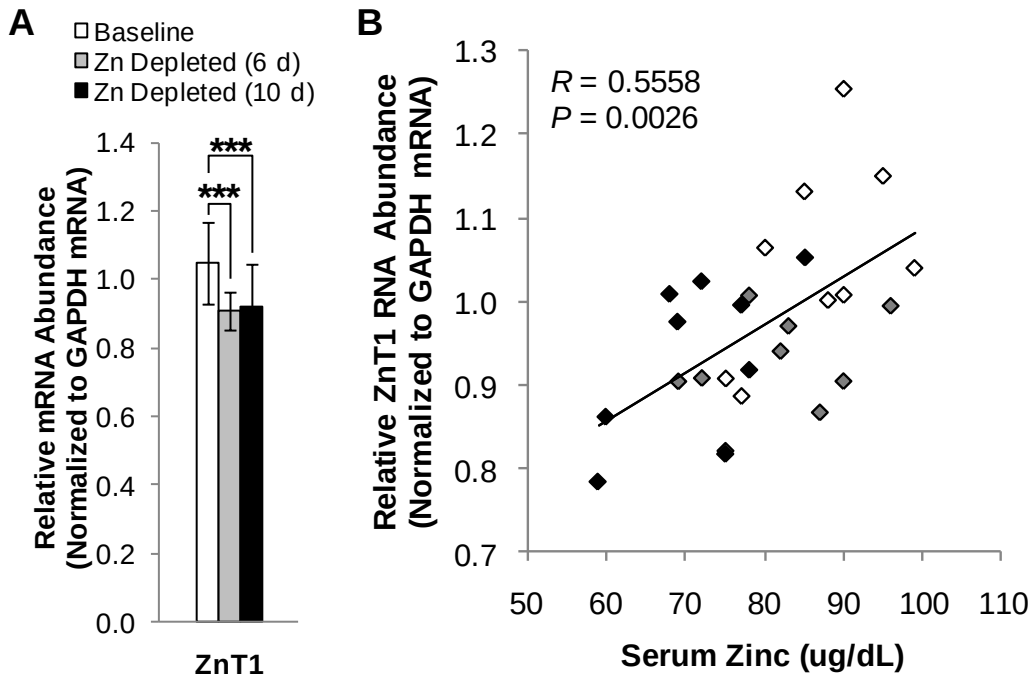


Figure 3-7. Effect of acute dietary zinc depletion on whole blood ZnT1 transcript levels. (A) Reduction in whole blood ZnT1 transcript levels by zinc restriction. ZnT1 mRNA abundance decreased in both PBMC and reticulocytes by zinc restriction. Values were normalized to GAPDH mRNA levels. Data are expressed as mean ± SD. *** indicates significant difference to baseline levels at $P < 0.001$ (n = 9 subjects). (B) Correlation with serum zinc levels was determined by the correlation coefficient ($R$) determined by linear regression analysis. White, baseline levels; grey, measures after 6 d of zinc depletion; black, measures after 10 d of zinc depletion.

**A**

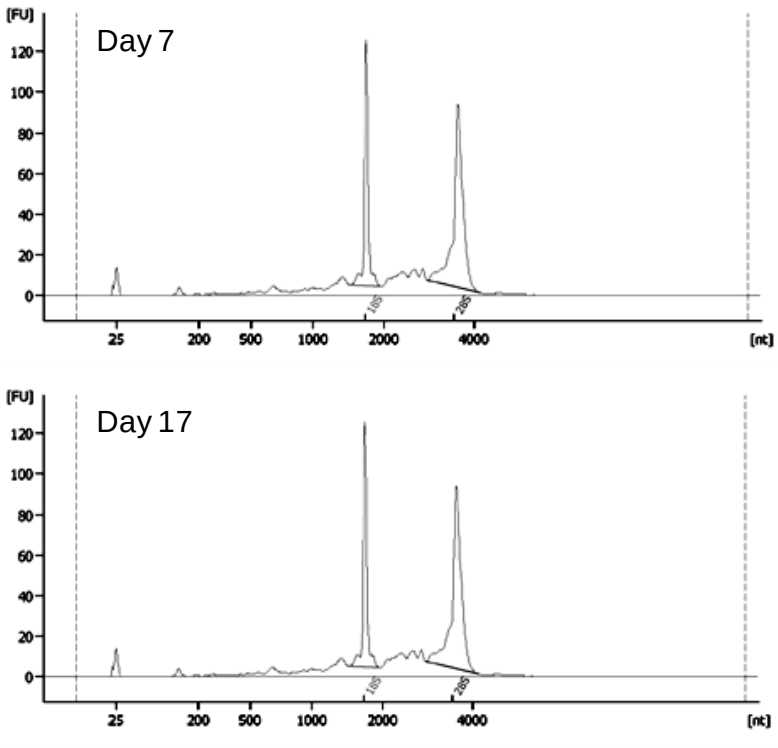


**B**

| Sample ID | RIN |
|---|---|
| 1-7 PAX | 9.0 |
| 1-17 PAX | 8.8 |
| 2-7 PAX | 8.4 |
| 2-17 PAX | 8.4 |
| 3-7 PAX | 8.7 |
| 3-17 PAX | 8.9 |
| 4-7 PAX | 9.1 |
| 4-17 PAX | 9.2 |
| 5-7 PAX | 9.0 |
| 5-17 PAX | 9.1 |
| 6-7 PAX | 9.1 |
| 6-17 PAX | 8.3 |
| 7-7 PAX | 9.1 |
| 7-17 PAX | 8.9 |
| 8-7 PAX | 9.3 |
| 8-17 PAX | 9.0 |
| 9-7 PAX | 9.1 |
| 9-17 PAX | 9.0 |

Figure 3-8. Quality assessment of whole blood RNA. Purity of RNA was determined by A260/A230 and A260/A280 ratios from the Nanodrop 1000. Ratios were 2.05~2.15 and 2.13~2.21, respectively. PAXgene system was used for RNA stabilization and isolation. Integrity of RNA was analyzed by using the Agilent 2100 Bioanalyzer. (A) Bioanalyzer electropherograms of RNA from whole blood collected on day 7 and 17 from subject 1 are presented as representative examples. (B) RNA integrity numbers (RIN) of whole blood RNA prepared by using the PAXgene system. All RNA samples were highly intact (RIN > 8.0).

**A**

| Sample | Input RNA | GLOBINclear RNA Recovered (Mean ± SD) |
|---|---|---|
| Baseline | 3 µg | 2.31 ± 0.32 µg |
| ZnD (10 d) | 3 µg | 2.34 ± 0.28 µg |

**B**

| Sample | Input RNA | cRNA Recovered (Mean ± SD) |
|---|---|---|
| Baseline | 0.20 µg | 13.67 ± 3.89 µg |
| ZnD (10 d) | 0.20 µg | 13.73 ± 2.33 µg |

**C**

| Sample | Input RNA | cRNA Recovered | |
|---|---|---|---|
| | | Pool PAX | Pool GRP |
| Baseline | 0.20 µg | 38.66 µg | 14.44 µg |
| ZnD (6 d) | 0.20 µg | 36.18 µg | 14.76 µg |
| ZnD (10 d) | 0.20 µg | 35.55 µg | 12.35 µg |

**D**

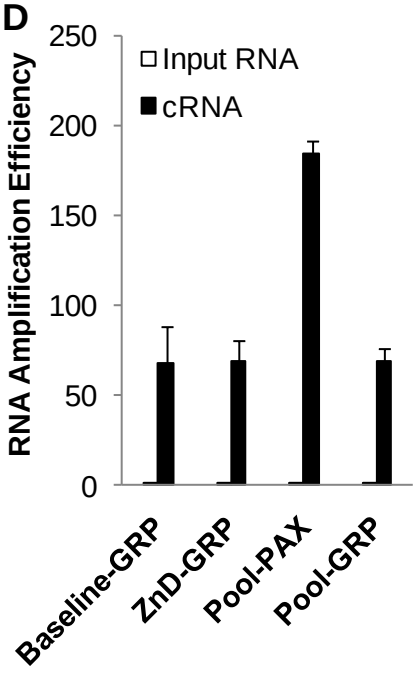


Figure 3-9. RNA recovery after processing for microarray analysis. (A) RNA recovery after globin RNA reduction by using GLOBINclear (Ambion). A260/A230 and A260/A280 ratios of the cRNA products of RNA amplification were at 2.12~2.31 and 2.19~2.30, respectively. (B) Yields of RNA after RNA amplification of individual whole blood RNA samples treated for globin RNA reduction. (C) RNA recovery of amplified pooled RNA samples processed without (PAX) or with the globin-reduction procedure (GRP). (D) Amplification efficiency, shown as folds of starting amount, of individual and pooled GRP, and pooled PAX samples.

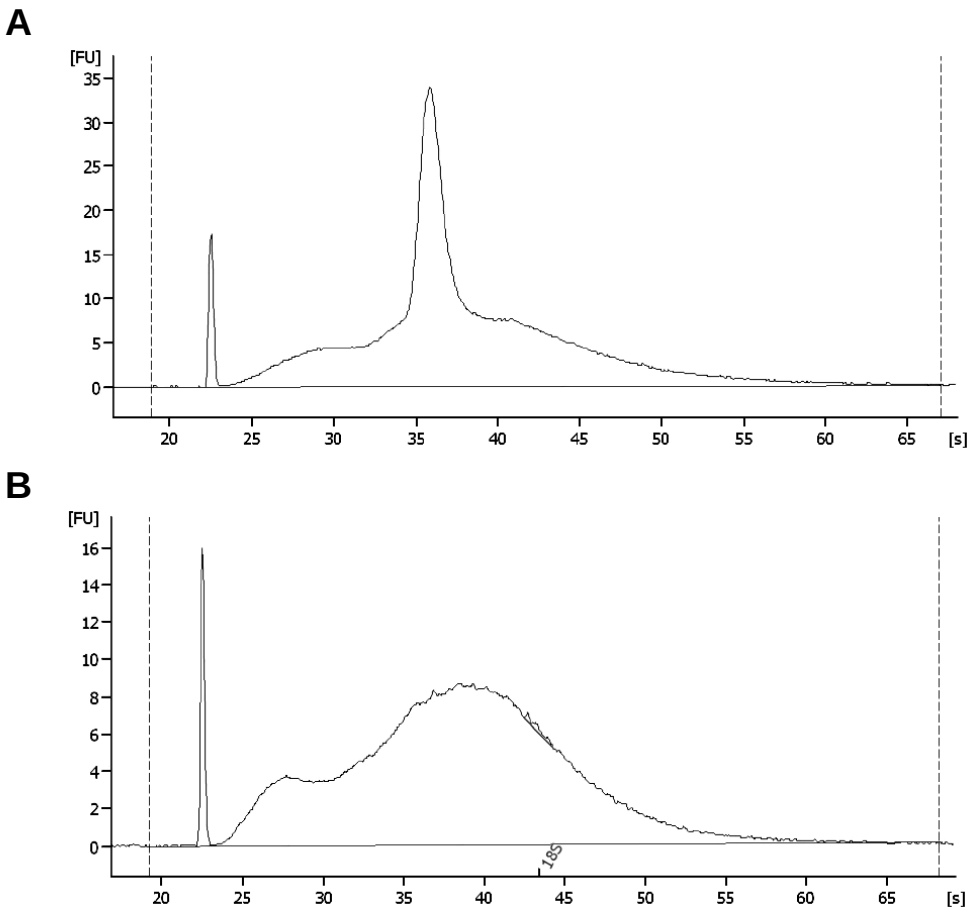


Figure 3-10. Quality of amplified cRNA assessed by Agilent 2100 Bioanalyzer. Representative electropherogram of amplified (A) whole blood RNA (PAX) and (B) globin RNA-reduced whole blood RNA (GRP) are shown. The peak only present in the electrophrogram of PAX indicates the highly abundant globin RNA content. Removal of this peak was confirmed by all globin RNA-reduced samples.

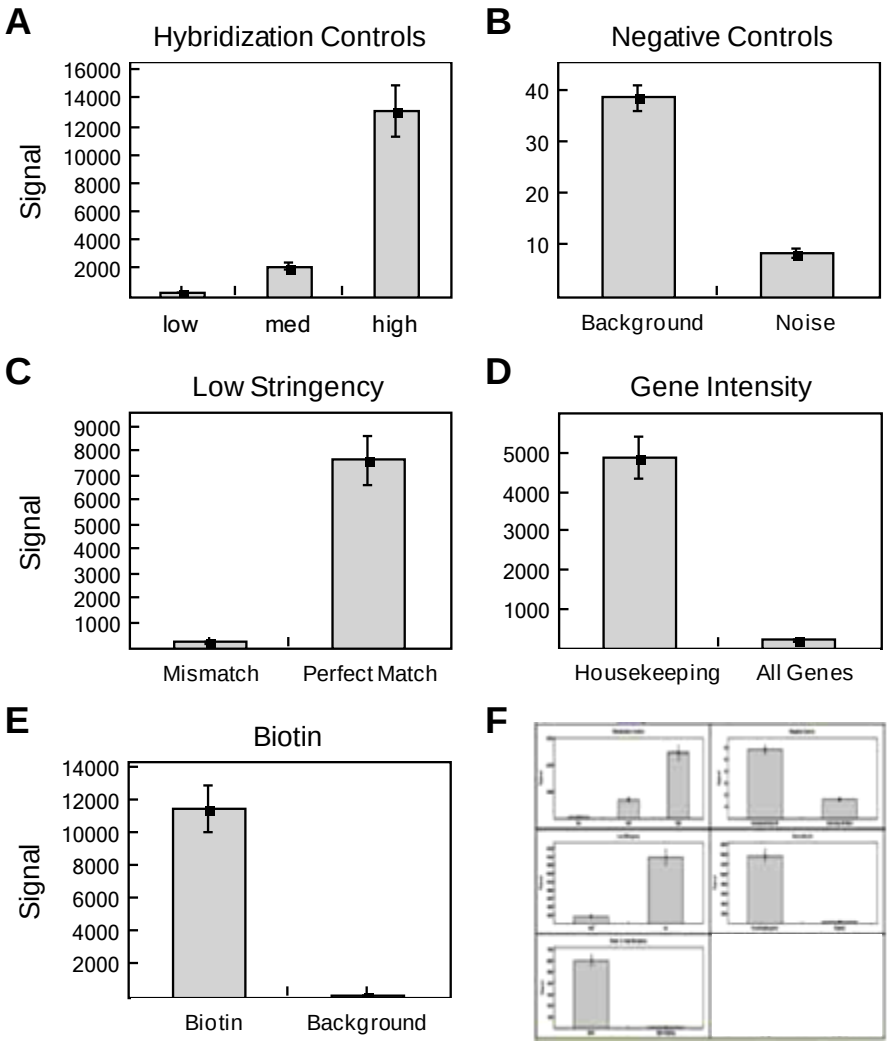


Figure 3-11. Quality assessment plots of microarray data generated by Genome Studio. (A) Hybridization controls, high > medium > low. (B) Negative controls (background and noise), low. (C) Low stringency control, perfect match > mismatch. (D) Gene intensity (housekeeping and all genes), higher than background (housekeeping > all genes). (E) Biotin, high. All parameters corresponded to (F) the expected values provided by Illumina. Data are expressed as mean ± SD (n = 24 arrays).

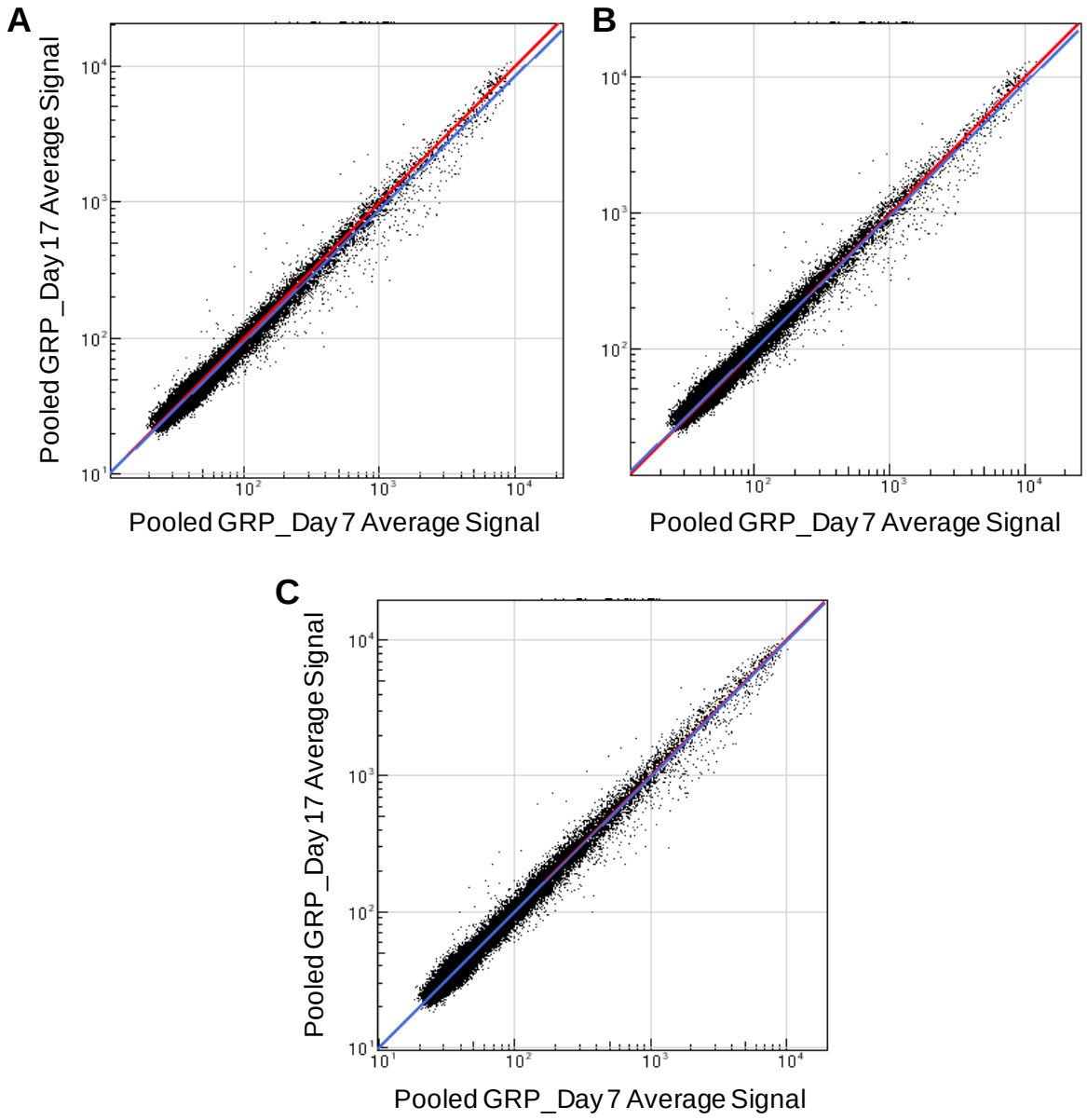


Figure 3-12. Scatter plots of microarray data before and after normalization of pooled whole blood RNA depleted of globin RNA (GRP) (Day 7 vs. Day 17). (A) No normalization. (B) Average normalization. (C) Quantile normalization. Quantile normalization, producing a highly symmetric distribution between day 7 and 17 values, was selected for the downstream data analyses.

Table 3-2. Number of differentially expressed genes determined by using various *P*-value and fold-change combinations

| | All Genes[1] | *P* < 0.05 | *P* < 0.01 | *P* < 0.005 | *P* < 0.001 | *P* < 0.0001 |
|---|---|---|---|---|---|---|
| Paired by Subjects[2] | | | | | | |
| All FC | 20,752 | 2,565 | 631 | 328 | 105 | 41 |
| FC > 1.1 | | 2,035 | 625 | 328 | 105 | 41 |
| FC > 1.2 | | 532 | 249 | 162 | 87 | 41 |
| FC > 1.5 | | 51 | 28 | 25 | 22 | 21 |
| FC > 2.0 | | 15 | 15 | 15 | 14 | 14 |
| Unpaired[3] | | | | | | |
| All FC | 20,752 | 1,256 | 221 | 108 | 44 | 10 |
| FC > 1.1 | | 1,017 | 213 | 107 | 44 | 10 |
| FC > 1.2 | | 292 | 106 | 73 | 38 | 10 |
| FC > 1.5 | | 29 | 24 | 23 | 18 | 9 |
| FC > 2.0 | | 15 | 15 | 14 | 14 | 8 |

[1] Genes of which detection *P*-value was lower than 0.05 in at least one sample.
[2] Pairwise comparison was conducted to identify genes of which transcript level was changed after dietary zinc restriction.
[3] Less differentially expressed genes were detected when inter-subject variability was taken into account by unpaired class comparison.

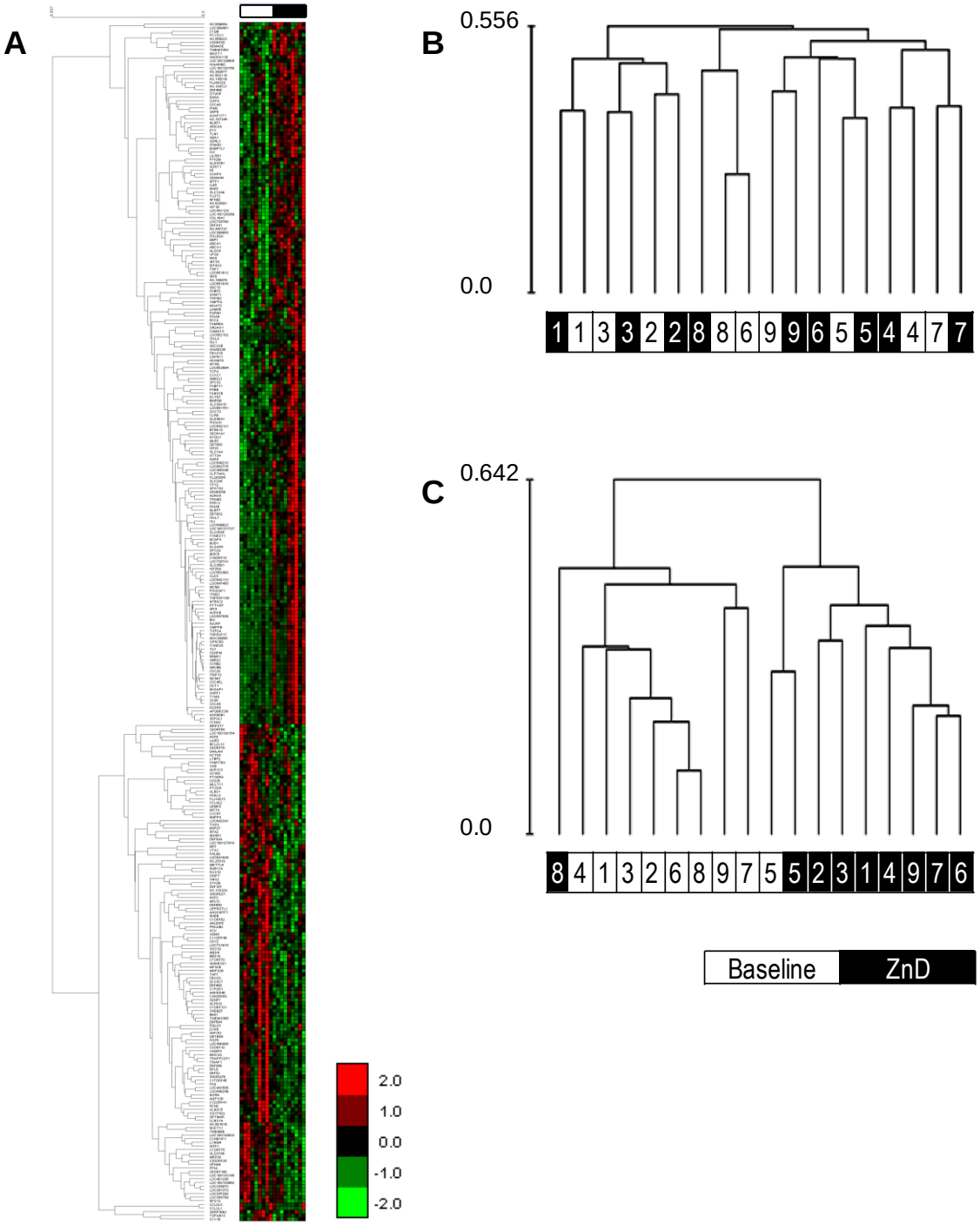


Figure 3-13. Differential expression of 328 genes identified by pairwise comparisons at $P < 0.005$. (A) Differentially expressed (DE) genes were clustered by average-linkage hierarchical clustering with Pearson correlation metric. Clustering of conditions by (B) all genes and (C) DE genes. Baseline and zinc-depleted conditions were partially separated when clustered by DE genes. Numbers indicated each individual subject (n = 9).

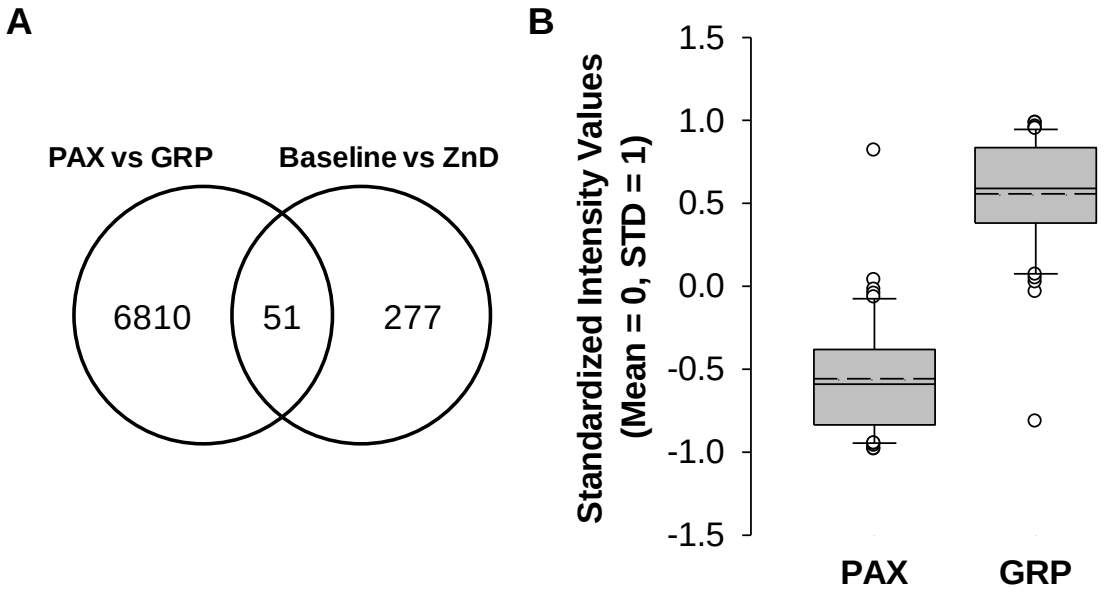


Figure 3-14. Effects of globin RNA reduction on the detection of differentially expressed genes. (A) Venn diagram showing the number of zinc-responsive genes undetected under the presence of globin RNA. RNA from whole blood collected on day 7, 13 and 17 were pooled, respectively. Signal intensity and detection *P*-values of microarray data from whole blood RNA (PAX) and globin RNA-depleted RNA (GRP) were compared. Transcripts were considered present when detection *P*-value was lower than 0.05 in at least one sample of each group. Differentially expressed genes (baseline vs. ZnD) were determined as for Figure 3-13. (B) Signal intensities of zinc-responsive gene transcripts affected by globin RNA in PAX and GRP samples. Solid and dashed lines across bars indicate median and mean values, respectively.

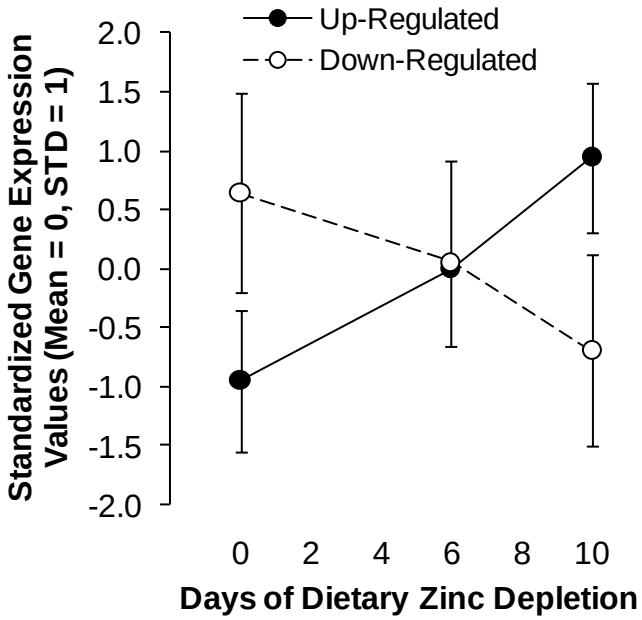


Figure 3-15. Temporal expression pattern of differentially expressed genes during dietary zinc depletion. RNA from whole blood collected on day 7, 13 and 17 were pooled, respectively, and treated for globin RNA depletion prior to microarray analysis. The up-regulated and down-regulated genes identified from day 7 and 17 samples from each individual show a temporal trend of increase and decrease, respectively, during the dietary zinc depletion phase.

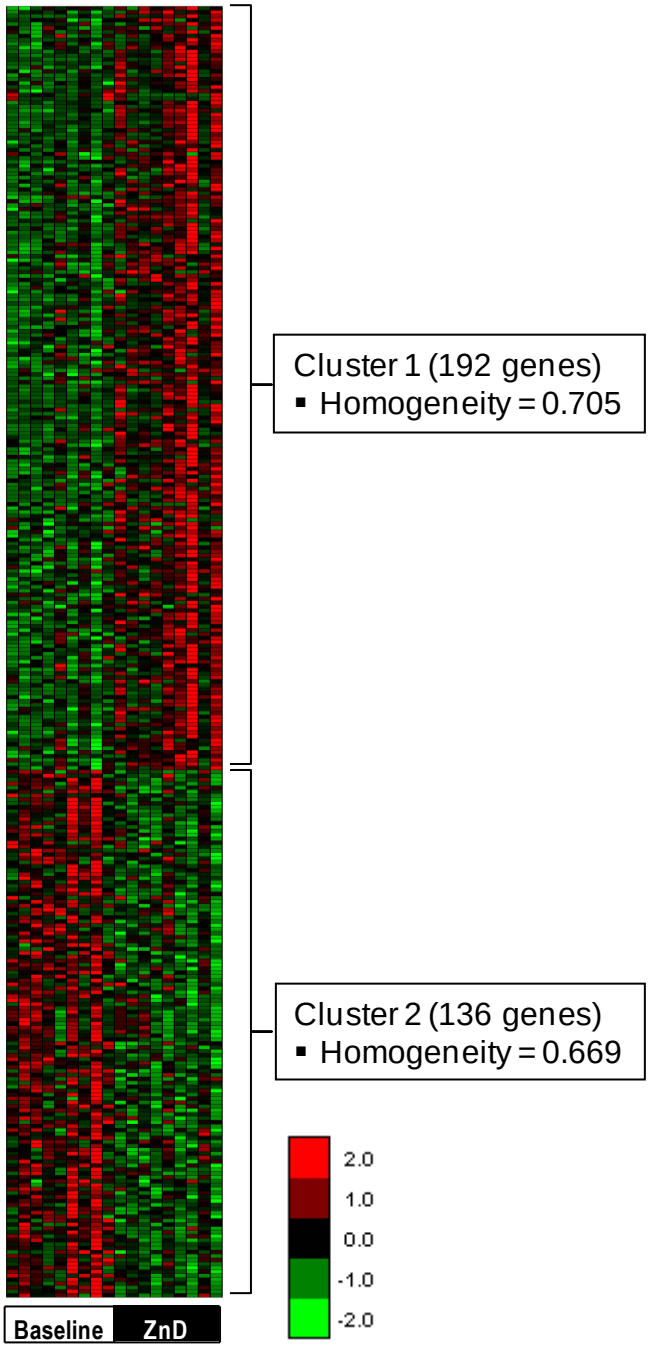


Figure 3-16. Clustering of zinc-responsive genes by expression patterns for functional interpretation. Differentially expressed (DE) genes identified by paired t-test at $P < 0.005$ (328 genes) were selected for functional enrichment analyses. K-means algorithm (k = 2) was used to cluster the genes by their mode of responsiveness o acute dietary zinc depletion. Cluster 1, up-regulated genes; cluster 2, down-regulated genes.

Table 3-3. Gene ontology (GO) enrichement by genes responsive to acute dietary zinc depletion[1]

| Gene Ontology Category | GO Number | *P*-Value | Corrected *P*-Value[2] | Frequency in Cluster (%)[3] | Gene List |
|---|---|---|---|---|---|
| Up-regulated Genes (Cluster 1) | | | | | |
| Nuclear Division | GO:0000280 | 3.90E-15 | 0.001 | 9.27 | DLGAP5, TPX2, NUSAP1, CDC20, BIRC5, AURKA, AURKB, UBE2C, DCTN1, SPC24, KIF2C, CDCA8, CCNB2, RCC2, NCAPG, BUB1, CCNA2, CDCA5 |
| Establishment of Organelle Localization | GO:0051656 | 3.69E-06 | 0.007 | 3.09 | DLGAP5, NUSAP1, BIRC5, COPG, MYH9, CDCA5 |
| Positive Regulation of Cell Cycle Process | GO:0090068 | 8.15E-06 | 0.014 | 2.06 | DLGAP5, NUSAP1, BIRC5, UBE2C |
| ATP Binding | GO:0005524 | 1.89E-05 | 0.029 | 13.4 | AURKA, ABCA1, AURKB, TK1, KIF2C, PTK2B, TAP1, BUB1, TRIP13, NLRP7, ABCB9, CAMK1G, AARS, TPX2, PIM2, MCM2, MYH9, MCM4, ABCG1, NLRP1, HYOU1, HSP90B1, UBA1, FBXO18, SEMA4A, KIF20A |
| Regulation of Mitotic Cell Cycle | GO:0007346 | 2.46E-05 | 0.032 | 3.6 | DLGAP5, BUB1, NUSAP1, BIRC5, UBE2C, CCNA2, CDT1 |

[1] Identified by Tool for Analysis of GO enrichments (TANGO) of EXPANDER with zinc-responsive genes determined by a pairwise comparison ($P < 0.005$). Threshold *P*-value for significance was set at 0.005.
[2] Empirical *P*-values corrected for multiple comparison computed by TANGO algorithm.
[3] Percentage of genes related to each functional class within the clusters generated by the K-means algorithm.

Table 3-4. Cis-regulatory elements enriched in the putative promoter regions (-1000~+200) of genes responsive to dietary zinc depletion[1]

| Transcription Factor | TRANSFAC ID | *P*-Value | Enrichment Factor[2] | Target Gene (Location of Putative TF Binding Site) |
|---|---|---|---|---|
| Up-regulated Genes (Cluster 1) | | | | |
| NF-Y | M00287 | 5.98E-7 | 1.692 | PDIA4(-61,-41,104), SPC24(-213,-115), NUSAP1(-59), CDCA5(-745), CIC(-765,-716), CDC45L(158), AARS(-51), TPX2(99,135), AURKA(-11,21), RRBP1(-60), SLC38A10(-85), SHMT1(-39), SDF2L1(-138,-19), UHRF1(-88), ALDH6A1(-226,-134,-91,-33,-5), FAM46A(-737), TK1(98,129), KIF20A(41), HSP90B1(-171,-118), SRPR(-257,-156), MCM4(-59), CDCA8(17), CXXC1(-923), MGC29506(-50), NARF(-122,-82,-46,-6), PRR11(-479,-345,-254,-133,-105,-39), PIM2(-124), UBE2C(-68,-37), SLC1A4(-181), CCNA2(-82), BUB1(-61,-35), GLDC(-97), SORT1(-189,-128), P4HB(-256,-140), MAGT1(-216,-169,-79), AURKB(-92), OTUD5(-847,-480), CCNB2(-100,-67), MLEC(-647,-129,-73), OXCT2(-294), TRPM3(-125), CDC20(-79,-34), SPCS2(-52), FBXO18(-97), PTK2B(133), DLGAP5(1,66), GMPPB(-190,-124,-51) |
| AP-2α | M00469 | 0.0020 | 1.605 | HYOU1(-240), ALOX5(-137), CLPTM1L(-811,-416), NUSAP1(-362), CIC(-771,-527,-490,-63), CDC45L(-423), RRBP1(-523), TXNDC11(15), TRAM2(-444,-395,-247), SLC38A10(-184), SDF2L1(55), ARID3A(-432,-237), FAM46A(-639), C19ORF10(-66), KIF1B(-403), DUSP5(-61), UBE2J1(-193), HSP90B1(-820), SRPR(-116), NARF(-539), PIM2(106), CDT1(-334), NLRP1(76), UBE2C(-336), SLC1A4(-656,60), SORT1(-296), P4HB(-703), MCM2(-133), OTUD5(-334), OXCT2(36), TLN1(-323), PTK2B(-277), DLGAP5(-158), APOBEC3B(-125), LAMA5(-213), NFKB2(-435), GMPPA(-678), GMPPB(-510) |
| ETF | M00695 | 9.4E-4 | 1.374 | PDIA4(-126,50), ALOX5(-911,-708,52), MTF1(-518), TYMS(-51,52,80,114), BIRC5(-52,110), ZYX(-541,15), CDC45L(-300,-285,199), TPX2(200), MGAT3(97,142), TRAM2(-469), SEC23B(-95), SDF2L1(29), UHRF1(18), SEC13(108), COL18A1(10), UBE2J1(-92), SRPR(-9), SPATS2(-430,-414), CDT1(46), PIM2(-401), SLC1A4(-208,-195), FAHD2B(-146,126,135), BIK(43), SLC35B1(-416,27), P4HB(-459), KIAA0226(-246,25), EHBP1L1(104), ADAM19(53), DENND5B(-114,37,148,157), KIF2C(-37), OTUD5(-408), TRPM3(-211,-91), FBXO18(-279,-60,-38), C4ORF28(-106), LAMA5(-969,15), ITM2C(52), SORL1(-723,86), HYOU1(-131), TRIP13(-315,-295,64), CKAP4(-211,-116), FLOT2(-132), CLPTM1L(-204,-87,-68), CIC(-745,-724,-468), AARS(-76), STT3A(-732), RRBP1(-118,193), TXNDC11(22), SLC38A10(4), SHMT1(-101,92,142), SIL1(17,47), IFNAR2(164), TK1(116), KIF1B(-928,-846,-732,-445), DUSP5(105), HSP90B1(-318), ZNF341(101), MCM4(-724), CDCA8(-56), ABCG1(-110), NARF(-438,-222,-213,126), BTBD12(10), PRR11(-709,-550), CCNA2(-30), BUB1(-39,34), UBA1(86,151), BMP8B(-243,198), MLEC(-227,-37), MYH9(89), CDC20(-305,-139), POLR2A(-388), GMPPA(-867), SEC61A1(176), GMPPB(-486) |

Table 3-4. Continued

| Transcription Factor | TRANSFAC ID | *P*-Value | Enrichment Factor[2] | Target Gene (Location of Putative TF Binding Site) |
|---|---|---|---|---|
| Down-regulated Genes (Cluster 2) | | | | |
| Elk-1 | M00025 | 0.0020 | 1.628 | LEMD3(-38), TMEM9B(-2), CREBZF(-905), ZNF256(-149), VTA1(-45), KCTD5(-124,9), CRYZ(-273), C9ORF78(6), ZNF594(-176,12), PQLC3(-731), LEPROTL1(-21), SLFN12(-748), RAB11A(-732,-223,-17), C1ORF52(-22,-1), PALB2(-116), SENP7(-123,-93), TAF7(-257), FLJ14213(-411), C20ORF30(-39), ZCCHC7(-6), COX7A2L(-778), ZNF550(-23), CRIPT(-3), MIS12(-92,-74) |
| TEF | M00672 | 0.0030 | 1.621 | C6ORF190(-38), ZNF187(-202,-140), PTGER2(-968,-827), KLRD1(-605), MS4A1(-547), GZMK(-451,-47), C9ORF78(-906), CCNB1IP1(-86), ZNF594(-951), TSPAN13(-553), RAB11A(-845), TAF7(-981,-876), RGS18(-306,49), SETMAR(-155), ERP27(-836,-181), FASLG(-286), AKR1C3(-172,-10), GNG2(-969), HOPX(-548), GK5(-667) |

[1] Identified by Promoter Integration in Microarray Analysis (PRIMA) of EXPANDER with zinc-responsive genes determined by a pairwise comparison ($P < 0.005$). Threshold *P*-value for significance was set at 0.005.
[2] Ratio of prevalence of TF hits in the cluster to that in all genes.

Table 3-5. Top 5 functions over-represented by all genes differentially expressed after acute dietary zinc depletion[1]

| Functional Category | *P*-Value[2] | Gene List |
|---|---|---|
| Cellular Assembly and Organization | 1.02E-08~2.38E-02 | DLGAP5, CDT1, KIF1B, NCAPG, CCNB2, AURKB, TAP1, ABCA1, MCM4, BIRC5, CCNA2, TOP2A, HJURP, KLHDC5, KIF2C, FASLG, RRBP1, NUSAP1, AURKA, LILRB1, RPA2, BUB1, WAS, DCTN1, MYH9, MIS12 |
| DNA Replication, Recombination, and Repair | 1.02E-08~2.5E-02 | DLGAP5, PTK2B, CDT1, NCAPG, HSF2, CCNB2, AURKB, MCM4, BIRC5, INTS3, CCNA2, BMI1, RARA, TOP2A, HJURP, CDCA5, KIF2C, FASLG, TYMS, SETMAR, TRIP13, CDC45, NUSAP1, DCK, SLX4, AURKA, RPA2, BUB1, MCM2, PPIA, BIK, MIS12, ALOX5, TK1 |
| Cell Cycle | 7.74E-08~2.23E-02 | KIF20A, DLGAP5, CDC20, CDT1, NCAPG, HSF2, CCNB2, AURKB, BIRC5, CCNA2, BMI1, CCNB1IP1, RARA, TOP2A, CD38, HJURP, CDCA5, KIF2C, TYMS, CDC45, TRIP13, IL4R, NUSAP1, CDCA8, SMARCE1, IRF9, AURKA, TPX2, MST4, ARID3A, BUB1, RPL5, MCM2, WAS, BIK, STX16, MYH9, RAB11A, DCTN1, MIS12, PIM2, UBE2C |
| Cellular Movement | 1.89E-06~2.23E-02 | KIF20A, LTBP2, PTK2B, CDC20, PTGDR, POU2AF1, HSF2, TLN1, AURKB, BIRC5, CD226, TOP2A, CD38, FASLG, LAMA5, NUSAP1, NFKB2, AURKA, CCR9, WAS, CXCR7, PPIA, CCL3L1/CCL3L3, MYH9, STX16, RAB11A, ALOX5 |
| Cancer | 8.23E-06~2.37E-02 | DLGAP5, AKR1C3, KIF1B, NLRP7, NCAPG, NLRP1, CCNB2, ABCG1, AURKB, BIRC5, BMI1, RARA, VPS8, FASLG, SLC2A5, CLNS1A, TYMS, IL4R, P4HB, CDCA8, EIF4G3, AURKA, NFKB2, IFNAR2, TPX2, PALB2, CCR9, CXCR7, ZYX, TRIAP1, PTGER2, ALOX5, TK1, UBE2C, CRYZ, KIF20A, TCF4, SLC1A4, CDC20, MS4A1, SOCS2, HYOU1, SPC24, SIL1, MCM4, IGLL1/IGLL5, MGAT3, CCNA2, DUSP5, HSP90B1, POLR2A, F5, PHGDH, TOP2A, CD38, CDCA5, SORT1, COL18A1, LAMA5, TRIP13, NUSAP1, IRF4, GZMK, UHRF1, DCK, MST4, ARID3A, SERPINE2, BUB1, HOPX, SDF2L1, MCM2, IGJ, PPIA, UBA1, TNFRSF13B, PIM2 |

[1] Identified by Ingenuity Pathway Analysis with zinc-responsive genes determined by a pairwise comparison ($P < 0.005$).
[2] Range of Fisher's exact test *P*-values of functional annotations assigned to each respective functional catagory.

Table 3-6. Top 5 functions over-represented by genes up-regulated after acute dietary zinc depletion[1]

| Functional Category | *P*-Value[2] | Gene List |
|---|---|---|
| Cell Cycle | 1.03E-08~1.64E-02 | KIF20A, DLGAP5, CDC20, CDT1, NCAPG, CCNB2, AURKB, BIRC5, CCNA2, RARA, TOP2A, CD38, HJURP, CDCA5, KIF2C, TYMS, CDC45, TRIP13, NUSAP1, IL4R, CDCA8, IRF9, AURKA, TPX2, ARID3A, BUB1, MCM2, WAS, BIK, MYH9, DCTN1, PIM2, UBE2C |
| Cellular Assembly and Organization | 1.9E-08~1.64E-02 | DLGAP5, PTK2B, CDT1, KIF1B, NCAPG, CCNB2, AURKB, TAP1, MCM4, ABCA1, BIRC5, CCNA2, TOP2A, HJURP, KIF2C, COL18A1, RRBP1, NUSAP1, UHRF1, AURKA, LILRB1, TPX2, BUB1, WAS, DCTN1, MYH9, ZYX |
| DNA Replication, Recombination, and Repair | 1.9E-08~1.64E-02 | DLGAP5, PTK2B, CDT1, NCAPG, CCNB2, MCM4, BIRC5, INTS3, CCNA2, RARA, TOP2A, CDCA5, HJURP, KIF2C, TYMS, CDC45, TRIP13, NUSAP1, SLX4, AURKA, TPX2, BUB1, MCM2, BIK, ALOX5, TK1 |
| Cancer | 1.88E-07~1.75E-02 | DLGAP5, KIF1B, NLRP7, NCAPG, NLRP1, CCNB2, ABCG1, AURKB, BIRC5, RARA, VPS8, SLC2A5, TYMS, IL4R, P4HB, CDCA8, EIF4G3, AURKA, NFKB2, IFNAR2, TPX2, CCR9, ZYX, ALOX5, TK1, UBE2C, KIF20A, TCF4, SLC1A4, CDC20, HYOU1, SPC24, SIL1, MCM4, IGLL1/IGLL5, MGAT3, CCNA2, DUSP5, HSP90B1, POLR2A, F5, PHGDH, TOP2A, CD38, CDCA5, SORT1, COL18A1, TRIP13, LAMA5, NUSAP1, IRF4, UHRF1, ARID3A, BUB1, SDF2L1, MCM2, IGJ, UBA1, TNFRSF13B, PIM2 |
| Genetic Disorder | 7.69E-07~1.72E-02 | DLGAP5, KIF1B, SLC38A10, NLRP1, CCNB2, ABCG1, TLN1, AURKB, ABCA1, BIRC5, TNFRSF17, INTS3, RARA, ALDH6A1, TYMS, PDIA5, IL4R, P4HB, CDCA8, SORL1, MAGT1, EIF4G3, AURKA, ZBTB43, NFKB2, IFNAR2, LILRB1, CCR9, FLOT2, ZYX, ALDH3B1, ALOX5, PACRGL, TK1, UBE2C, TCF4, SLC1A4, PTK2B, CDC20, CKAP4, SIL1, MCM4, IGLL1/IGLL5, TRPM3, CCNA2, DUSP5, HSP90B1, SEC61A1, POLR2A, F5, SEC23B, ADAM19, TOP2A, PHGDH, CD38, SORT1, HJURP, CDCA5, SEMA4A, COL18A1, SEMA3E, TRIP13, CDC45, CIC, LAMA5, IRF4, UHRF1, SLC35B1, COPG, SDF2L1, MCM2, WAS, IGJ, MYH9, DCTN1, SLC12A9, SPATS2, UBA1, TNFRSF13B, GLDC |

[1] Identified by Ingenuity Pathway Analysis with zinc-responsive genes determined by a pairwise comparison ($P < 0.005$).
[2] Range of Fisher's exact test *P*-values of functional annotations assigned to each respective functional category.

Table 3-7. Top 5 functions over-represented by genes down-regulated after acute dietary zinc depletion[1]

| Functional Category | *P*-Value[2] | Gene List |
|---|---|---|
| Cell Death | 1.02E-04~4.93E-02 | CLNS1A, SETMAR, GZMK, CD160, DCK, PTGDR, KLRD1, SOCS2, HSF2, MS4A1, SMARCE1, SEDLP, SERPINE2, MST4, BCL2L13, FAU, BMI1, PPIA, CD226, CCL3L1/CCL3L3, GNG2, TRIAP1, PTGER2, FASLG |
| Cell-mediated Immune Response | 1.02E-04~4.05E-02 | KLRD1, CD226, CCL3L1/CCL3L3, FASLG |
| Cellular Development | 1.02E-04~4.55E-02 | AKR1C3, KLRD1, STK39, SMARCE1, TSPAN13, TAF7, MST4, BMI1, CXCR7, PPIA, CD226, PTGER2, FASLG |
| Cellular Function and Maintenance | 1.02E-04~4.55E-02 | KLRD1, PPIA, HSF2, CRIPT, SMARCE1, CD226, PTGER2, FASLG |
| Hematological System Development and Function | 1.02E-04~4.55E-02 | CLNS1A, BMI1, PTGDR, CXCR7, KLRD1, PPIA, SOCS2, CD226, CCL3L1/CCL3L3, PTGER2, FASLG, SERPINE2 |

[1] Identified by Ingenuity Pathway Analysis with zinc-responsive genes determined by a pairwise comparison ($P < 0.005$).
[2] Range of Fisher's exact test *P*-values of functional annotations assigned to each respective functional category.

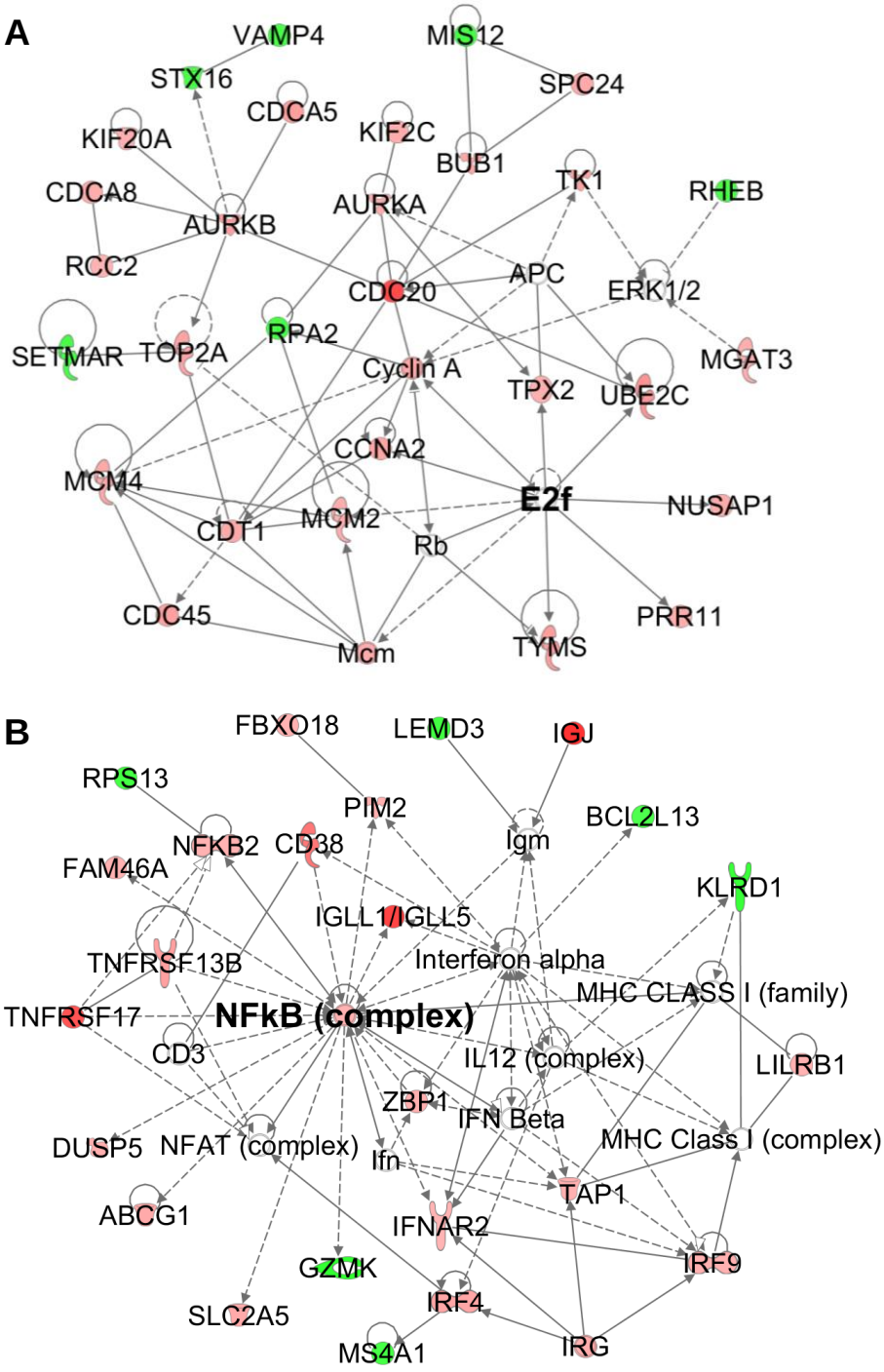


Figure 3-17. Functional networks of genes differentially expressed after acute dietary zinc depletion. Top two networks identified by Ingenuity Pathway Analysis. Each is associated with (A) cell cycle, cellular movement, cellular assembly and organization, and (B) cellular growth and proliferation, hematological system development and function, cellular development, respectively. Red, up-regulated by zinc restriction; green, down-regulated by zinc restriction.

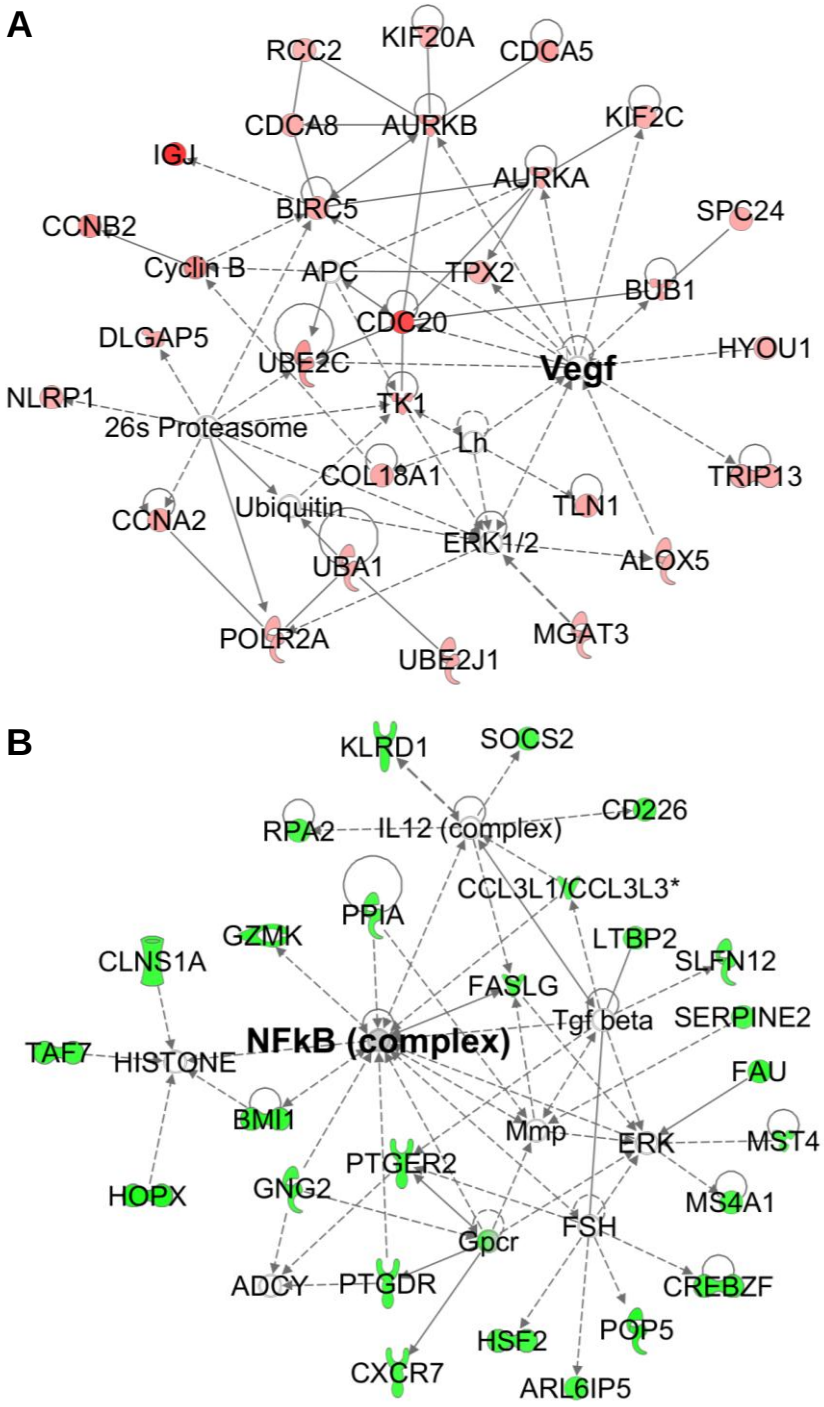


Figure 3-18. Functional network enriched by genes up-regulated and down-regulated after acute dietary zinc depletion. (A) Top network of up-regulated genes associated with cellular assembly and organization, DNA replication, recombination and repair, and cell cycle. (B) Top network of down-regulated genes associated with cell death, cell-mediated immune response and cellular development. Red, up-regulated by zinc restriction; green, down-regulated by zinc restriction.

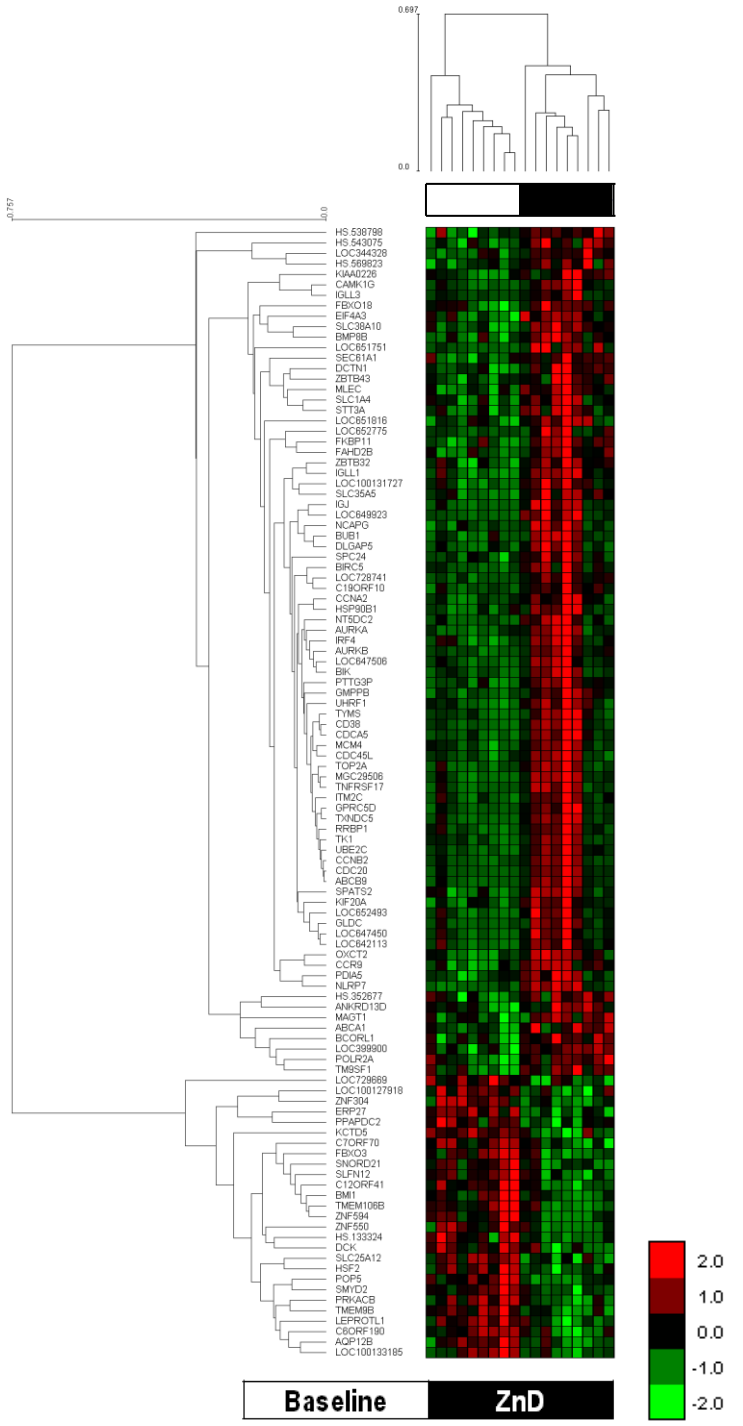


Figure 3-19. Differential expression of 203 genes identified by unpaired t-test at $P < 0.005$. Differentially expressed (DE) genes were clustered by average-linkage hierarchical clustering with Pearson correlation metric. A clear distinction between baseline and zinc-depleted condition is shown when clustering is conducted with the DE genes.

Table 3-8. Genes holding the potential as an indicator of dietary zinc deficiency in individuals[1]

| Gene Symbol | Entrez ID | Gene Name | Fold-Change (ZnD/Baseline) | *P*-Value | FDR |
|---|---|---|---|---|---|
| CDC20 | 991 | cell division cycle 20 homolog (S. cerevisiae) | 2.69 | 2.00E-07 | 0.00124 |
| TXNDC5 | 81567 | thioredoxin domain containing 5 (endoplasmic reticulum) | 2.73 | 5.00E-07 | 0.00173 |
| MZB1 | 51237 | marginal zone B and B1 cell-specific protein | 2.07 | 7.00E-07 | 0.00182 |
| IGJ | 3512 | immunoglobulin J polypeptide, linker protein for immunoglobulin alpha and mu polypeptides | 4.22 | 1.00E-06 | 0.00189 |
| IGLL1 | 3543 | immunoglobulin lambda-like polypeptide 1 | 2.77 | 1.00E-06 | 0.00189 |
| CD38 | 952 | CD38 molecule | 2.03 | 2.07E-05 | 0.01780 |
| GLDC | 2731 | glycine dehydrogenase (decarboxylating) | 2.49 | 2.30E-06 | 0.00367 |
| TNFRSF17 | 608 | tumor necrosis factor receptor superfamily, member 17 | 2.55 | 1.85E-05 | 0.01740 |

[1] Baseline and post-zinc depletion values were grouped as to represent zinc-adequate (ZnA) and zinc-deficient (ZnD) conditions. Total of 8 well-characterized genes were identified to be significantly different between each group ($P < 0.005$ by t-test without pairing) with a fold-change larger than 2 (n = 9). FDR, false discovery rate.

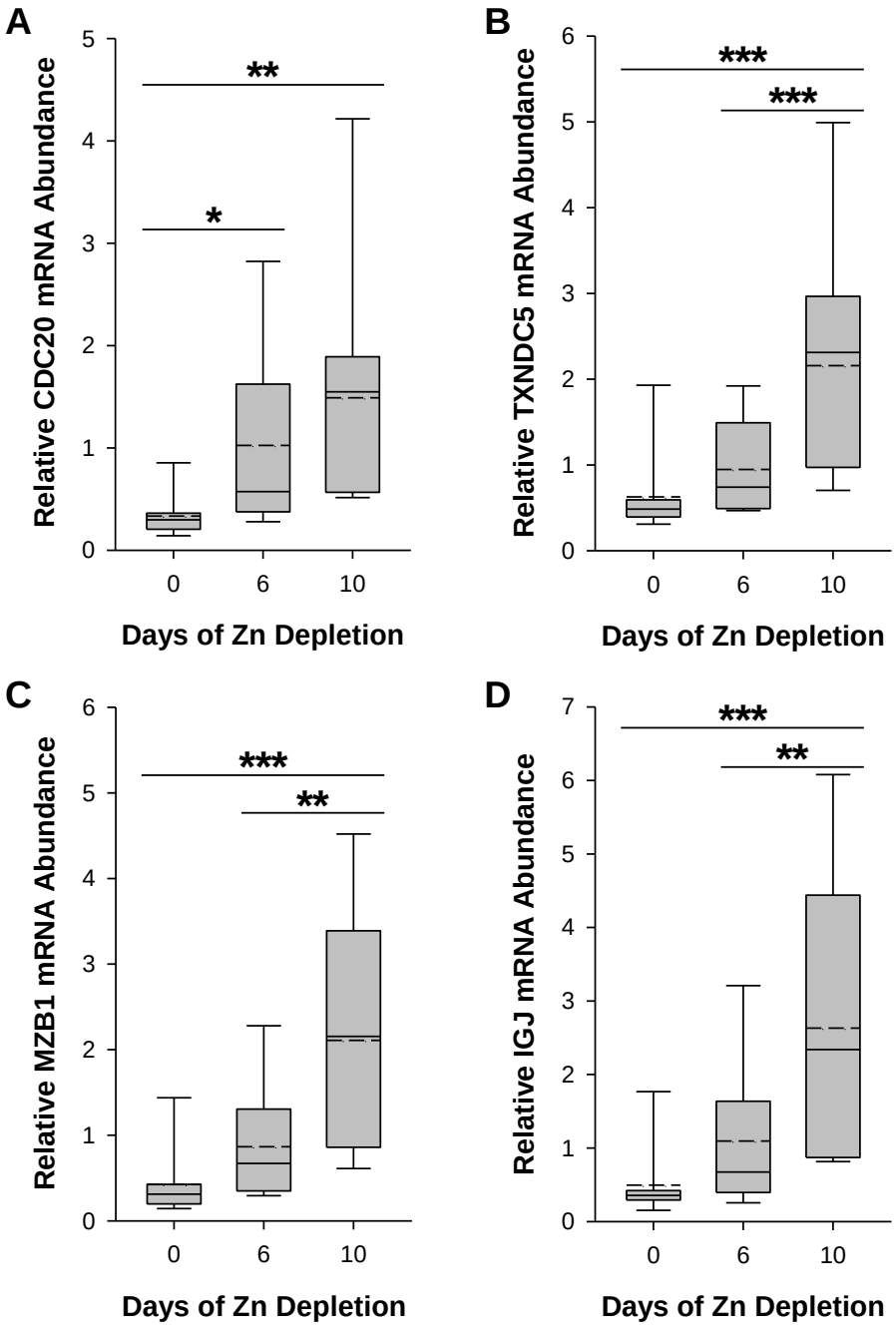


Figure 3-20. Validation of microarray data using qPCR. Relative transcript levels of (A) CDC20, (B) TXNDC5, (C) MZB1 (MGC29506) and (D) IGJ in whole blood RNA during dietary zinc depletion were measured by qPCR. Values were normalized to GAPDH mRNA levels. Solid and dashed lines across bars indicate median and mean values, respectively. Values significantly different to respective baseline levels are *, $P < 0.05$; **, $P < 0.01$; ***, $P < 0.001$ (n = 9 subjects).

# CHAPTER 4
# EFFECTS OF ACUTE DIETARY ZINC DEPLETION ON WHOLE BLOOD CYTOKINE RELEASE INDUCED BY *EX VIVO* IMMUNOCHALLENGES

## Introductory Remarks

The essentiality of adequate zinc intake has been derived from its involvement in various physiological events including immunity. The association of dietary zinc deficiency with clinical symptoms reflecting impaired immunity, such as thymic atrophy and increased risks of bacterial, viral and fungal infections, imply the significance of sufficient zinc supply for maintenance of the immune system (1, 2, 22). Additionally, low serum zinc levels have been associated with a decrease in cytokine production by leukocytes in humans (63, 96). The beneficial effects of zinc supplementation on the activation of immune cells, i.e., granulocytes, lymphocytes and monocytes, have been shown by increases in cytokine production induced by *ex vivo* immunostimulation with human subjects (41). Recent *in vitro* and animal experiments indicate the necessity of zinc and zinc transporter function for the expression of genes responsible for immune responses (22). Direct involvement of zinc molecules in the signaling pathways mediating in activation and cytokine production of T-cells and dendritic cells has been identified (51, 52). Consequently, inadequate dietary intake of zinc leads to a modulation in immunity, and thus functional assessment of these features may provide means for the diagnosis of dietary zinc deficiency.

Whole blood cytokine assays, which involve *ex vivo* challenge of cells to either lipopolysaccharides (LPS) or phytohemagglutinin (PHA), have been employed as a method to evaluate the *in vivo* effects of various conditions on immune response (113). Research with whole blood assays implies the appropriateness of this methodology as a diagnostic tool for various conditions such as tuberculosis (114), sepsis (115), multiple

sclerosis (116) and HIV infection (117). Additionally, association of immunity with vitamin A store levels (118) and serum high-density lipoportein levels (119) was identified by using this approach.

The classical approach for the identification of responses of a protein to a biological effect is based on immunological labeling of the target protein and visualization by an enzyme-conjugated protein that produces colorometric, autoradiographic or chemiluminescent signals upon substrate treatment. Relevant techniques include western analysis and enzyme-linked immunosorbent assay (ELISA). Multi-analyte ELISA arrays have been used for the identification of molecular effects of a treatment on proteins involved in certain pathways such as cytokines and other markers of immune response. The platform provides ELISA assays for the quantitation of multiple proteins on a 96-well plate template, and thus allows the simultaneous evaluation of the effects of a biological variable on the protein expression levels. The limitation of these techniques are that the proteins of interest should be identified prior to the experiment is conducted. However, when researchers have an idea of the affected list of proteins based on previous findings from relevant research, these tools enable multiplexing which markedly reduces labor- and cost-intensity. Additionally, by utilizing commercially available platforms along with standard peptides, the inter-laboratory variable can be minimized particularly with regards of the nature of the technique allowing absolute quantitation.

The aim of the study was to determine the effects of acute dietary zinc depletion on the levels of whole blood cytokine release induced by *ex vivo* exposure to LPS or PHA using the recently introduced multi-analyte ELISA array platform. The validity of

this approach for the diagnosis of zinc deficiency was further assessed by absolute quantitation of secreted cytokine levels by using single-analyte ELISA arrays as well. Additionally, differential expression of zinc transporters by *ex vivo* activation and the effect of the hosts' zinc intake level on its profile were assessed by qPCR.

## Results

### Inflammatory Cytokine Production by Whole Blood

Whole blood cytokine assay was implemented as an approach to test if the modulating effects of zinc on the capability of immune cell activation can be used as a tool for identifying dietary zinc deficiency. To identify the cytokines of which production induced by immunostimulation is affected by dietary zinc depletion, cell-free supernatants collected on day 7 and 17 were pooled and analyzed using a multi-analyte ELISA array designed for human inflammatory cytokines. Among the twelve cytokines tested, only TNFα showed a noticeable effect of dietary zinc depletion on its production induced by challenges with LPS and PHA (Figure 4-1). In order to confirm this effect of dietary zinc deprivation, supernatant collected from individual whole blood-incubations were subject to ELISA specific for IL-1β, IFNγ and TNFα quantitation. Prominent induction of the monokine IL-1β by LPS confirmed the activation of monocytes present in the whole blood samples during the *ex vivo* immunostimulation (Figure 4-2). A substantial increase in lymphokine IFNγ secretion indicated the successful activation of lymphocytes in the PHA-treated whole blood samples as well (Figure 4-3). As observed by the multi-analyte screening with pooled samples, there were no differences between whole blood samples collected before (baseline) and after dietary zinc depletion (Zn depleted) by IL-1β and IFNγ responses to LPS or PHA. In contrast, whole blood samples collected at the post-depletion phase secreted significantly lower TNFα in

response to immunostimulation than those collected at the baseline (Figure 4-4), indicating the presence of a zinc effect on a pathway specific to the production of this cytokine.

**Zinc Transporter Transcript Levels**

The critical roles of zinc and its transporters in immune response implicate the possibilities of zinc transporter expression induced by immune cell activation to respond to the host's dietary zinc status. Heparin was used as an anticoagulant for the whole blood samples for the cytokine assays. It is of note that residual heparin present in the whole blood RNA can inhibit reverse transcriptase and polymerase activity (120, 121), and thus RNA purification by LiCl prior to qPCR assays was essential (Figure 4-5). Among the zinc homeostatic gene transcripts measured, only MT mRNA levels showed a statistically significant response to LPS challenge, while MT, ZnT6, Zip1, Zip3, Zip6, Zip8 and Zip14 transcripts were up-regulated in response to activation by PHA (Figure 4-6). Only PHA-induced Zip8 expression was responsive to acute dietary zinc depletion with an approximate decrease of 50%.

## Discussion

Impaired immunity is one of the most extensively characterized outcomes of zinc deficiency by various types of research (95-97). The clinical significance of adequate zinc intake has been substantiated by epidemiological data identifying higher risks of morbidity and mortality from infectious diseases including pneumonia and malaria in populations with high prevalence of zinc deficiency (23, 88). Previously, we have shown the synergistic effects of zinc supplementation on the expression of cytokine genes induced by immune cell activation (41). The dependence of these genes on zinc transporter activity (51, 52) also underlines the importance of constant zinc levels in the

cells conferring immune response. Corresponding to these aspects of zinc in immunity, functional network analysis of our microarray data, presented in the preceding chapter, identified an overrepresentation of transcripts for genes down-regulated during zinc depletion that are associated with cell-mediated immune response. Thus, as an approach to functionally assess the effects of low zinc ingestion on the host's immune response, we implemented a standardized method, i.e., whole blood cytokine assay, involving an *ex vivo* challenge and quantitative measures of cytokine release (113). Successes in discrimination between patients of various diseases and healthy individuals by using this means implicate its practicality for molecular diagnosis (114-117).

The results of the present study indicate the potential of TNFα production levels induced by blood cell activation as an indicative marker of the host's zinc status. The *in vitro* effect of zinc on TNFα secretion from blood cells induced by immunoactivators including LPS and PHA has been well-documented elsewhere (122). It is of note that zinc alone can function as an immunoactivator, particularly, by inducing TNF production (62). The *in vivo* effects of dietary zinc levels on immune cell activation, measured by relevant cytokine transcript levels, were recently shown by a dietary human study with regimen of supplemental zinc. Consumption of zinc supplements for a 10-day period resulted in enhancement in activation-induced TNFα, IFNγ and IL-1β gene expression of monocytes, T-lymphocytes and granulocytes, respectively (41). The increase in TNFα expression by high zinc intake agrees with the repression by zinc depletion observed in the present study. In agreement to the observations in the current study, the effects of zinc on cytokine production were limited to the cells exposed to *ex vivo*

immunoactivators in the previous study on zinc supplementation. This activation-dependent zinc-responsiveness of cytokine expression emphasizes the significance of sufficient dietary zinc intake for populations, particularly, at higher risks of infection or immunological disorders.

A previous microarray study with immune cell lines identified tumor necrosis factors as central regulators of the biological events associated with the genes influenced by zinc availability (90). Additionally, NFκB, a major regulator of TNFα gene expression, was present in the functional network composed of the down-regulated genes identified by our transcriptome analysis. These bioinformatic data suggest that impaired TNFα production upon activation may be a consequence of impairment in NFκB activity under low zinc conditions. Mechanistic studies with various immune and cancer cell models further support our hypothesis of the involvement of NFκB in conferring the zinc effects on immunoactivator-induced TNFα gene expression (106-108). It is of note that two TNF receptor superfamily genes, TNFRSF17and TNFRSF13B, were identified as zinc-responsive by the microarray experiments of the current study. Both receptor genes produced higher transcript levels after the consumption of the zinc-deficient diet. Upon recognition by TNF receptors, TNFα triggers a feedback inhibitory mechanism of TNFα gene expression by attenuating the transactivation potential of its inducer NFκB (123). These suggest that the negative feedback regulation enhanced by higher receptor activities may account for the reduced LPS- or PHA-induced TNFα production by blood cells from zinc-depleted individuals.

The whole blood model has been implemented as a means to evaluate the immune system of patients under various clinical conditions (113). The use of whole

blood for biomolecular diagnostics holds several advantages over the use of isolated blood mononuclear cells. The lack of extensive processing for cellular fractionation enables the implementation of assays in a timely efficient manner and under such conditions where specific laboratory equipment or reagents are absent. Additionally, because whole blood culturing conveys all blood components to the *ex vivo* cellular environment, the cytokine assay results allow the prediction of the *in vivo* outcome of immune cell activation under the physiological condition of interest. The use of inappropriate anticoagulants can markedly affect the results, and thus relevant precaution during blood sampling was taken for the current study. Even though, other anticoagulants hold the advantage for PCR-based assays (85), heparin was selected as an anticoagulant for the presented experiments. EDTA and citric acid-based reagents were excluded due to their respective potential to chelate zinc (124) and to modulate plasma or cellular metabolite concentrations (46) which would potentially modulate the zinc bioavailability during *in vitro* incubation. The limitation of heparin, inhibiting reverse transcriptase and DNA polymerase activities during qPCR (120, 121), was overcome by implementing an additional step of RNA purification by using lithium chloride (85).

The release of zinc ions compartmentalized in intracellular vesicles to the cytosol has been suggested as a regulatory mechanism of various signaling pathways mediating immune responses (21, 22). In addition to its effects on the DNA binding activity of transcription factors, zinc molecules exploit their regulatory role as inhibitors or activators of enzymes involved in the regulation of signaling molecules, such as phosphatases and kinases (51, 125-129). Zinc transporters, Zip8 and Zip6, have been shown to mediate the redistribution of cellular zinc during the activation of T-

lymphocytes (51) and dendritic cells (52), respectively. Among the responses of zinc transporter transcripts to *ex vivo* challenging, that of Zip8 mRNA to PHA treatment was most prominent in the current study. These results from the whole blood model were comparable to those from a previous screening carried out with isolated human primary T-cells (51). RNA interference of lymphocyte Zip8 resulted in impaired activation of T-lymphocytes as indicated by a reduction in the expression levels of an activation marker gene, IFNγ (51). Potentiating effect of zinc on the activation of T-cells was also shown by this study. The NFκB-mediated regulation of Zip8 has been suggested by its responsiveness to TNFα (130). Even though the depressing effect of dietary zinc depletion on the activation-induced TNFα levels was also identified by LPS-treated blood, the down-regulation of Zip8 under such conditions was only present in PHA-treated whole blood culture. Thus, it is unlikely that TNFα is mediating the down-regulation of Zip8 by the host's suboptimal zinc intake. Consequently, future research for the identification of a zinc-responsive regulatory factor specifically mediating the attenuation of Zip8 responses to T-lymphocyte activation is warranted.

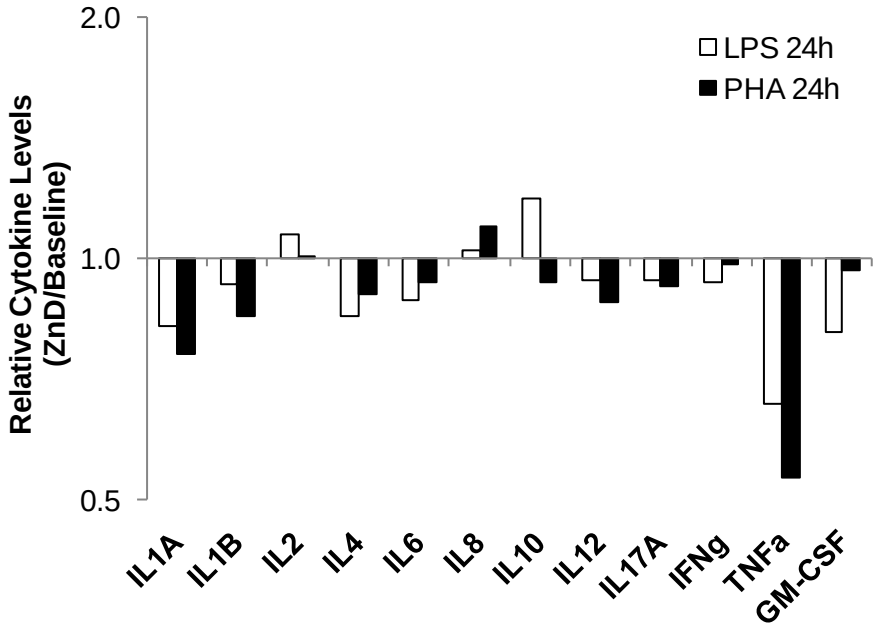


Figure 4-1. Effects of acute dietary zinc depletion on whole blood cytokine production induced by LPS and PHA *in vitro*. Heprainized whole blood collected on day 0 (baseline) and day 10 (ZnD) of zinc depletion were incubated with LPS (1 µg/mL) or PHA (10 µg/mL) for 24 h. Cell-free supernatants were pooled for the screening measures by a cytokine-focused multi-analyte ELISA array. Values of zinc-depleted status are expressed as ratios relative to the baseline levels in a log-2 scale (Pooled samples from n = 8 subjects).

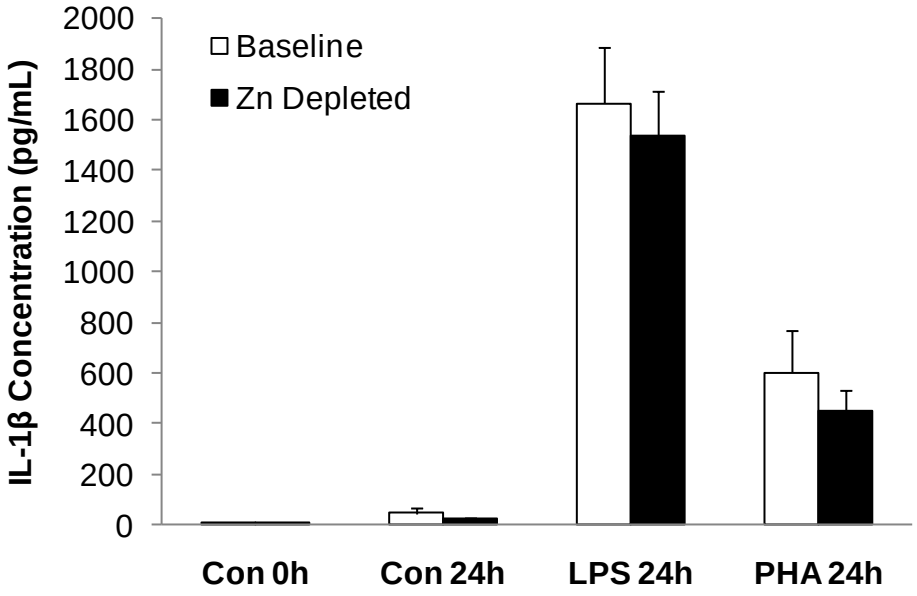


Figure 4-2. Confirmation of LPS-induced monocyte activation in whole blood *in vitro*. Cell-free supernatant was collected from whole blood exposed to LPS or PHA for 24 h. Levels of a monokine, IL-1β, in each individual sample were measured by using a single-analyte ELISA array. Absolute concentrations deduced from a standard curve generated with synthetic IL-1β peptides. Data are expressed as mean ± SD (n = 8 subjects).

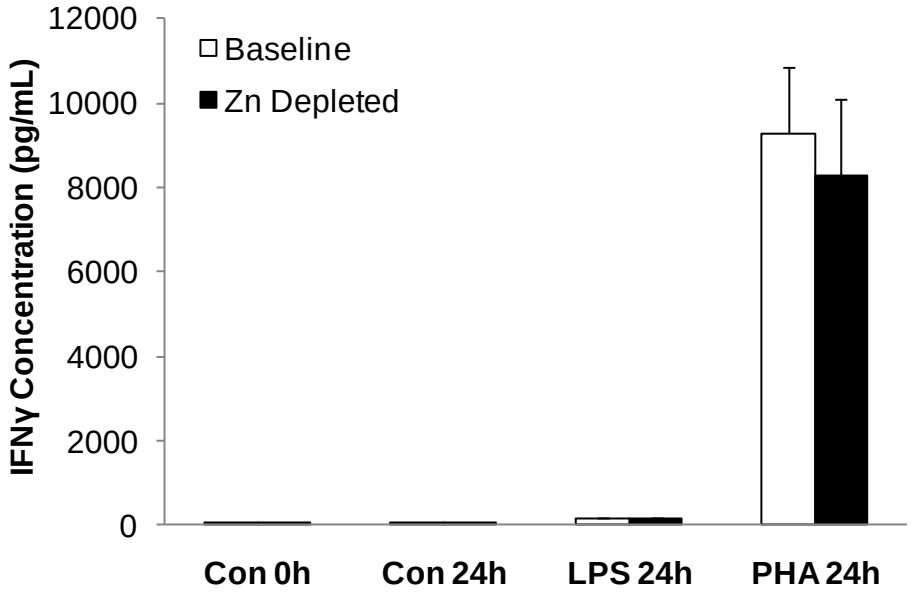


Figure 4-3. Confirmation of PHA-induced lymphocyte activation in whole blood *in vitro*. Cell-free supernatant was collected from whole blood exposed to LPS or PHA for 24 h. Levels of a lymphokine, IFNγ, in each individual sample were measured by using a single-analyte ELISA array. Absolute concentrations were deduced from a standard curve generated with synthetic IFNγ peptides. Data are expressed as mean ± SD (n = 8 subjects).

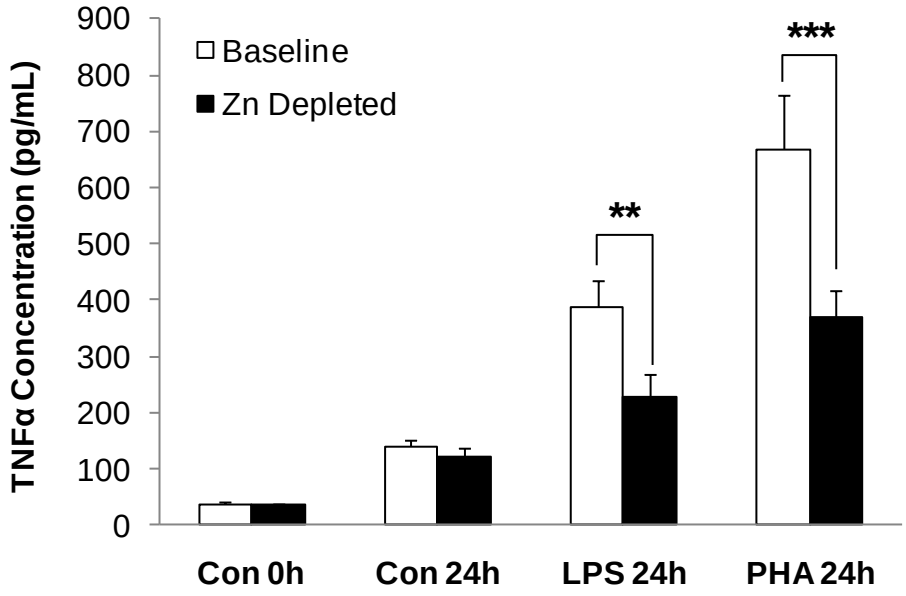


Figure 4-4. Confirmation of the repression in LPS- and PHA-induced TNFα production by acute dietary zinc depletion. Cell-free supernatant was collected from whole blood exposed to LPS or PHA for 24 h. TNFα levels of each individual sample were measured by using a single-analyte ELISA array. Absolute concentrations were deduced from a standard curve generated with synthetic TNFα peptides. Data are expressed as mean ± SD. Values significantly different to respective baseline levels are **, $P < 0.01$; ***, $P < 0.001$ (n = 8 subjects).

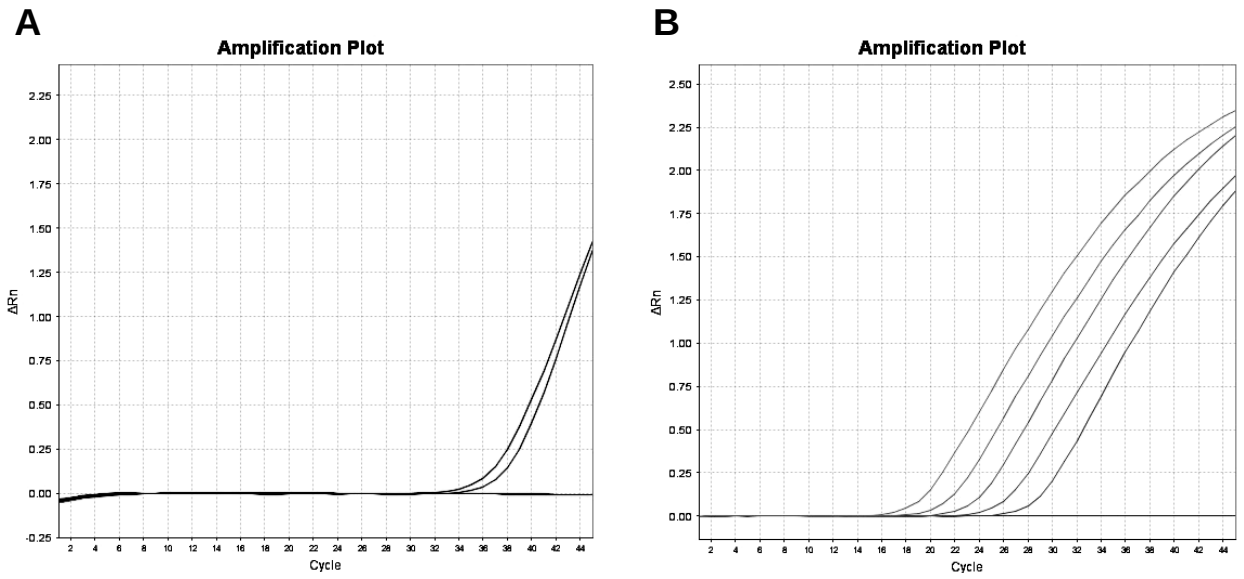


Figure 4-5. Effects of residual heparin in RNA samples on PCR amplification. (A) Amplification plot of MT transcripts in standards prepared by 1/5-serial dilution of RNA isolated from heparinized whole blood. Amplification was detected only when standards were sufficiently diluted in nuclease-free water. (B) Amplification plot of MT transcripts in standards prepared by 1/5-serial dilution of RNA purified by $LiCl_2$ after isolated from heparinized whole blood. All standards produced amplification products by qPCR.

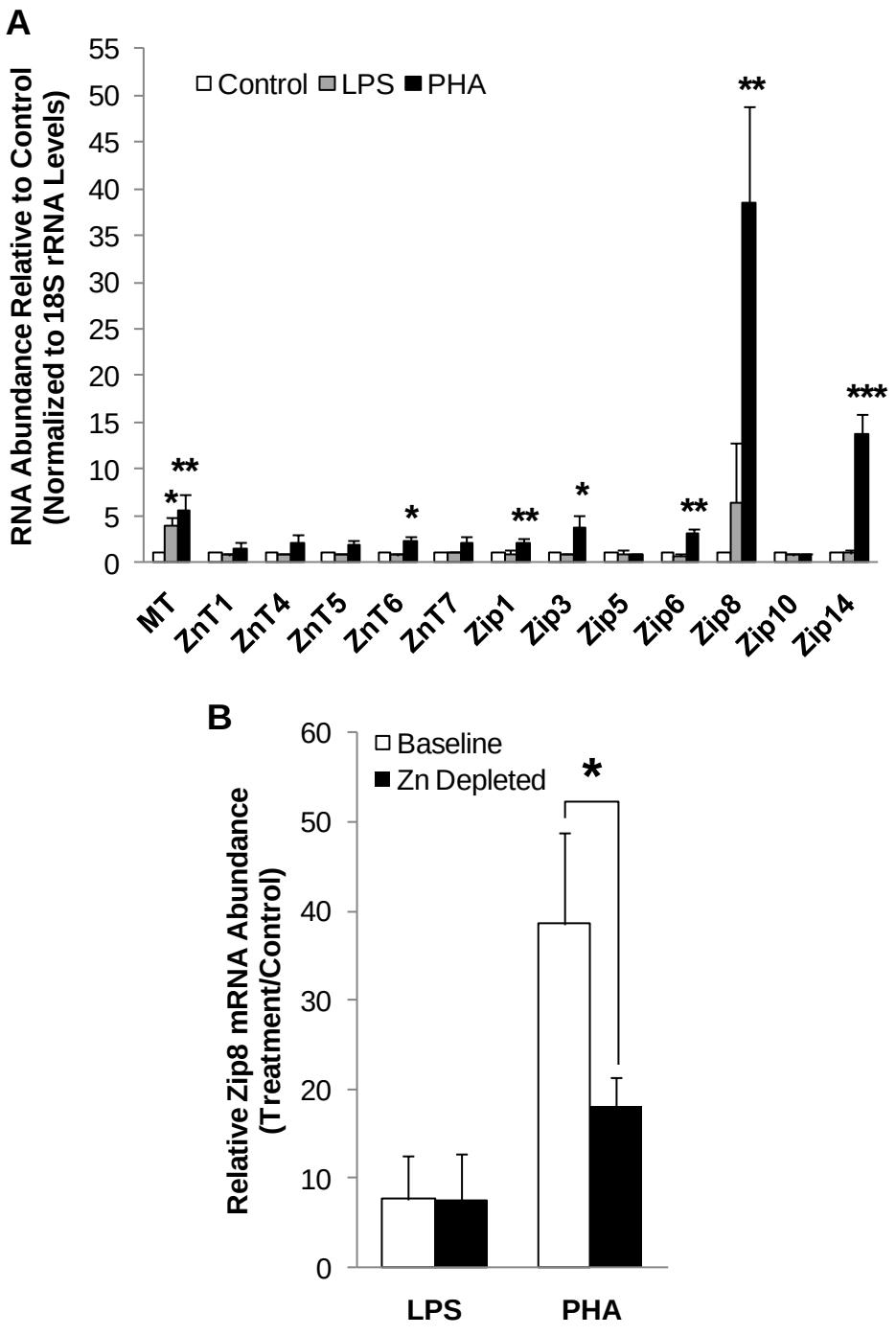


Figure 4-6. Effects of immunostimulation on zinc-related gene transcripts in whole blood. (A) Responsiveness of whole blood MT and zinc transporter transcripts to LPS- or PHA-induced activation. Values were normalized to 18S rRNA levels and control levels for each individual were set at 1. (B) Repression in PHA-induced Zip8 transcript levels by acute dietary zinc depletion. Data are expressed as mean ± SD. Values significantly different to respective baseline levels are *, $P < 0.05$; **, $P < 0.01$; ***, $P < 0.001$ (n = 3 subjects).

# CHAPTER 5
# SERUM MICRORNA AS BIOMARKERS OF DIETARY ZINC STATUS

## Introductory Remarks

The recent discovery of microRNA (miRNA) has introduced a promoter-independent regulatory mechanism of gene expression. Target transcripts of these small non-protein-conding RNA are determined by conserved sequences present in the 3'-untranslated region (3'-UTR) which are complementary to the sequence of the functioning miRNA (131). The biogenesis of functional miRNA from their gene transcript (primary miRNA; pri-miRNA) requires two major steps of processing each mediated by the Microprocessor (Drosha-DGCR8 complex) and Dicer which generate and trim precursor-miRNA (pre-miRNA), respectively (132, 133). The single-stranded mature form of miRNA incorporates into the RNA-induced silencing complex (RISC) via Argonaute (Ago) proteins and binds to its recognition site at the targeted transcript. Inhibition of gene expression occurs by the induction of gene transcript decay through deadenylation pathways and translational repression by obstructing the initiation and elongation of peptide synthesis (131).

Serum microRNA (miRNA) profiles have been shown to reflect the developmental and metastatic stage of various cancer types (134), and thus have become an emerging target for cancer biomarker research. The use of serum miRNA as a diagnostic tool has been supported by its high stability and low variability among individuals in a healthy state (135-137). The highly stable nature of miRNA in serum, which contains a substantial amount of RNase activity, is maintained by its presence in cell-derived exosomes (138, 139). Even though the complete physiological role of circulating miRNA is yet to be known, its function as a mediator of intercellular communication has

been suggested (139). Serum miRNAs are secreted from cells via an energy-dependent export mechanism (140) and their sources are not limited to blood cells (136, 137). In other words, the profile of circulating miRNAs reflects the effect of clinical conditions on the miRNA profile of various tissues, which enables the detection of cancers also unrelated to the hematological system.

Thus, characterization of serum miRNA would be a feasible approach for biomarker discovery in not only cancer research but also the nutrition field. We hypothesized that miRNA levels in serum may be modulated by dietary zinc depletion and thus hold the potential of being a diagnostic tool for zinc deficiency. As the first attempt to comprehensively assess the zinc effect on miRNA in human, our data introduce miRNAs likely to mediate post-transcriptional regulation of genes under dietary zinc deprivation.

## Results

Major advantages of using serum miRNA include its resistance against *ex vivo* temperature fluctuation and its low inter-individual variability (135-137). By using a standardized protocol for the isolation of total RNA from serum and a qPCR-based tool for miRNA detection (87), we implemented the concept developed by cancer biomarker research to the field of nutrient status assessment. Due to the relatively short history of research related to serum miRNA, there is no known endogenous housekeeping transcript that can serve as a means of normalization. Thus, equal amount of synthetic cel-miR-39 was added into the samples prior to the RNA isolation process. Ct values acquired by the amplification of this exogenous control validate the experimental protocol by indicating consistent yield of serum RNA recovery (Figure 5-1).

To identify the miRNA circulating in serum that can serve as a biomarker of zinc deficiency, total RNA from pooled sera collected before and after dietary zinc depletion was assessed by using a qPCR array focused on those identified to be present in human serum. Among the serum miRNAs measured, total of twenty were shown to respond to the dietary zinc depletion regimen by fold-changes above 1.5 and with Ct values below 35 (Figure 5-2A). It is of note that the majority of differentially regulated miRNA showed a trend of decreased abundance in their response to acute dietary zinc depletion (Figure 5-2B). Further analysis with sera collected after zinc repletion was conducted to determine if the effects of zinc deprivation can be reversed by dietary zinc replenishment. Consequently, we identified nine miRNA (miR-10b, miR-155, miR-200b, miR-296-5p, miR-375, miR-92a, miR-145, miR-204, miR-211) responding to dietary zinc deprivation and supplementation in opposite modes (Figure 5-3).

## Discussion

In 2005, the estimated number of miRNAs in human genome was approximately 800 (141). Currently, there are 1,424 human miRNAs deposited in the miRBase database (release 17) (142) which indicates the contribution of this small miRNA family to the regulation of gene expression to be greater than that expected at the initial stage of discovery. More than 45,000 target sites are conserved within 3'-UTRs of human gene products, and above 60% of protein-coding transcripts are estimated to be under the regulation by miRNAs (143). Understanding of the role of miRNA in the regulation of genes related to nutrient metabolism is fairly limited (144-146). To date, published experimental evidence of the effects of zinc on miRNA expression is nonexistant, and relevant information was identified only through conference reports and as a part of a book chapter, noted as unpublished data. The enhanced miR-34a, miR-1274a, miR-

140 and miR-1949 expression in the small intestine of zinc-deficient mice identified by microarray analysis is of most relevance (147). The presence of two zinc-responsive miRNA involved in the regulation of Zip5 by supplemental zinc has also been described, however, without details (148). Dietary zinc deprivation has been shown to cause up-regulation of miR-31 and miR-183, and down-regulation of miR-183 in precancerous esophagus of rats (99). Modulation in the miRNA profile was suggested by the authors as an underlying mechanism by which zinc exerts its anti-tumorigenic property. Based on our knowledge, the evaluation of serum miRNA profiles during differential dietary zinc intakes conducted by the current study is the first attempt to identify the effects of zinc on miRNA metabolism in humans.

The transcriptional machinery of microRNA gene expression, generally mediated by RNA polymerase II, shares its regulatory components with that of protein-coding transcripts (132). A recent computational analysis of the regulatory elements at the promoter region of miRNA genes identified putative transcription factors involved in the regulation of miRNA gene expression (112). The zinc-sensing transcription factor, MTF-1, was predicted as one of the five master-regulators of human pre-miRNA expression. It is of note that two other predicted master-regulators, NF-Y and AP-2α, were identified as putative transcription factors eliciting the effects of dietary zinc depletion on gene expression by the microarray dataset of the current study. These findings suggest the possible regulatory role of zinc in multiple miRNA gene expression via modulated transcription factor activity.

As an approach to identify the miRNA responsive to zinc, we utilized a commercially developed PCR array platform focused on miRNA known to be present in

serum. Due to the activity of serum miRNA research in the cancer field, most of the miRNAs assessed have been identified as regulators of oncogenes or tumor suppressors (149, 150). The normal biological role of circulating miRNA remains unclear. However, its energy-dependent export by tissues and stable form in the blood circulation suggest its potential to function as an inter-cellular or -organ messenger (138-140). Delivery of miRNA, eliciting protumorigenic effects, secreted from cancerous tissues to healthy tissues may partially contribute to the metastasis of cancer. Conversely, miRNA with antitumoigenic effects may mediate the defense mechanism against carcinogenesis. Among the miRNA screened, miR-204 and miR-296-5p showed the highest responsiveness of down-regulation to dietary zinc depletion. It is of note that both of these miRNA have been recently characterized to hold suppressing effects on oncogene expression. The adhesion, migration and invasion of squamous cell carcinoma of the head and neck were reduced by restoration of miR-204 *in vitro* (151). Ectopic expression of miR-296 resulted in the repression of an oncogene, high-motility group AT-hook gene 1, in various types of prostate cancer cells, and suppressed cell proliferation and invasion were observed as consequences of miR-296 activity (152). These findings suggest the therapeutic properties of these zinc-responsive miRNA on tumor progression, and imply their involvement in the mechanism of the predisposition to cancer by zinc deficiency.

The tissues producing the modulated serum miRNA profile by zinc deficiency were not identified by the current study, and thus the effect of zinc on tissue miRNA expression needs to be further explored. As identified by TargetScan (Table 5-1), several zinc-related genes are potential targets of the differentially expressed serum

miRNA.  Thus, the zinc-responsive serum miRNA provided here may function as candidate miRNAs for future studies focusing on the role of miRNAs in the regulation of biological events affected by the levels of dietary zinc intake.

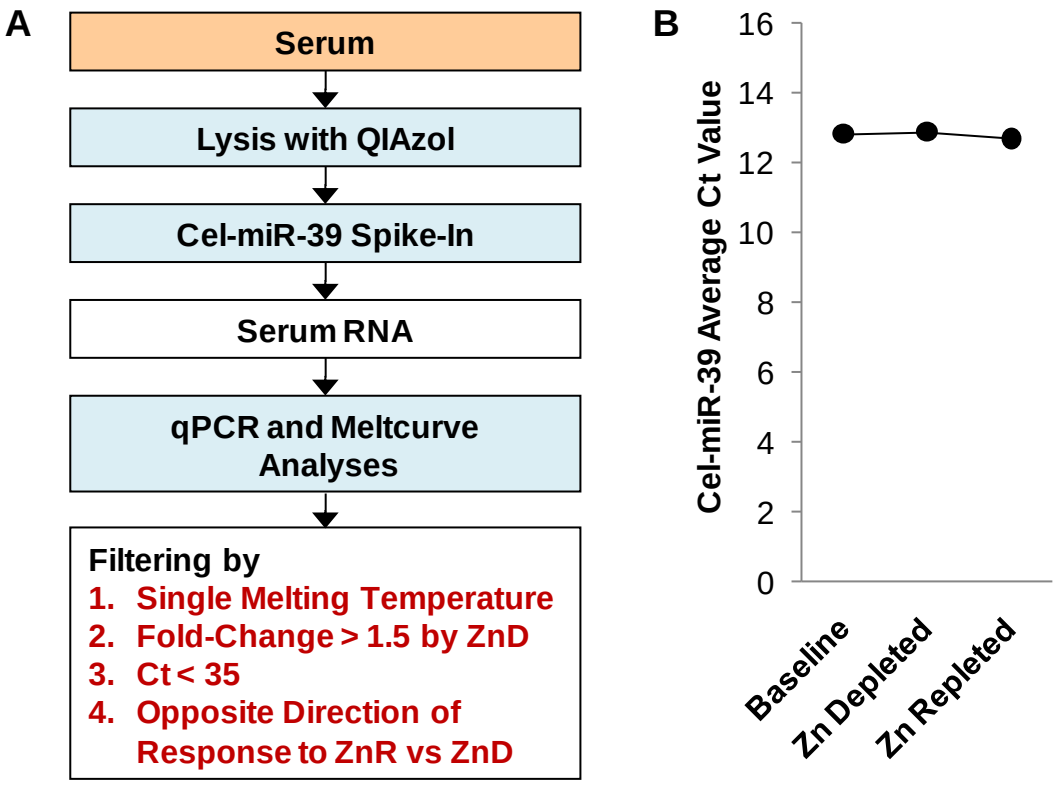


Figure 5-1. Serum processing for miRNA isolation. (A) Schematic workflow of serum RNA isolation and data analysis. (B) Yield of cel-miR-39 spiked into serum prior to RNA isolation. Synthetic Caenorhabditis elegans miR-39 was incorporated into serum samples prior to RNA isolation and served as a normalization means during the downstream quantitative analyses. Data of sera from subjects at day 7, day 17 and day 24 are shown.

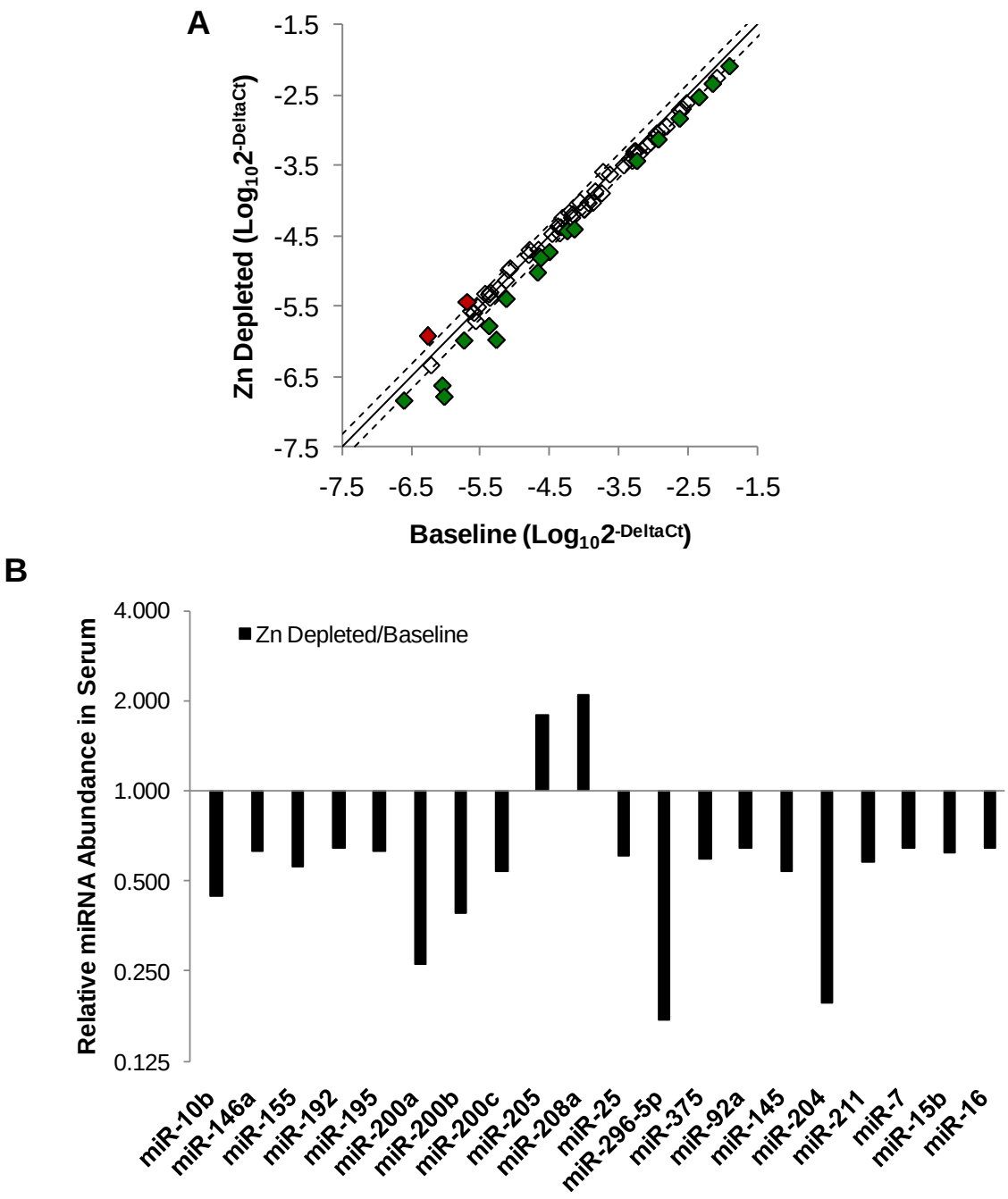


Figure 5-2. Identification of serum miRNAs responsive to acute dietary zinc depletion using a qPCR-based array. Circulating miRNA were isolated from pooled sera collected on baseline (day 7) and post-depletion phase (day 17), and were quantified by using a qPCR array focused on miRNA known to be present in human serum. (A) A scatter plot indicating the miRNA of which levels were modulated by fold-changes above 1.5 under dietary zinc restriction. Red, up-regulated; green, down-regulated. (B) Relative abundance of serum miRNAs affected by dietary zinc depletion. Values were normalized to cel-miR-39 levels.

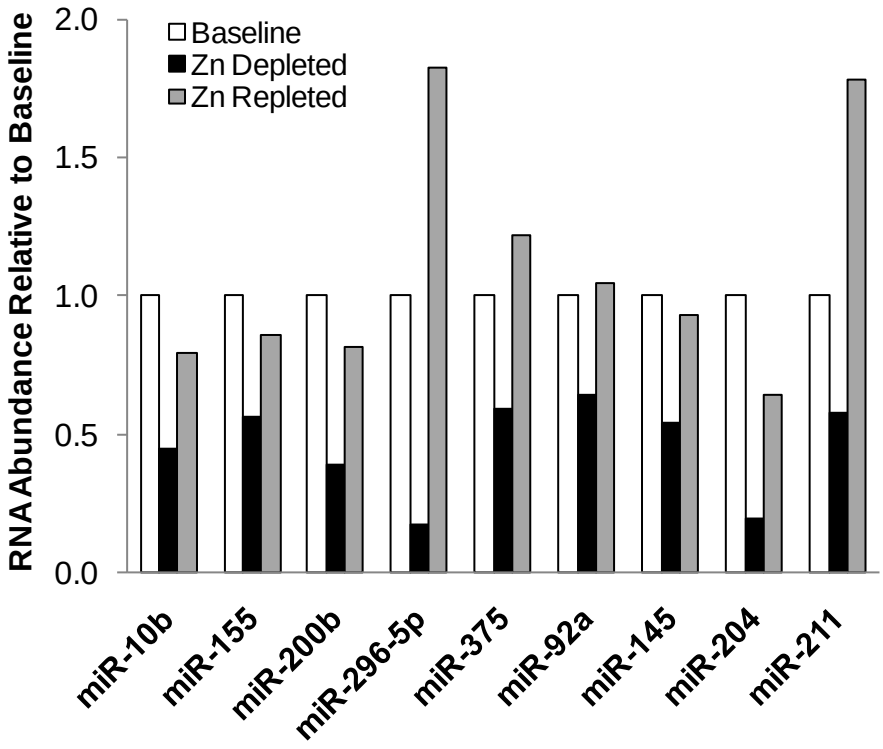


Figure 5-3. Effects of dietary zinc intake levels on circulating serum miRNA levels. Serum miRNA responding to zinc restriction and repletion in opposite directions were selected as candidate biomarkers reflecting dietary zinc intake levels. Values were normalized to cel-miR-39 levels and baseline levels were set at 1.

Table 5-1. Zinc-related genes targeted by the zinc-responsive serum miRNA[1]

| Representative miRNA | Target gene | Conserved sites | | | | Poorly conserved sites | | | | Total Context Score | Aggregate $P_{CT}$ [2] |
|---|---|---|---|---|---|---|---|---|---|---|---|
| | | total | 8mer | 7mer-m8 | 7mer-1A | total | 8mer | 7mer-m8 | 7mer-1A | | |
| hsa-miR-10b | MTF1 | 1 | 0 | 0 | 1 | 1 | 0 | 1 | 0 | -0.19 | 0.41 |
| hsa-miR-92a | MTF1 | 2 | 1 | 0 | 1 | 1 | 0 | 0 | 1 | -0.31 | >0.99 |
| hsa-miR-145 | MTF1 | 1 | 0 | 1 | 0 | 1 | 0 | 0 | 1 | -0.35 | 0.69 |
| hsa-miR-375 | KLF4 | 1 | 0 | 0 | 1 | 0 | 0 | 0 | 0 | -0.13 | 0.38 |
| hsa-miR-145 | KLF4 | 1 | 0 | 0 | 1 | 0 | 0 | 0 | 0 | -0.09 | 0.61 |
| hsa-miR-296-5p | SLC30A3 | 1 | 0 | 1 | 0 | 1 | 0 | 1 | 0 | -0.27 | N/A |
| hsa-miR-155 | SLC39A10 | 1 | 1 | 0 | 0 | 0 | 0 | 0 | 0 | -0.25 | <0.10 |
| hsa-miR-200b | SLC39A14 | 1 | 0 | 1 | 0 | 0 | 0 | 0 | 0 | -0.29 | 0.70 |

[1] Predicted by TargetScan release 5.1.
[2] $P_{CT}$, the probability of conserved targeting.

# CHAPTER 6
# ERYTHROCYTE MEMBRANE ZINC TRANSPORTERS AND DEMATIN LEVELS IN HUMANS UNDER SHORT-TERM DIETARY ZINC RESTRICTION

## Introductory Remarks

The homeostatic regulation of zinc is crucial during the maturation of erythroid progenitor cells. More than 90% of erythrocyte zinc functions as a component essential for the activity of zinc metalloenzymes, such as carbonic anhydrase and Cu/Zn-superoxide dismutase (153). Master transcription factors involved in the erythropoietin (EPO)-induced gene expression include zinc-finger transcription factors GATA-1 and erythroid Krüppel-like factor (EKLF) (154, 155). Zinc is also important for the maintenance of the membrane integrity of erythrocytes, as indicated by higher osmotic fragility of red cells from zinc-deficient animals (156). However, an excess in cellular zinc at the terminal phase of erythropoiesis can be detrimental due to its interference with iron molecules during hemoglobin biosynthesis (93, 94).

Differential expression of metallothionein (MT) and zinc transporters have been identified as regulatory mechanisms of cellular zinc homeostasis (8, 9). Reduction in red cell MT protein levels by acute dietary zinc depletion has been previously shown (42, 43). Recently, we have identified the presence of zinc transporters ZnT1, Zip8 and Zip10 in the plasma membrane fraction of mouse erythrocytes (14). Temporal expression patterns of these transporter genes indicated higher zinc import and export during the early and late stage of terminal erythroid differentiation, respectively. The zinc transporter system was shown to be influenced by the host's zinc status in mice. After the mice were fed a zinc-deficient diet for three weeks, an increase in Zip10 and a decrease in ZnT1 protein levels occurred in the erythrocyte membrane. Additionally, higher $^{65}$Zn uptake was observed in erythrocytes collected from zinc-restricted animals.

This study was conducted to determine if the erythroid ZnT1, Zip8 and Zip10 expression is present in humans, and to assess their potential of being a status assessment tool of human dietary zinc deficiency. Additionally, levels of a protein recognized non-specifically by the Zip8 antibody in the plasma membrane were identified as zinc-responsive, indicating its potential as a zinc biomarker.

## Results

### Erythrocyte Zinc Transporter Expression during Low Zinc Intake

Western analyses by using in-house designed antibodies against human ZnT1, Zip8 and Zip10 successfully produced positive signals from erythrocyte samples (Figure 6-1), confirming the screening results from the previous animal experiments (14). Specificity of signals was determined by preabsorption controls, indicating the estimated molecular weight of human ZnT1, Zip8 and Zip10 in erythrocytes to be 130~150 kDa, 150 kDa and 40 kDa, respectively. The prominent band at 50 kDa produced by the Zip8 antibody did not disappear by peptide competition, and thus was considered non-specific. A shift in the migration of ZnT1 by PNGase-F treatment indicates the glycosylation of this transporter in human erythrocyte. In contrast to our findings from the mouse experiments, there were no significant changes in the zinc transporters by dietary zinc depletion (Figure 6-2). However, signal intensities from the non-specific band produced by the Zip8 antibody were significantly higher in the membrane fraction of erythrocytes collected after the depletion phase.

### Identification of Dematin as a Zinc-Responsive Erythrocyte Membrane Protein

The zinc-responsive protein non-specifically detected by the human Zip8 antibody was further characterized by proteomic approaches including immunoprecipitation and mass spectrometry. After enriching the protein of interest by immunoprecipitation with

the human Zip8 antibody, protein samples were subject to SDS-PAGE and subsequent gel staining or western analysis. Due to its molecular weight at approximately 50 kDa based on the known size of IgG heavy chain (55 kDa), it was of importance to confirm the separation between these two proteins which were highly abundant in the immunoprecipitated samples prior to band excision for protein identification (Figure 6-3A). Western analysis using the secondary antibody against rabbit IgG identified three bands originating from the Zip8 antibody used for immunoprecipitation, of which two representing heavy chains (40 and 55 kDa) and another identifying the light chain (25 kDa). Reprobing the membrane with the Zip8 antibody and its respective secondary antibody enabled the discrimination of the signal produced by the protein of interest (50 kDa) from that originating from the heavy chain of IgG. By matching with the western blot based on molecular weight markers, the region corresponding to the size of the non-specific band was excised from the stained gel for protein identification by liquid chromatography-mass spectrometry (Figure 6-3B).

The protein profile identified from the mass spectrum of the digested sample was composed of eleven proteins (Figure 6-4A). Among these, the long isoform of dematin was detected with the highest normalized spectrum counts. The predicted molecular weight of 46 kDa was closest to that of the non-specific band size detected by western analysis using the Zip8 antibody (50 kDa). A spectrum representative of those exclusively corresponding to the amino acid sequence of dematin is presented in Figure 6-4B. Approximately 20% of the complete amino acid sequence of dematin was covered by seven associated tryptic peptides identified by the mass spectrum (Figure 6-4C). This coverage rate was highest among all proteins detected, suggesting the

nature of the unknown protein producing non-specific band by Zip8 antibody to be dematin.

The protein identity determined by mass spectrometry and the presence of dematin in the membrane fraction of human erythrocyte was validated by western analysis of samples immunoprecipitated with an antibody designed to target dematin. A strong signal corresponding to a molecular weight of 50 kDa was produced by probing the immunoprecipitated samples by the human Zip8 antibody (Figure 6-5A). Western analyses of samples from blood collected before and after dietary zinc depletion confirmed the zinc-responsiveness of membrane dematin levels in human erythrocytes (Figure 6-5B). A significant increase with a fold-change of 2 was observed by low zinc ingestion. The estimated molecular weight and the magnitude of response determined by the dematin antibody were comparable to those detected by the non-specific signals from the human Zip8 antibody. No change in the Zip8 levels by the dietary treatment confirms the observation shown in Figure 6-2.

## Discussion

The presence of ZnT1, Zip8 and Zip10 in the plasma membrane of mouse erythrocytes was previously identified by using a battery of in-house made antibodies targeting zinc transporters (14). Differential expression of these transporter genes during terminal erythroid differentiation was shown by using a primary cell model inducible by EPO treatment *in vitro* (14). Up-regulation of the importers, Zip8 and Zip10, preceded the induction of ZnT1 by EPO. These findings implicate the involvement of zinc transporter activity in the development of optimal zinc balance required for the transactivation of genes by zinc-finger transcription factors (154, 155) and hemoglobin synthesis during the differentiation process (93, 94). The results from the current study

confirm the expression of these transporter proteins in the plasma membrane of human red cells.

The enhancement in erythrocyte zinc uptake by low dietary levels of zinc has been identified in animal models (14, 157-159). However, the underlying molecular mechanism remains unclear. The down-regulation of ZnT1 and the up-regulation of Zip10 observed in erythrocytes of zinc-deficient mice (14) suggest these transporters as factors exerting this effect of zinc deficiency. It is of note that MTF-1 has been shown to mediate the zinc-responsive transcription of both ZnT1 and Zip10, however, towards the opposite mode of response (4-6). Upon zinc-sensing, nuclear translocation of MTF-1 and its binding to the MRE motif occurs for the activation and repression of ZnT1 and Zip10, respectively. The recently discovered mechanism for Zip10 repression by MTF-1 involves its binding to an MRE downstream from the transcription start site, resulting in the inhibition of the movement of RNA polymerase II (6). Based on these, we postulated that the differential expression of ZnT1 and Zip10 observed in mouse erythrocytes is meditated by the zinc-dependent activation of MTF-1 during their gene expression at the terminal stage of erythropoiesis.

Even though the observations from the mouse model agree with the mode of MTF-1-meditated regulation of ZnT1 and Zip10 by zinc, there were no changes in the zinc transporter proteins of human erythrocytes by acute dietary zinc depletion. During the differentiation of erythroid progenitors to reticulocytes, enucleation occurs, and thus the capability of these cells to carry out gene regulation is lost. Thus, the erythrocyte proteome is dependent on that formed during the preceding differentiation stage. The estimated life-span of human erythrocytes and mouse red cells are 120 d and 40 d,

respectively (160). The dietary zinc regimen of the current human study for zinc depletion was limited to 10 d, which covers less than 10% of the life-span of circulating erythrocytes. Thus, a substantial portion of circulating erythrocytes collected after the zinc depletion phase would be those formed under adequate zinc conditions. The length of the zinc depletion period in mice approximated 50% of the life-span of their red cells (14), consequently a higher portion of erythrocytes in the bloodstream are produced during zinc deprivation. Additionally, as indicated by changes in plasma/serum zinc levels observed in the mouse and human subjects (approximately 60% vs. 20% reduction), the severity of zinc deficiency induced by the 21-d dietary zinc deprivation in mice was greater than that produced by the 10-d dietary regimen applied to the human subjects. This indicates the murine model of zinc deficiency is close to moderate or severe deficiency, while the human model used represents conditions of short-term modest dietary zinc deprivation. Consequently, the potential of erythrocyte ZnT1 and Zip10 levels for the diagnosis of chronic dietary zinc deficiency in human needs to be further investigated.

Among the zinc transporters of which proteins were detected in the plasma membrane of red cells, only ZnT1 transcripts were identified to reflect the host's zinc intake levels in reticulocytes. Reticulocyte transcript levels reflect a gene expression profile at the very late stage of erythropoiesis. Induction of Zip10 expression by EPO was only observed at the early stage of terminal erythroid differentiation in mice (14). In contrast, repression of ZnT1 transcripts by zinc chelation was present at a later stage of the 24-h differentiation period (14). These results indicate the effect of zinc on Zip10 transcription in human erythroid progenitor cells may be limited to the early phase of

EPO-induced terminal differentiation as reflected by the absence of differences between the baseline and post-depletion levels of Zip10 mRNA in reticulocytes.

Dematin, a protein initially identified as protein 4.9 in the membrane of human red cells (161), functions as an actin-bundling protein located at the junctional complex, i.e., spectrin-actin junction, of the erythrocyte membrane skeleton (162). Along with other core constituents of the membrane skeleton such as spectrin, actin, adducin and protein 4.1 (163, 164), dematin has been shown to be essential for the maintenance of the cellular morphology, motility and membrane structural integrity (165, 166). In the current study, the level of erythrocyte dematin in the plasma membrane was shown to be highly sensitive to the host's zinc status. Its rapid response implicates the presence of a posttranslational regulatory mechanism mediating the effects of zinc on this protein. Two protein kinases, cyclic adenosine monophosphate-dependent protein kinase (PKA) and protein kinase C (PKC), are involved in the regulation of the actin cytoskeleton, and both have been shown to phosphorylate dematin *in vitro* (167). In particular, phosphorylation by PKA, of which activity in red cells is evident (168), exerts an inhibitory effect on the actin-bundling activity of dematin by causing a conformational change in the headpiece domain (167, 169-171). Zinc has been shown to predominantly inhibit the hydrolysis of cyclic adenosine monophosphate (cAMP) and cyclic guanosine monophosphate (cGMP) by phosphodiesterase (PDE) acitivity *in vitro* (172). Additionally, this inhibitory effect on PDE activity has been recently suggested as an indirect mechanism for zinc to enhance PKA activity in immune cells (129). Conversely, suboptimal zinc conditions may result in lower PKA activity, and thus lead to less phosphorylation of dematin. The inhibitory effect of phosphorylation on the actin-

binding of dematin can be reversed by phosphatase treatment (167). The capability of zinc to inhibit phosphatase activities has been identified in various signaling pathways (51, 125-127). Taken these together with the observations of the present study, dietary zinc depletion may increase the translocation of cytosolic dematin to the plasma membrane by disrupting the balance between PKA and phosphatase activities.

Phosphorylation of the component proteins associated with the junctional complex by modulated PKC activity can also lead to the formation of an instable membrane skeleton (173). However, the phosphorylation of dematin by PKC has been shown to have no effects on its actin-bundling activity (167). It is of note that cytosolic translocation of membrane adducin, which is another actin-binding protein anchoring the junctional complex to the plasma membrane, by PKC activity resulted in the redistribution of another membrane PKC-independent skeletal protein, spectrin, to the cytoplasm (174). Thus, impaired PKC activity can also lead to the internalization of membrane dematin in an indirect manner. In contrast to PKA, PKC can be directly regulated by zinc (128). Upon binding to its metal-binding site, zinc increases the activity of PKC and also induces the translocation of cytosolic PKC to the plasma membrane. This mode of regulation agrees with the present observation of decreased membrane levels of a cytoskeletal protein under a zinc-depleted condition, and thus suggests PKC as another possible mediator of the effects of dietary zinc depletion on membrane dematin levels.

Impaired cellular membrane stability and increased osmotic fragility have been identified in red cells of zinc-deficient animals (156). Whether excess of dematin in the membrane complex produces beneficial or detrimental effects to the structural integrity

of normal erythrocytes is unclear. Overexpression of dematin has been shown to alter the cellular phenotype of prostate cancer cells towards that of normal prostate epithelial cells (175). It is of note that, respective overexpression of the core and headpiece domain of dematin also caused phenotypic changes such as cytoplasmic shrinkage, extensive filopodial extensions, and inlamellopodial extensions of the cancer cells. Thus, the increase in membrane dematin levels may contribute to the effect of zinc deficiency on red cell integrity, particularly, by causing a dysfunctional assembly of the actin-based erythrocyte cytoskeleton.

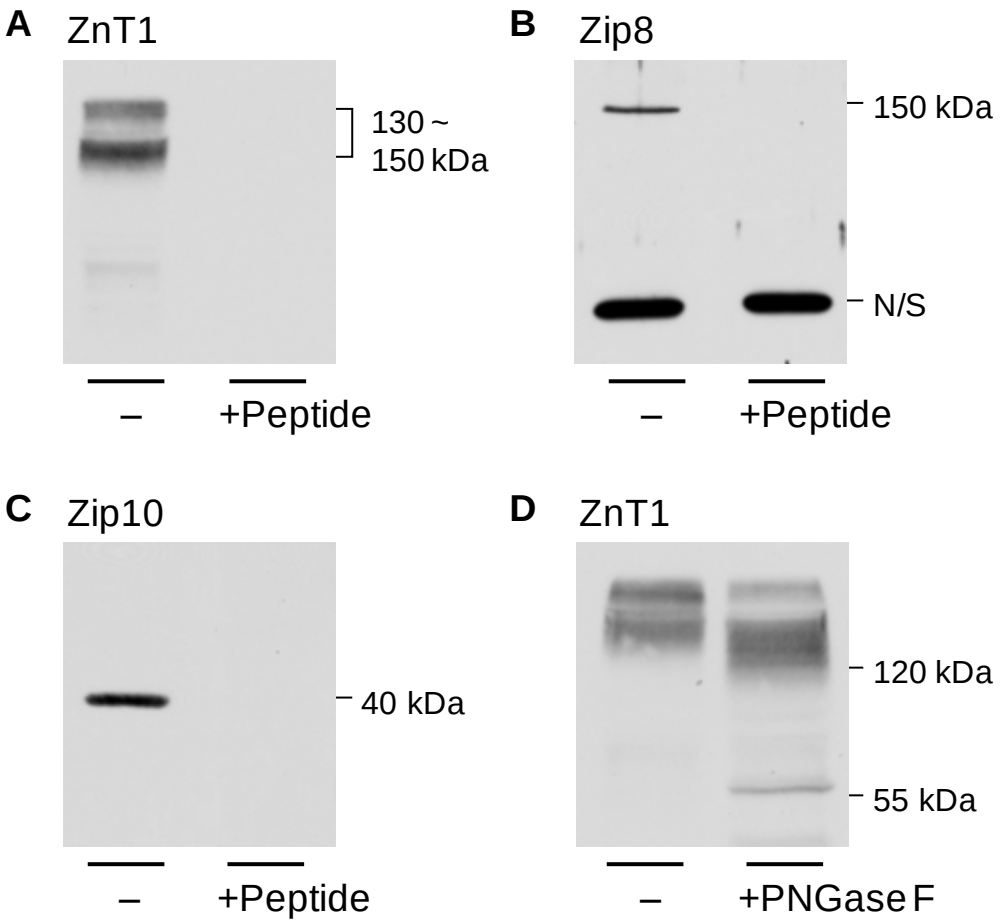


Figure 6-1. Zinc Transporter Expression in Human Erythrocyte Membrane. The presence of (A) ZnT1, (B) ZIP8 and (C) ZIP10 in erythrocyte ghosts was detected by western analysis. Specificity of signals was determined by preincubating each primary antibody with respective antigenic peptides. (D) Glycosylation of ZnT1 was identified by PNGase-F treatment.

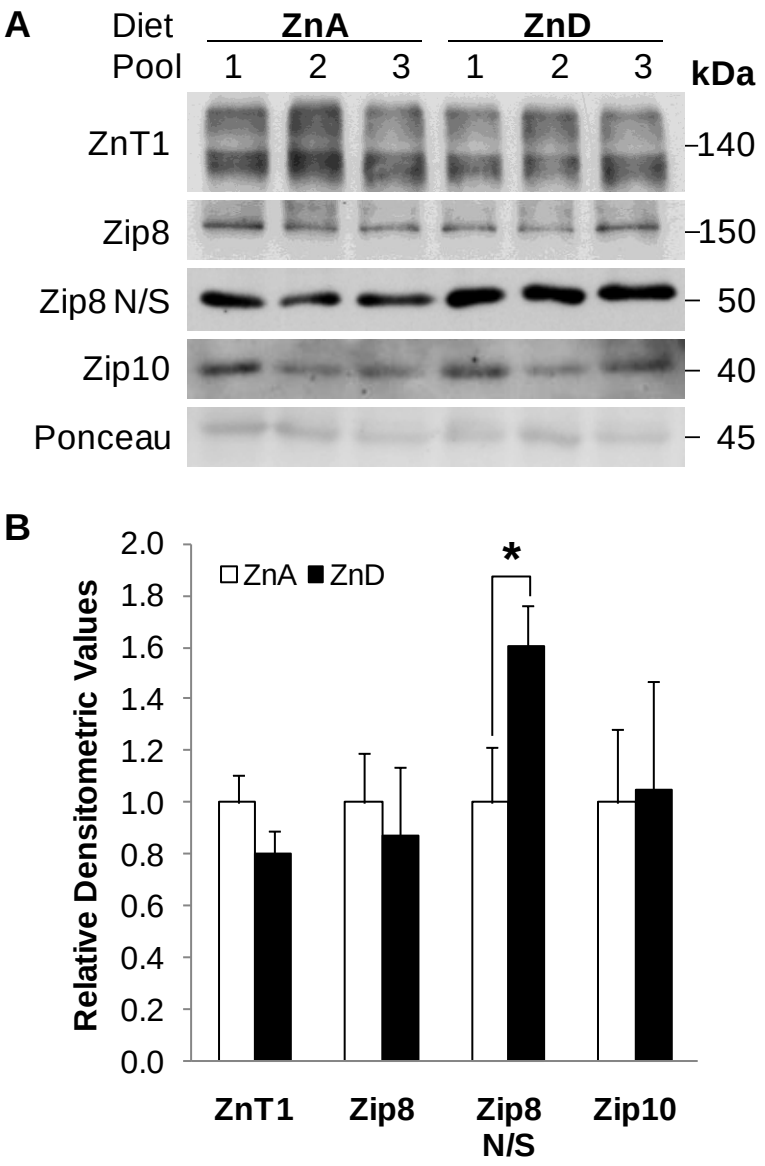


Figure 6-2. Effects of acute dietary zinc depletion on zinc transporter expression in human erythrocytes. (A) The expression of each transporter was identified by western analysis with respective antibodies. N/S indicates the non-specific band that is zinc-responsive and is detected with the Zip8 antibody. (B) Signal intensities quantified by densitometric analysis. Data are expressed as mean ± SD and statistically significant differences are *, $P < 0.05$ (n = 3 subjects in each pooled sample).

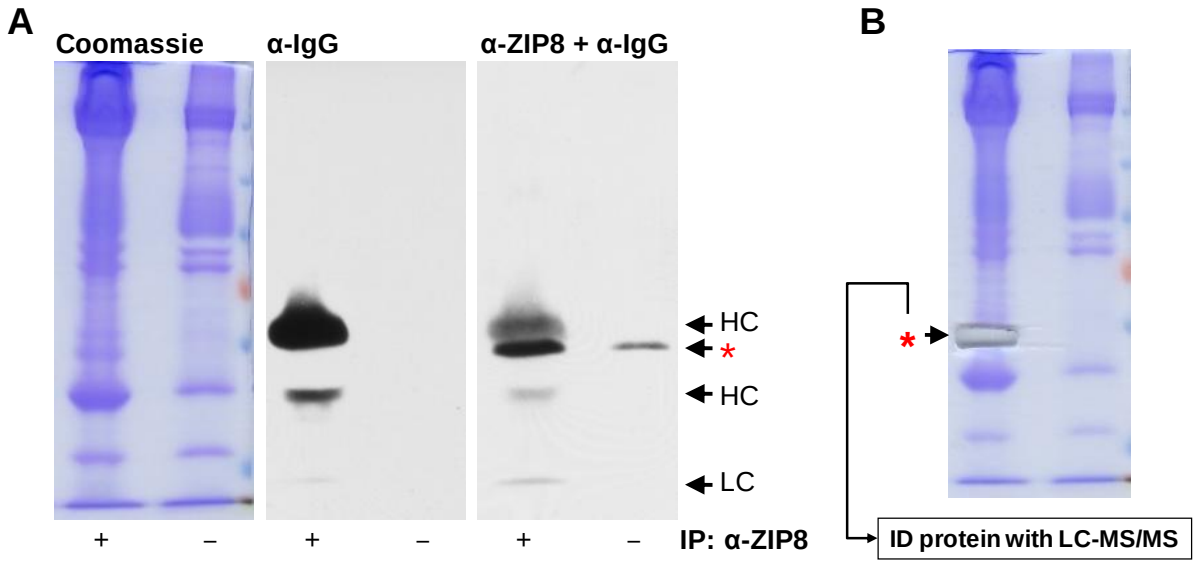


Figure 6-3. Isolation of the peptide producing a non-specific band with the Zip8 antibody by immunoprecipitation. (A) Staining and labeling of immunoprecipitated erythrocyte membrane proteins by using Coomassie Blue and respective antibodies. HC and LC indicate heavy chain and light chain, respectively. Position of the non-specific band is annotated by a red asterisk. (B) Excision of the region migrating at the size of the non-specific protein for mass spectrometry analysis.

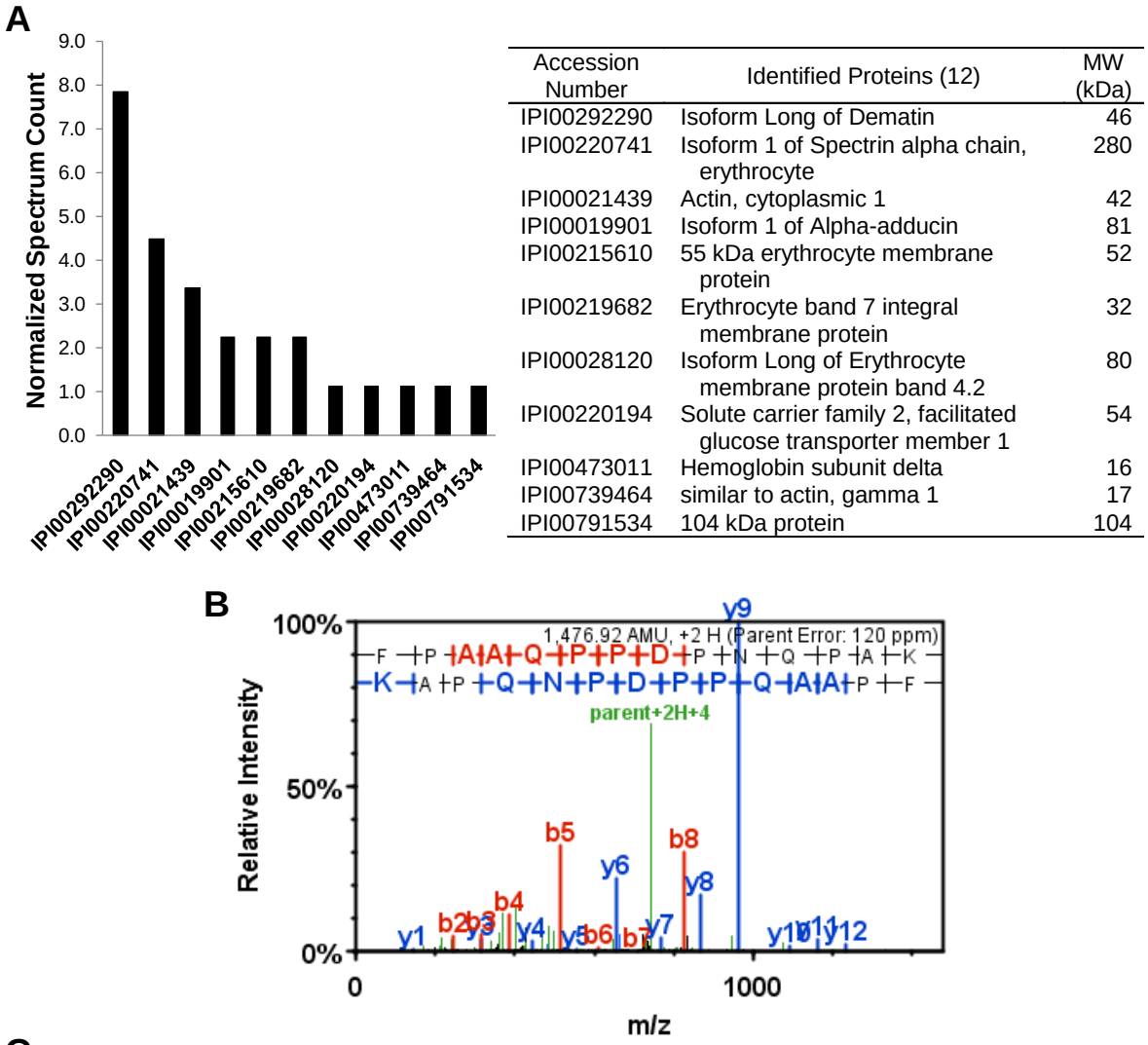


Figure 6-4. Identification of the protein non-specifically detected by the hZip8 antibody. Protein samples were trypsinized and were subject to liquid chromatography coupled with tandem mass spectrometry (LC-MS/MS). (A) Dematin, with an expected molecular weight (MW) of 46 kDa, showing the highest normalized spectrum count among the twelve identified proteins. (B) Representative mass spectrum of dematin. (C) Identified peptide sequences unique for dematin by LC-MS/MS.

| Accession Number | Identified Proteins (12) | MW (kDa) |
|---|---|---|
| IPI00292290 | Isoform Long of Dematin | 46 |
| IPI00220741 | Isoform 1 of Spectrin alpha chain, erythrocyte | 280 |
| IPI00021439 | Actin, cytoplasmic 1 | 42 |
| IPI00019901 | Isoform 1 of Alpha-adducin | 81 |
| IPI00215610 | 55 kDa erythrocyte membrane protein | 52 |
| IPI00219682 | Erythrocyte band 7 integral membrane protein | 32 |
| IPI00028120 | Isoform Long of Erythrocyte membrane protein band 4.2 | 80 |
| IPI00220194 | Solute carrier family 2, facilitated glucose transporter member 1 | 54 |
| IPI00473011 | Hemoglobin subunit delta | 16 |
| IPI00739464 | similar to actin, gamma 1 | 17 |
| IPI00791534 | 104 kDa protein | 104 |

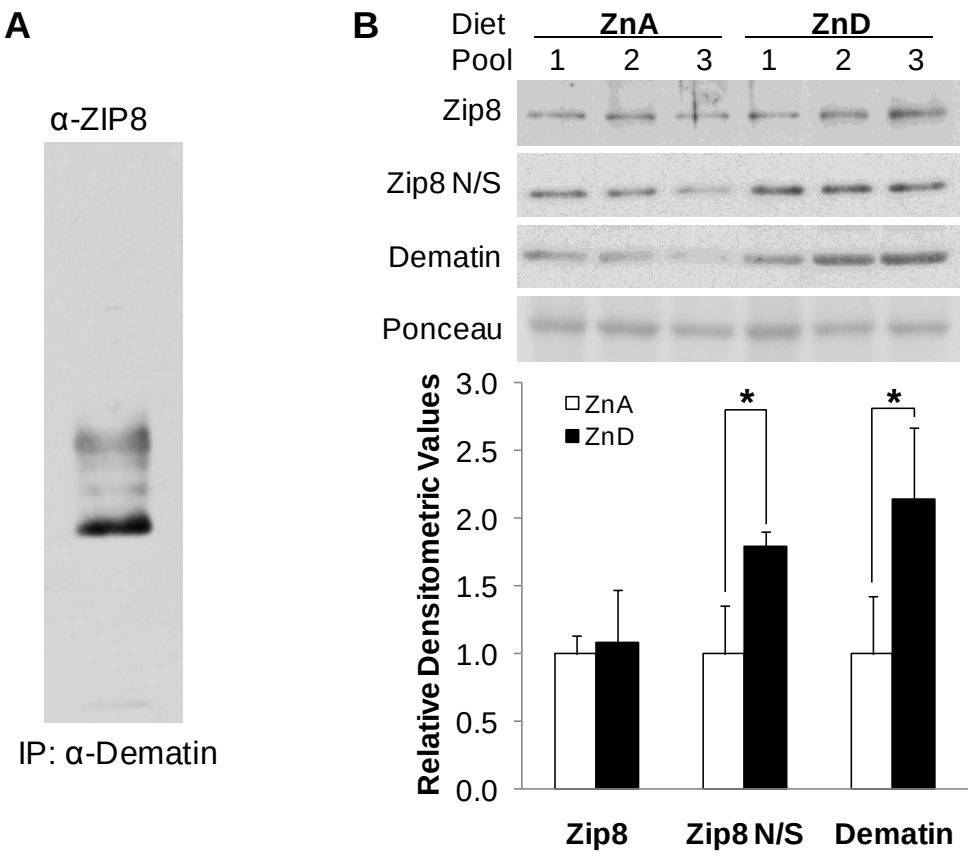


Figure 6-5. Confirmation of protein identity determined by mass spectrometry analysis. (A) Western analysis with a rabbit anti-Zip8 polyclonal antibody of erythrocyte membrane proteins immunoprecipitated by a mouse polyclonal anti-dematin antibody. (B) Responsiveness of erythrocyte membrane dematin to acute dietary zinc depletion. Signal intensities quantified by densitometric analysis. Data are expressed as mean ± SD and statistically significant differences are *, $P < 0.05$ (n = 3 subjects in each pooled sample).

# CHAPTER 7
# CONCLUSIONS AND FUTURE DIRECTIONS

The presence of a reliable biomarker is a prerequisite for employing a preventive or prognositic policy on a population suffering from clinical outcomes associated with malnutrition. Identification of a specific and sensitive assessment tool for individuals with zinc deficiency has been a long-term goal in zinc research. The current study was conducted primarily to identify biomolecules holding the potential to reflect the host's zinc status in blood and buccal specimens. Given the function of metallothionein and zinc transporters mediating the regulation of cellular zinc homeostasis, the effects of acute dietary zinc depletion on the transcript abundance of these zinc homeostatic genes in blood cells and buccal epithelial mucosa were determined. MT, ZnT1, ZnT4, ZnT5, and Zip3 responded to a short-term zinc depletion regimen in a cell type-specific manner. Based on the significance in changes by zinc depletion and their correlation with serum zinc concentrations, PBMC and whole blood ZnT1 levels were identified as candidate molecules holding potentials of being an assessment tool for dietary zinc status. The well-known regulatory mechanism of ZnT1 by the zinc-sensing transcription factor MTF-1 (4) further validates the findings of the present study.

As a standard approach for identifying gene transcripts responding to modulated metabolic or clinical conditions, microarray analysis with stabilized whole blood was conducted. It is of interest that the gene products responsive to acute dietary zinc depletion were mostly associated to cell cycle regulation and immune response. VEGF, a therapeutic target molecule for cancer treatment, and NFκB, a transcription factor mediating gene expression related to cell proliferation and immune response, were suggested as putative regulatory factors mediating the effects of low zinc ingestion on

the whole blood transcriptome profile. These correspond to previous findings describing the significance of zinc in the maintenance of host defense (95-97) and its protective role against cancer development (98, 99). Among those differentially expressed during zinc depletion, eight well-characterized gene transcripts, IGJ, CDC20, MZB1, IGLL1, TXNDC5, CD38, GLDC and TNFRSF17, were determined as genes highly responsive to dietary zinc restriction. The molecular mechanism exerting the modulation of these genes by zinc restriction, and the specificity of their responsiveness to zinc should be determined by future research.

The functional significance of zinc in pathways mediating immune response was confirmed by the depression of LPS- and PHA-induced TNFα release from whole blood by acute dietary zinc restriction. The mode of TNFα response by the activated whole blood samples to suboptimal zinc ingestion corresponds to 1) the implications of impaired NFκB activity by the down-regulated genes in the microarray dataset of the current study and 2) the enhancement of TNFα gene expression observed in a previous dietary study focused on the effects of zinc supplementation (41). It is of note that a standardized commercial ELISA kit was used for the absolute quantitation of cytokines in order to enable comparisons among data produced by the current study and those from future studies requiring dietary zinc assessment.

Erythrocyte ZnT1 and Zip10 respond to zinc depletion in mice, however, in an opposite manner (14). *In vitro* experiments with mouse erythroid progenitor cells indicate the regulation of these genes to be present during terminal erythroid differentiation. The mode of responses of erythroid ZnT1 and Zip10 to dietary zinc depletion agree with the previous findings of MTF-1-meditated activation of ZnT1 and

repression of Zip10 gene expression under high zinc conditions (4-6). In contrast to the observations in the animal study, no changes in erythrocyte ZnT1 and Zip10 protein levels were identified in humans under dietary zinc restriction. Differences in the length of experimental zinc depletion, life-span of circulation red cells, and the magnitude in reduction of serum zinc concentrations between the human and mouse model indicate the former to represent conditions of acute short-term zinc depletion, while the latter mimics extended dietary zinc deficiency resulting in higher severity. Therefore, detection of the zinc-responsiveness of erythrocyte ZnT1 and Zip10 proteins may be limited to conditions of chronic and severe zinc deficiency. Future human studies with experimental models of long-term dietary zinc restriction or supplementations are required to further confirm this hypothesis.

The erythrocyte membrane level of dematin, a protein functioning as a core component of the cytoskeletal complex, was identified to be responsive to short-term dietary zinc depletion. As described above there were no changes in the levels of ZnT1 and Zip10 proteins in erythrocytes. Both are known to be regulated by zinc at the transcript level (4-6). Taking this into account, the presence of a posttranslational regulatory mechanism exerting the effect of zinc on dematin can be speculated. Involvement of protein kinases and phosphatases in the regulation of the actin-bundling activity of cytoskeletal proteins, including dematin, is of particular relevance (167, 173). It is of note that zinc has been shown to enhance PKA and PKC activity (128, 129) and also inhibit various phosphatases (125-127). Collectively, the observations of higher membrane dematin in red cells under the zinc-restricted condition may be due to a modulation in the phosphorylation status of dematin or other proteins involved in the

assembly of the cykoskelatal complex on the intracellular side of the plasma membrane. Future *in vitro* mechanistic studies focusing on the effects of zinc on 1) the activities of erythrocyte PKA, PKC, and phosphatases, 2) the phosphorylation degree of cytoskeletal proteins, and 3) the cellular distribution of relevant proteins will allow the identification of a novel role of zinc contributing to the morphology, motility and integrity of circulating erythrocytes (156).

Serum miRNA profiles of cancer patients have been extensively characterized in cancer biomarker studies, particularly, due to its highly stable nature *ex vivo* (135-137). Modulation in the profile of serum miRNAs was identified as a consequence of dietary zinc depletion by the current biomarker study. Among the responsive miRNAs, miR-204 and miR-296-5p showed the highest responsiveness to zinc restriction. Reversal effects of supplemental zinc on these miRNA levels further potentiates their property as indicators of the host's dietary zinc status. It is of note that both miR-204 and miR-296-5p have been shown to target genes involved in tumor development and progression (151, 152). The differential responses of circulating miRNAs to dietary zinc levels imply their possible role in the post-transcriptional regulation of protein-coding gene products related to zinc metabolism as well.

Even though several hypothesis-driven *in vitro* and *in vivo* studies have suggested the potential of zinc homeostatic gene products and metalloenzyme activities as zinc biomarkers, their limited practicality for larger sample sizes hinders the implementation of relevant population-based validation studies. Based on an in-depth analysis of the transcriptome of blood cells and serum by using novel molecular techniques enabling sample stabilization and high-throughput analysis, a plethora of biomolecules were

identified as potential diagnostic indices of suboptimal zinc consumption. It is of note that the following aspects were taken into consideration during the experimental design to allow the application of the current findings to future verification studies and, eventually, to the field of nutrient assessment: 1) noninvasiveness of the sampling process, 2) reasonable cost of the implemented technique for quantitative measures (i.e., cost-effectiveness), 3) minimal requirement of skills and laboratory devices for sample processing and analysis, 4) stability of samples or target molecules, particularly, during transportation after the collection or processing, and 5) availability of a standardized protocol covering the processes from sample collection to analytical assessments.

In conclusion, the present study on the effects of acute dietary zinc depletion produced a plethora of indicative molecular indices implying the physiological effects of dietary zinc in the human body. Transcripts of blood genes associated with cell cycle regulation, host defense and the regulation of zinc homeostasis hold the potential to indicate the dietary zinc status of individuals. TNFα release from whole blood under immunostimulation was clearly depressed by suboptimal zinc intake. These strongly agree with the biological roles of zinc in immunity and cell proliferation characterized by previous *in vitro* and *in vivo* experiments. The clinical implications and relevant molecular mechanisms of the modulation in erythrocyte membrane dematin and serum miRNAs by dietary zinc restriction remain unclear, and thus require further exploration. By using novel techniques enabling sample stabilization and high-throughput data analyses along with cost-effectiveness, this study may also provide insights into the

standardization of experimental designs for future nutritional or clinical biomarker studies.

# APPENDIX A
# SCREENING QUESTIONNAIRE

## SCREENING: SUBJECT ELIGIBILITY CRITERIA

Please mark (X) Yes or No for each criterion:

**INCLUSION CRITERIA**

| Yes | No | |
|---|---|---|
| ☐ | ☐ | 1. Subject is a male between 21 and 35 years of age. |
| ☐ | ☐ | 2. Subject weighs at least 110 pounds. |
| ☐ | ☐ | 3. Subject is willing to discontinue all dietary supplements. |
| ☐ | ☐ | 4. Subject is willing to follow the guidelines for dietary restriction. |
| ☐ | ☐ | 5. Subject is willing to consider the GCRC as his only dietary source for 17 days. |
| ☐ | ☐ | 6. Subject is willing to consume dietary supplements provided as pills for 24 days. |
| ☐ | ☐ | 7. Subject is willing to visit the GCRC at the scheduled dates and times. |

- Day 0 to 17 – 06:30 AM and 05:00 PM (twice a day)
- Day 20, 24 – 06:30 AM

| | | |
|---|---|---|
| ☐ | ☐ | 8. Subject is willing to consume a liquid diet, exclusively, as their only source of food for 10 days. |
| ☐ | ☐ | 9. Subject is willing to give 5 mL of blood for the screening process. |
| ☐ | ☐ | 10. Subject is willing to give blood samples, totaling 125.5 mL, during the dietary restriction. |
| ☐ | ☐ | 11. Subject is willing to provide mouth skin swabs three times during the dietary restriction. |

Qualified if all "Yes" boxes are marked: ☐ Criteria Met

**EXCLUSION CRITERIA**

| Yes | No | |
|---|---|---|
| ☐ | ☐ | 1. Subject is a student or an advisee of any investigators involved in this project. |
| ☐ | ☐ | 2. Subject is a current smoker. |
| ☐ | ☐ | 3. Subject consumes alcohol at the rate of more than 2 drinks per day. |
| ☐ | ☐ | 4. Subject is under a routine consumption of medications/drugs. |
| ☐ | ☐ | 5. Subject has a history of any chronic diseases. |
| ☐ | ☐ | 6. Subject had a recent surgery. |
| ☐ | ☐ | 7. Subject is wearing a denture or has been using denture cream. |
| ☐ | ☐ | 8. Subject has been consuming supplements containing zinc (or zinc lozenges) within the previous 7 days. |
| ☐ | ☐ | 9. Subject is a vegetarian. |
| ☐ | ☐ | 10. Subject has a history of allergic or adverse reactions to a certain food component. |

If yes, please specify: _____.

Qualified if all "No" boxes are marked: ☐ Criteria Met

| |
|---|
| Name: |
| Call back number: ( ) |
| Cell phone number: ( ) |
| Address: |
| E-mail: |
| Qualified: ☐ Yes ☐ No |

APPENDIX B
POST-PARTICIPATION SURVEY

## POST-STUDY SURVEY:
## COMPIANCE TO THE DIETARY REGIMEN

Please mark (X) Yes or No for each criterion:

| Yes | No | |
|---|---|---|
| ☐ | ☐ | 1. All meals provided by the GCRC were completely consumed, and none was shared by others or thrown away. |
| ☐ | ☐ | 2. During the first 17 days of participation, I did not consume any food items or beverages that were not provided by the GCRC. |
| ☐ | ☐ | 3. I had an experience of sickness (such as symptoms of common cold or allergy) while participating in the study. |
| ☐ | ☐ | 4. I have taken medications or drugs during (or at any point of) the study period. |
| ☐ | ☐ | 5. I took dietary supplements that were not provided by the GCRC while being in the study. |
| ☐ | ☐ | 6. I consumed alcohol while being in the study. |
| ☐ | ☐ | 7. I had smoked one or more cigarettes (or any other tobacco products) while being in the study. |
| ☐ | ☐ | 8. I have been aware of and compliant to the guidelines for the dietary restriction of this study. |

* If you have any other comments or issues to notify, please write in the blank below.

# APPENDIX C
# LIST OF GENES DIFFERENTIALLY EXPRESSED BY ACUTE DIETARY ZINC DEPLETION

Table C-1. List of genes up-regulated by acute dietary zinc depltion ranked by fold-changes (ZnD/Baseline values)[1]

| Gene Symbol | Entrez ID | Gene Name | Fold-Change | Parametric *P*-Value | FDR |
|---|---|---|---|---|---|
| LOC651751 | 651751 | similar to Ig kappa chain V-II region RPMI 6410 precursor | 4.32 | < 1e-07 | < 1e-07 |
| IGJ | 3512 | immunoglobulin J polypeptide, linker protein for immunoglobulin alpha and mu polypeptides | 4.22 | 1.00E-06 | 0.00189 |
| LOC649923 | 649923 | similar to Ig gamma-2 chain C region | 3.51 | 3.00E-07 | 0.00124 |
| LOC642113 | 642113 | Ig kappa chain V-III region HAH-like | 3.05 | < 1e-07 | < 1e-07 |
| LOC652493 | 652493 | ig kappa chain V-I region HK102-like | 3.05 | 6.00E-07 | 0.00178 |
| LOC647450 | 647450 | similar to Ig kappa chain V-I region HK101 precursor | 2.87 | 3.00E-07 | 0.00124 |
| LOC647506 | 647506 | similar to Ig kappa chain V-I region HK101 precursor | 2.77 | 9.00E-07 | 0.00189 |
| IGLL1 | 3543 | immunoglobulin lambda-like polypeptide 1 | 2.77 | 1.00E-06 | 0.00189 |
| TXNDC5 | 81567 | thioredoxin domain containing 5 (endoplasmic reticulum) | 2.73 | 5.00E-07 | 0.00173 |
| CDC20 | 991 | cell division cycle 20 homolog (S. cerevisiae) | 2.69 | 2.00E-07 | 0.00124 |
| TNFRSF17 | 608 | tumor necrosis factor receptor superfamily, member 17 | 2.55 | 0.0000185 | 0.0174 |
| GLDC | 2731 | glycine dehydrogenase (decarboxylating) | 2.49 | 2.30E-06 | 0.00367 |
| LOC652102 | 652102 | similar to Ig heavy chain V-I region HG3 precursor | 2.46 | 1.07E-03 | 0.208 |
| MZB1 | 51237 | marginal zone B and B1 cell-specific protein | 2.07 | 0.0000007 | 0.00182 |
| CD38 | 952 | CD38 molecule | 2.03 | 2.07E-05 | 0.0178 |
| ABCB9 | 23457 | ATP-binding cassette, sub-family B (MDR/TAP), member 9 | 1.85 | 2.20E-06 | 0.00367 |
| IGLL3 | 91353 | immunoglobulin lambda-like polypeptide 3, pseudogene | 1.85 | 0.0001122 | 0.0541 |
| LOC652775 | 652775 | similar to Ig kappa chain V-V region L7 precursor | 1.81 | 0.0014877 | 0.232 |
| LOC649210 | 649210 | similar to Ig lambda chain V region 4A precursor | 1.73 | 3.13E-03 | 0.273 |
| CCNB2 | 9133 | cyclin B2 | 1.70 | 0.0000182 | 0.0174 |
| ITM2C | 81618 | integral membrane protein 2C | 1.70 | 2.23E-05 | 0.0178 |
| ABCA1 | 19 | ATP-binding cassette, sub-family A (ABC1), member 1 | 1.69 | 0.0000061 | 0.00791 |
| GPRC5D | 55507 | G protein-coupled receptor, family C, group 5, member D | 1.67 | 0.000022 | 0.0178 |
| UBE2C | 11065 | ubiquitin-conjugating enzyme E2C | 1.59 | 0.0000044 | 0.00652 |
| NLRP7 | 199713 | NLR family, pyrin domain containing 7 | 1.51 | 8.19E-05 | 0.0447 |
| LOC728741 | 728741 | hypothetical LOC728741 | 1.50 | 0.0000118 | 0.0129 |
| APOBEC3B | 9582 | apolipoprotein B mRNA editing enzyme, catalytic polypeptide-like 3B | 1.49 | 0.0007272 | 0.168 |
| LOC652694 | 652694 | similar to Ig kappa chain V-I region HK102 precursor | 1.46 | 0.0025921 | 0.265 |
| AURKB | 9212 | aurora kinase B | 1.45 | 0.0000497 | 0.0316 |
| TYMS | 7298 | thymidylate synthetase | 1.44 | 1.90E-04 | 0.0787 |
| CDCA5 | 113130 | cell division cycle associated 5 | 1.43 | 0.0000691 | 0.0387 |

Table C-1. Continued

| Gene Symbol | Entrez ID | Gene Name | Fold-Change | Parametric *P*-Value | FDR |
|---|---|---|---|---|---|
| LOC651612 | 651612 | hypothetical protein LOC651612 | 1.43 | 0.0025996 | 0.265 |
| POU2AF1 | 5450 | POU class 2 associating factor 1 | 1.42 | 0.0000075 | 0.00915 |
| SORL1 | 6653 | sortilin-related receptor, L(DLR class) A repeats containing | 1.42 | 1.65E-03 | 0.245 |
| HSP90B1 | 7184 | heat shock protein 90kDa beta (Grp94), member 1 | 1.42 | 0.0017993 | 0.248 |
| HS.520591 | | - | 1.42 | 1.87E-03 | 0.248 |
| SEMA4A | 64218 | sema domain, immunoglobulin domain (Ig), transmembrane domain (TM) and short cytoplasmic domain, (semaphorin) 4A | 1.42 | 0.0034833 | 0.278 |
| TNFRSF13B | 23495 | tumor necrosis factor receptor superfamily, member 13B | 1.41 | 0.0002692 | 0.102 |
| TK1 | 7083 | thymidine kinase 1, soluble | 1.40 | 0.0003142 | 0.107 |
| CDC45L | 8318 | cell division cycle 45 homolog (S. cerevisiae) | 1.40 | 3.64E-04 | 0.118 |
| FKBP11 | 51303 | FK506 binding protein 11, 19 kDa | 1.40 | 0.0003749 | 0.12 |
| RRBP1 | 6238 | ribosome binding protein 1 homolog 180kDa (dog) | 1.37 | 0.0000325 | 0.0241 |
| TOP2A | 7153 | topoisomerase (DNA) II alpha 170kDa | 1.36 | 0.0000993 | 0.0503 |
| NT5DC2 | 64943 | 5'-nucleotidase domain containing 2 | 1.36 | 0.0002826 | 0.103 |
| NCAPG | 64151 | non-SMC condensin I complex, subunit G | 1.36 | 0.0017575 | 0.247 |
| BIK | 638 | BCL2-interacting killer (apoptosis-inducing) | 1.35 | 0.0006896 | 0.163 |
| SDF2L1 | 23753 | stromal cell-derived factor 2-like 1 | 1.35 | 0.0009311 | 0.191 |
| F5 | 2153 | coagulation factor V (proaccelerin, labile factor) | 1.35 | 0.0044828 | 0.305 |
| UHRF1 | 29128 | ubiquitin-like with PHD and ring finger domains 1 | 1.34 | 3.62E-05 | 0.0259 |
| C19ORF10 | 56005 | chromosome 19 open reading frame 10 | 1.34 | 0.000042 | 0.0281 |
| LOC100131727 | 100131727 | hypothetical protein LOC100131727 | 1.34 | 0.0002553 | 0.0984 |
| SLC35A5 | 55032 | solute carrier family 35, member A5 | 1.33 | 1.09E-04 | 0.0538 |
| CAMK1G | 57172 | calcium/calmodulin-dependent protein kinase IG | 1.33 | 0.0001167 | 0.055 |
| IRF4 | 3662 | interferon regulatory factor 4 | 1.32 | 0.0000085 | 0.0098 |
| DENND5B | 160518 | DENN/MADD domain containing 5B | 1.32 | 0.0000583 | 0.0336 |
| CCNA2 | 890 | cyclin A2 | 1.32 | 0.0009848 | 0.195 |
| ASAP1IT1 | 29065 | ASAP1 intronic transcript 1 (non-protein coding) | 1.32 | 0.0041321 | 0.295 |
| LOC100129905 | 100129905 | ribosomal protein S27 pseudogene 19 | 1.31 | 0.0043965 | 0.305 |
| PTTG3P | 26255 | pituitary tumor-transforming 3, pseudogene | 1.30 | 0.000091 | 0.0472 |
| SLC38A10 | 124565 | solute carrier family 38, member 10 | 1.29 | 0.0000394 | 0.0272 |
| GMPPB | 29925 | GDP-mannose pyrophosphorylase B | 1.29 | 0.0000578 | 0.0336 |
| BUB1 | 699 | budding uninhibited by benzimidazoles 1 homolog (yeast) | 1.29 | 0.0028315 | 0.269 |
| OXCT2 | 64064 | 3-oxoacid CoA transferase 2 | 1.28 | 0.0000521 | 0.0318 |
| MCM4 | 4173 | minichromosome maintenance complex component 4 | 1.28 | 0.000169 | 0.0746 |
| PHGDH | 26227 | phosphoglycerate dehydrogenase | 1.28 | 0.0002838 | 0.103 |

Table C-1. Continued

| Gene Symbol | Entrez ID | Gene Name | Fold-Change | Parametric *P*-Value | FDR |
|---|---|---|---|---|---|
| BIRC5 | 332 | baculoviral IAP repeat containing 5 | 1.28 | 0.0004178 | 0.129 |
| TLN1 | 7094 | talin 1 | 1.28 | 0.0013616 | 0.231 |
| HS.184721 | | - | 1.28 | 0.0024909 | 0.265 |
| LOC441124 | 441124 | hypothetical gene supported by AK093729; BX647918 | 1.28 | 0.0045759 | 0.305 |
| CKAP4 | 10970 | cytoskeleton-associated protein 4 | 1.28 | 0.0047783 | 0.309 |
| CCR9 | 10803 | chemokine (C-C motif) receptor 9 | 1.27 | 0.0000053 | 0.00733 |
| PDIA5 | 10954 | protein disulfide isomerase family A, member 5 | 1.27 | 0.0002362 | 0.0942 |
| COL18A1 | 80781 | collagen, type XVIII, alpha 1 | 1.27 | 0.0024194 | 0.265 |
| ABCG1 | 9619 | ATP-binding cassette, sub-family G (WHITE), member 1 | 1.26 | 0.0000169 | 0.0174 |
| SLC2A5 | 6518 | solute carrier family 2 (facilitated glucose/fructose transporter), member 5 | 1.26 | 0.0003109 | 0.107 |
| MTF1 | 4520 | metal-regulatory transcription factor 1 | 1.26 | 0.0007353 | 0.168 |
| CDT1 | 81620 | chromatin licensing and DNA replication factor 1 | 1.26 | 0.0020703 | 0.258 |
| STT3A | 3703 | STT3, subunit of the oligosaccharyltransferase complex, homolog A (S. cerevisiae) | 1.25 | 0.0001593 | 0.0726 |
| TRAM2 | 9697 | translocation associated membrane protein 2 | 1.25 | 0.0004935 | 0.142 |
| AURKA | 6790 | aurora kinase A | 1.25 | 0.0006783 | 0.163 |
| HS.157344 | - | - | 1.25 | 0.0009777 | 0.195 |
| POLR2A | 5430 | polymerase (RNA) II (DNA directed) polypeptide A, 220kDa | 1.25 | 0.0020028 | 0.258 |
| LOC642131 | 642131 | putative V-set and immunoglobulin domain-containing protein 6-like | 1.25 | 0.0030141 | 0.27 |
| SPC24 | 147841 | SPC24, NDC80 kinetochore complex component, homolog (S. cerevisiae) | 1.25 | 0.0044094 | 0.305 |
| DLGAP5 | 9787 | discs, large (Drosophila) homolog-associated protein 5 | 1.24 | 0.0015724 | 0.24 |
| NUSAP1 | 51203 | nucleolar and spindle associated protein 1 | 1.24 | 0.0029244 | 0.27 |
| UBE2J1 | 51465 | ubiquitin-conjugating enzyme E2, J1 (UBC6 homolog, yeast) | 1.23 | 0.0000268 | 0.0206 |
| HS.352677 | - | - | 1.23 | 0.0001848 | 0.0782 |
| TRIP13 | 9319 | thyroid hormone receptor interactor 13 | 1.23 | 0.0006141 | 0.159 |
| WAS | 7454 | Wiskott-Aldrich syndrome (eczema-thrombocytopenia) | 1.23 | 0.0011971 | 0.224 |
| ARID3A | 1820 | AT rich interactive domain 3A (BRIGHT-like) | 1.23 | 0.0018194 | 0.248 |
| CENPM | 79019 | centromere protein M | 1.23 | 0.0024777 | 0.265 |
| UBA1 | 7317 | ubiquitin-like modifier activating enzyme 1 | 1.23 | 0.0032981 | 0.276 |
| BMP8B | 656 | bone morphogenetic protein 8b | 1.22 | 0.0006654 | 0.163 |
| SPATS2 | 65244 | spermatogenesis associated, serine-rich 2 | 1.22 | 0.0008565 | 0.187 |
| SLC12A9 | 56996 | solute carrier family 12 (potassium/chloride transporters), member 9 | 1.22 | 0.00092 | 0.191 |
| SLC1A4 | 6509 | solute carrier family 1 (glutamate/neutral amino acid transporter), member 4 | 1.22 | 0.0012287 | 0.228 |

Table C-1. Continued

| Gene Symbol | Entrez ID | Gene Name | Fold-Change | Parametric *P*-Value | FDR |
|---|---|---|---|---|---|
| TXNDC11 | 51061 | thioredoxin domain containing 11 | 1.22 | 0.002231 | 0.265 |
| LOC440348 | 440348 | nuclear pore complex interacting protein-like 2 | 1.22 | 0.0023746 | 0.265 |
| HJURP | 55355 | Holliday junction recognition protein | 1.22 | 0.0032498 | 0.276 |
| ZNF341 | 84905 | zinc finger protein 341 | 1.22 | 0.0034433 | 0.278 |
| ZYX | 7791 | zyxin | 1.22 | 0.0043195 | 0.302 |
| LOC100128269 | 100128269 | hypothetical LOC100128269 | 1.22 | 0.0049398 | 0.314 |
| ZBTB43 | 23099 | zinc finger and BTB domain containing 43 | 1.21 | 0.0004846 | 0.142 |
| KIF1B | 23095 | kinesin family member 1B | 1.21 | 0.0007647 | 0.171 |
| SNORA11B | 100124539 | small nucleolar RNA, H/ACA box 11B (retrotransposed) | 1.21 | 0.0009366 | 0.191 |
| KIF2C | 11004 | kinesin family member 2C | 1.21 | 0.0009411 | 0.191 |
| MAGT1 | 84061 | magnesium transporter 1 | 1.21 | 0.0011432 | 0.218 |
| PRR11 | 55771 | proline rich 11 | 1.21 | 0.0013451 | 0.231 |
| MCM2 | 4171 | minichromosome maintenance complex component 2 | 1.21 | 0.0017097 | 0.247 |
| ALOX5 | 240 | arachidonate 5-lipoxygenase | 1.21 | 0.002618 | 0.265 |
| TCF4 | 6925 | transcription factor 4 | 1.21 | 0.0029275 | 0.27 |
| NARF | 26502 | nuclear prelamin A recognition factor | 1.21 | 0.0036279 | 0.285 |
| SORT1 | 6272 | sortilin 1 | 1.21 | 0.0045313 | 0.305 |
| CDCA8 | 55143 | cell division cycle associated 8 | 1.20 | 0.001591 | 0.241 |
| LAMA5 | 3911 | laminin, alpha 5 | 1.20 | 0.0023538 | 0.265 |
| HYOU1 | 10525 | hypoxia up-regulated 1 | 1.20 | 0.0026657 | 0.266 |
| HS.143018 | - | - | 1.20 | 0.0035111 | 0.278 |
| FAHD2B | 151313 | fumarylacetoacetate hydrolase domain containing 2B | 1.20 | 0.0047638 | 0.309 |
| ZBTB32 | 27033 | zinc finger and BTB domain containing 32 | 1.19 | 0.0003531 | 0.116 |
| MGAT3 | 4248 | mannosyl (beta-1,4-)-glycoprotein beta-1,4-N-acetylglucosaminyltransferase | 1.19 | 0.000672 | 0.163 |
| ADAM19 | 8728 | ADAM metallopeptidase domain 19 | 1.19 | 0.0008079 | 0.178 |
| DCTN1 | 1639 | dynactin 1 | 1.19 | 0.0014801 | 0.232 |
| SEMA3E | 9723 | sema domain, immunoglobulin domain (Ig), short basic domain, secreted, (semaphorin) 3E | 1.19 | 0.0015156 | 0.235 |
| GMPPA | 29926 | GDP-mannose pyrophosphorylase A | 1.19 | 0.0016243 | 0.244 |
| LOC651816 | 651816 | similar to Ubiquitin-conjugating enzyme E2S (Ubiquitin-conjugating enzyme E2-24 kDa) (Ubiquitin-protein ligase) (Ubiquitin carrier protein) (E2-EPF5) | 1.19 | 0.0023823 | 0.265 |
| SEC61A1 | 29927 | Sec61 alpha 1 subunit (S. cerevisiae) | 1.19 | 0.002402 | 0.265 |
| EHBP1L1 | 254102 | EH domain binding protein 1-like 1 | 1.19 | 0.0024833 | 0.265 |

Table C-1. Continued

| Gene Symbol | Entrez ID | Gene Name | Fold-Change | Parametric *P*-Value | FDR |
|---|---|---|---|---|---|
| CIC | 23152 | capicua homolog (Drosophila) | 1.19 | 0.0028768 | 0.27 |
| FLOT2 | 2319 | flotillin 2 | 1.19 | 0.0032535 | 0.276 |
| RARA | 5914 | retinoic acid receptor, alpha | 1.19 | 0.0033469 | 0.276 |
| DUSP5 | 1847 | dual specificity phosphatase 5 | 1.19 | 0.0043166 | 0.302 |
| OR2AG1 | 144125 | olfactory receptor, family 2, subfamily AG, member 1 | 1.18 | 0.0004701 | 0.141 |
| LOC399900 | 399900 | hypothetical LOC399900 | 1.18 | 0.000509 | 0.144 |
| SPCS2 | 9789 | signal peptidase complex subunit 2 homolog (S. cerevisiae) | 1.18 | 0.0005436 | 0.146 |
| ZBP1 | 81030 | Z-DNA binding protein 1 | 1.18 | 0.0009123 | 0.191 |
| LOC399491 | 399491 | GPS, PLAT and transmembrane domain-containing protein | 1.18 | 0.0010411 | 0.204 |
| KIF20A | 10112 | kinesin family member 20A | 1.18 | 0.0026819 | 0.266 |
| COPG | 22820 | coatomer protein complex, subunit gamma | 1.18 | 0.0027871 | 0.269 |
| OTUD5 | 55593 | OTU domain containing 5 | 1.18 | 0.0043392 | 0.302 |
| MYH9 | 4627 | myosin, heavy chain 9, non-muscle | 1.18 | 0.0048114 | 0.309 |
| SEC13 | 6396 | SEC13 homolog (S. cerevisiae) | 1.17 | 0.0014051 | 0.231 |
| VPS8 | 23355 | vacuolar protein sorting 8 homolog (S. cerevisiae) | 1.17 | 0.0014412 | 0.232 |
| PARM1 | 25849 | prostate androgen-regulated mucin-like protein 1 | 1.17 | 0.0014727 | 0.232 |
| SRPR | 6734 | signal recognition particle receptor (docking protein) | 1.17 | 0.0016889 | 0.247 |
| PIM2 | 11040 | pim-2 oncogene | 1.17 | 0.0020115 | 0.258 |
| TPX2 | 22974 | TPX2, microtubule-associated, homolog (Xenopus laevis) | 1.17 | 0.0021016 | 0.258 |
| LOC100130168 | 100130168 | hypothetical protein LOC100130168 | 1.17 | 0.0023524 | 0.265 |
| HS.562118 | - | - | 1.17 | 0.0025938 | 0.265 |
| NLRP1 | 22861 | NLR family, pyrin domain containing 1 | 1.17 | 0.0028257 | 0.269 |
| HS.569823 | - | - | 1.17 | 0.0028932 | 0.27 |
| KIAA0226 | 9711 | KIAA0226 | 1.17 | 0.0029328 | 0.27 |
| TAP1 | 6890 | transporter 1, ATP-binding cassette, sub-family B (MDR/TAP) | 1.17 | 0.0029947 | 0.27 |
| MLEC | 9761 | malectin | 1.17 | 0.0032293 | 0.276 |
| CXXC1 | 30827 | CXXC finger protein 1 | 1.17 | 0.0033412 | 0.276 |
| AARS | 16 | alanyl-tRNA synthetase | 1.17 | 0.0036372 | 0.285 |
| C1QB | 713 | complement component 1, q subcomponent, B chain | 1.17 | 0.0040823 | 0.295 |
| KIAA0492 | 57238 | KIAA0492 protein | 1.17 | 0.0041365 | 0.295 |
| HS.447737 | - | - | 1.17 | 0.0045788 | 0.305 |
| HS.559654 | - | - | 1.16 | 0.0014509 | 0.232 |
| LOC728790 | 728790 | hypothetical LOC728790 | 1.16 | 0.0021339 | 0.26 |
| ALDH6A1 | 4329 | aldehyde dehydrogenase 6 family, member A1 | 1.16 | 0.0026201 | 0.265 |
| IL4R | 3566 | interleukin 4 receptor | 1.16 | 0.0029048 | 0.27 |
| PDIA4 | 9601 | protein disulfide isomerase family A, member 4 | 1.16 | 0.0041813 | 0.296 |

Table C-1. Continued

| Gene Symbol | Entrez ID | Gene Name | Fold-Change | Parametric *P*-Value | FDR |
|---|---|---|---|---|---|
| ALDH3B1 | 221 | aldehyde dehydrogenase 3 family, member B1 | 1.16 | 0.0046729 | 0.307 |
| ZNF486 | 90649 | zinc finger protein 486 | 1.16 | 0.0046782 | 0.307 |
| IRF9 | 10379 | interferon regulatory factor 9 | 1.16 | 0.0047607 | 0.309 |
| TMEM106A | 113277 | transmembrane protein 106A | 1.16 | 0.0047759 | 0.309 |
| INTS3 | 65123 | integrator complex subunit 3 | 1.15 | 0.0011132 | 0.214 |
| SIL1 | 64374 | SIL1 homolog, endoplasmic reticulum chaperone (S. cerevisiae) | 1.15 | 0.0020861 | 0.258 |
| FKBP2 | 2286 | FK506 binding protein 2, 13kDa | 1.15 | 0.0023331 | 0.265 |
| BTBD12 | 84464 | SLX4 structure-specific endonuclease subunit homolog (S. cerevisiae) | 1.15 | 0.0023915 | 0.265 |
| NFKB2 | 4791 | nuclear factor of kappa light polypeptide gene enhancer in B-cells 2 (p49/p100) | 1.15 | 0.0033623 | 0.276 |
| SLC35B1 | 10237 | solute carrier family 35, member B1 | 1.15 | 0.004008 | 0.295 |
| C4ORF28 | 133015 | PARK2 co-regulated-like | 1.15 | 0.0045292 | 0.305 |
| P4HB | 5034 | prolyl 4-hydroxylase, beta polypeptide | 1.15 | 0.0047315 | 0.309 |
| PTK2B | 2185 | PTK2B protein tyrosine kinase 2 beta | 1.15 | 0.0049749 | 0.315 |
| FBXO18 | 84893 | F-box protein, helicase, 18 | 1.14 | 0.0005795 | 0.154 |
| LILRB1 | 10859 | leukocyte immunoglobulin-like receptor, subfamily B (with TM and ITIM domains), member 1 | 1.14 | 0.0020484 | 0.258 |
| PCYOX1 | 51449 | prenylcysteine oxidase 1 | 1.14 | 0.0025229 | 0.265 |
| CLPTM1L | 81037 | CLPTM1-like | 1.14 | 0.0030232 | 0.27 |
| FAM46A | 55603 | family with sequence similarity 46, member A | 1.14 | 0.0034408 | 0.278 |
| CAPN11 | 11131 | calpain 11 | 1.14 | 0.0040412 | 0.295 |
| EIF4G3 | 8672 | eukaryotic translation initiation factor 4 gamma, 3 | 1.14 | 0.0045359 | 0.305 |
| HS.188979 | - | - | 1.13 | 0.0013004 | 0.231 |
| TRPM3 | 80036 | transient receptor potential cation channel, subfamily M, member 3 | 1.13 | 0.0018613 | 0.248 |
| FLJ44124 | 641737 | hypothetical LOC641737 | 1.13 | 0.0022495 | 0.265 |
| FLJ20254 | 54867 | transmembrane protein 214 | 1.13 | 0.0039144 | 0.295 |
| IFNAR2 | 3455 | interferon (alpha, beta and omega) receptor 2 | 1.12 | 0.0021891 | 0.265 |
| RCC2 | 55920 | regulator of chromosome condensation 2 | 1.12 | 0.0038441 | 0.295 |
| SEC23B | 10483 | Sec23 homolog B (S. cerevisiae) | 1.11 | 0.0041106 | 0.295 |
| SHMT1 | 6470 | serine hydroxymethyltransferase 1 (soluble) | 1.10 | 0.0036726 | 0.286 |

[1] Determined by paired t-test at $P < 0.005$ and a permutation of 10,000 (n = 9). FDR, false discovery rate.

Table C-2. List of genes down-regulated by acute dietary zinc depltion ranked by fold-changes (ZnD/Baseline values)[1]

| Gene Symbol | Entrez ID | Gene Name | Fold-Change | Parametric *P*-Value | FDR |
|---|---|---|---|---|---|
| HOPX | 84525 | HOP homeobox | -1.43 | 0.0001609 | 0.0726 |
| AKR1C3 | 8644 | aldo-keto reductase family 1, member C3 (3-alpha hydroxysteroid dehydrogenase, type II) | -1.41 | 0.0048328 | 0.309 |
| POP5 | 51367 | processing of precursor 5, ribonuclease P/MRP subunit (S. cerevisiae) | -1.37 | 0.0000503 | 0.0316 |
| RPL5 | 6125 | ribosomal protein L5 | -1.35 | 0.003269 | 0.276 |
| LOC100133185 | 100133185 | hypothetical LOC100133185 | -1.33 | 0.0004762 | 0.141 |
| LOC338870 | 338870 | ribosomal protein S12 pseudogene 23 | -1.32 | 0.0000862 | 0.0459 |
| C6ORF190 | 387357 | thymocyte selection associated | -1.32 | 0.0004691 | 0.141 |
| LOC391370 | 391370 | ribosomal protein S12 pseudogene 4 | -1.32 | 0.0006724 | 0.163 |
| CD160 | 11126 | CD160 molecule | -1.32 | 2.00E-03 | 0.258 |
| ENPP4 | 22875 | ectonucleotide pyrophosphatase/phosphodiesterase 4 (putative) | -1.32 | 0.0023961 | 0.265 |
| GZMK | 3003 | granzyme K (granzyme 3; tryptase II) | -1.30 | 0.0023638 | 0.265 |
| RCN2 | 5955 | reticulocalbin 2, EF-hand calcium binding domain | -1.30 | 0.0033195 | 0.276 |
| TRAPPC2P1 | 10597 | trafficking protein particle complex 2 pseudogene 1 | -1.30 | 0.0041531 | 0.295 |
| CRYZ | 1429 | crystallin, zeta (quinone reductase) | -1.30 | 0.0044254 | 0.305 |
| TMEM106B | 54664 | transmembrane protein 106B | -1.28 | 3.93E-04 | 0.123 |
| LOC441506 | 441506 | similar to laminin receptor 1 | -1.28 | 9.06E-04 | 0.191 |
| BMI1 | 648 | BMI1 polycomb ring finger oncogene | -1.28 | 0.0023516 | 0.265 |
| C17ORF45 | 125144 | non-protein coding RNA 188 | -1.28 | 0.0025859 | 0.265 |
| ZNF594 | 84622 | zinc finger protein 594 | -1.27 | 0.0005382 | 0.146 |
| FAU | 2197 | Finkel-Biskis-Reilly murine sarcoma virus (FBR-MuSV) ubiquitously expressed | -1.27 | 0.0013918 | 0.231 |
| LAIR2 | 3904 | leukocyte-associated immunoglobulin-like receptor 2 | -1.27 | 0.0020925 | 0.258 |
| RGS18 | 64407 | regulator of G-protein signaling 18 | -1.27 | 0.0024428 | 0.265 |
| ANKRD46 | 157567 | ankyrin repeat domain 46 | -1.27 | 0.003684 | 0.286 |
| C12ORF41 | 54934 | chromosome 12 open reading frame 41 | -1.25 | 0.0002883 | 0.103 |
| LEPROTL1 | 23484 | leptin receptor overlapping transcript-like 1 | -1.25 | 5.22E-04 | 0.144 |
| KLRD1 | 3824 | killer cell lectin-like receptor subfamily D, member 1 | -1.25 | 0.0006852 | 0.163 |
| DCK | 1633 | deoxycytidine kinase | -1.25 | 0.0029953 | 0.27 |
| ZCCHC7 | 84186 | zinc finger, CCHC domain containing 7 | -1.25 | 0.0032017 | 0.274 |
| LOC100133662 | 100133662 | hypothetical protein LOC100133662 | -1.23 | 0.0005223 | 0.144 |
| LOC388789 | 388789 | hypothetical LOC388789 | -1.23 | 1.83E-03 | 0.248 |
| TGDS | 23483 | TDP-glucose 4,6-dehydratase | -1.23 | 2.73E-03 | 0.267 |
| TRIAP1 | 51499 | TP53 regulated inhibitor of apoptosis 1 | -1.23 | 0.0031114 | 0.273 |
| CREBZF | 58487 | CREB/ATF bZIP transcription factor | -1.23 | 0.0031873 | 0.274 |

Table C-2. Continued

| Gene Symbol | Entrez ID | Gene Name | Fold-Change | Parametric *P*-Value | FDR |
|---|---|---|---|---|---|
| TAF7 | 6879 | TAF7 RNA polymerase II, TATA box binding protein (TBP)-associated factor, 55kDa | -1.23 | 0.0039695 | 0.295 |
| PTGDR | 5729 | prostaglandin D2 receptor (DP) | -1.22 | 0.0002983 | 0.105 |
| PTGER2 | 5732 | prostaglandin E receptor 2 (subtype EP2), 53kDa | -1.22 | 0.0009335 | 0.191 |
| CLNS1A | 1207 | chloride channel, nucleotide-sensitive, 1A | -1.22 | 0.0016481 | 0.245 |
| GNG2 | 54331 | guanine nucleotide binding protein (G protein), gamma 2 | -1.22 | 0.0019601 | 0.257 |
| ZNF256 | 10172 | zinc finger protein 256 | -1.22 | 3.28E-03 | 0.276 |
| LOC648249 | 648249 | similar to 40S ribosomal protein SA (p40) (34/67 kDa laminin receptor) (Colon carcinoma laminin-binding protein) (NEM/1CHD4) (Multidrug resistance-associated protein MGr1-Ag) | -1.22 | 0.0040863 | 0.295 |
| CCL4L2 | 388372 | chemokine (C-C motif) ligand 4-like 2 | -1.20 | 0.0000194 | 0.0175 |
| C16ORF63 | 123811 | FGFR1OP N-terminal like | -1.20 | 0.0017643 | 0.247 |
| C9ORF78 | 51759 | chromosome 9 open reading frame 78 | -1.20 | 0.0018299 | 0.248 |
| LOC440055 | 440055 | ribosomal protein S12 pseudogene 22 | -1.20 | 0.0022964 | 0.265 |
| MOCS2 | 4338 | molybdenum cofactor synthesis 2 | -1.20 | 0.0025874 | 0.265 |
| BBS10 | 79738 | Bardet-Biedl syndrome 10 | -1.20 | 0.0030162 | 0.27 |
| ZNF32 | 7580 | zinc finger protein 32 | -1.20 | 0.003189 | 0.274 |
| TSPAN13 | 27075 | tetraspanin 13 | -1.20 | 0.0039988 | 0.295 |
| ZNF480 | 147657 | zinc finger protein 480 | -1.19 | 0.0001729 | 0.0747 |
| MED30 | 90390 | mediator complex subunit 30 | -1.19 | 0.0003468 | 0.116 |
| AQP12B | 653437 | aquaporin 12B | -1.19 | 0.0009562 | 0.193 |
| FAM179A | 165186 | family with sequence similarity 179, member A | -1.19 | 0.0011852 | 0.224 |
| ZNF550 | 162972 | zinc finger protein 550 | -1.19 | 0.0024386 | 0.265 |
| COX7A2L | 9167 | cytochrome c oxidase subunit VIIa polypeptide 2 like | -1.19 | 0.0025752 | 0.265 |
| FLJ14213 | 79899 | proline rich 5 like | -1.19 | 0.0028075 | 0.269 |
| HSF2 | 3298 | heat shock transcription factor 2 | -1.19 | 0.002991 | 0.27 |
| ARL6IP5 | 10550 | ADP-ribosylation-like factor 6 interacting protein 5 | -1.19 | 0.0033878 | 0.277 |
| LEMD3 | 23592 | LEM domain containing 3 | -1.19 | 0.0034091 | 0.277 |
| CXCR7 | 57007 | chemokine (C-X-C motif) receptor 7 | -1.19 | 0.0034953 | 0.278 |
| SNORD21 | 6083 | small nucleolar RNA, C/D box 21 | -1.19 | 0.0040171 | 0.295 |
| C1ORF52 | 148423 | chromosome 1 open reading frame 52 | -1.19 | 0.0046506 | 0.307 |
| KCTD5 | 54442 | potassium channel tetramerisation domain containing 5 | -1.18 | 0.0002354 | 0.0942 |
| SMARCE1 | 6605 | SWI/SNF related, matrix associated, actin dependent regulator of chromatin, subfamily e, member 1 | -1.18 | 0.0002561 | 0.0984 |
| C7ORF70 | 84792 | chromosome 7 open reading frame 70 | -1.18 | 0.0007107 | 0.166 |
| CYP2R1 | 120227 | cytochrome P450, family 2, subfamily R, polypeptide 1 | -1.18 | 0.0007449 | 0.168 |
| HSF5 | 124535 | heat shock transcription factor family member 5 | -1.18 | 0.0014013 | 0.231 |

Table C-2. Continued

| Gene Symbol | Entrez ID | Gene Name | Fold-Change | Parametric *P*-Value | FDR |
|---|---|---|---|---|---|
| LOC641844 | 641844 | SDHDP2 succinate dehydrogenase complex, subunit D, integral membrane protein pseudogene 2 | -1.18 | 0.0014446 | 0.232 |
| CD226 | 10666 | CD226 molecule | -1.18 | 0.0017396 | 0.247 |
| C1ORF75 | 55248 | transmembrane protein 206 | -1.18 | 0.0017485 | 0.247 |
| STK39 | 27347 | serine threonine kinase 39 | -1.18 | 0.0020663 | 0.258 |
| METTL4 | 64863 | methyltransferase like 4 | -1.18 | 0.0020985 | 0.258 |
| LOC401206 | 401206 | ribosomal protein S25 pseudogene 6 | -1.18 | 0.0026953 | 0.266 |
| MIS12 | 79003 | MIS12, MIND kinetochore complex component, homolog (S. pombe) | -1.18 | 0.0031138 | 0.273 |
| C3ORF10 | 55845 | chromosome 3 open reading frame 10 | -1.18 | 0.0038643 | 0.295 |
| CRIPT | 9419 | cysteine-rich PDZ-binding protein | -1.18 | 0.0039907 | 0.295 |
| RPS13 | 6207 | ribosomal protein S13 | -1.18 | 0.0039929 | 0.295 |
| SENP7 | 57337 | SUMO1/sentrin specific peptidase 7 | -1.18 | 0.0040921 | 0.295 |
| SLFN12 | 55106 | schlafen family member 12 | -1.16 | 0.0005855 | 0.154 |
| SLC27A5 | 10998 | solute carrier family 27 (fatty acid transporter), member 5 | -1.16 | 0.0006825 | 0.163 |
| LOC100130154 | 100130154 | similar to thymosin, beta 10 | -1.16 | 0.001321 | 0.231 |
| PRKAB2 | 5565 | protein kinase, AMP-activated, beta 2 non-catalytic subunit | -1.16 | 0.0013488 | 0.231 |
| RPA2 | 6118 | replication protein A2, 32kDa | -1.16 | 0.0014052 | 0.231 |
| MED4 | 29079 | mediator complex subunit 4 | -1.16 | 0.0018549 | 0.248 |
| FASLG | 356 | Fas ligand (TNF superfamily, member 6) | -1.16 | 0.001886 | 0.249 |
| MS4A1 | 931 | membrane-spanning 4-domains, subfamily A, member 1 | -1.16 | 0.002495 | 0.265 |
| HS.25318 | | - | -1.16 | 0.002686 | 0.266 |
| LOC100127918 | 100127918 | similar to small ubiquitin-related modifier 2 | -1.16 | 0.0035131 | 0.278 |
| RAB11A | 8766 | RAB11A, member RAS oncogene family | -1.16 | 0.0040014 | 0.295 |
| KPNA5 | 3841 | karyopherin alpha 5 (importin alpha 6) | -1.16 | 0.0044516 | 0.305 |
| SETMAR | 6419 | SET domain and mariner transposase fusion gene | -1.16 | 0.004666 | 0.307 |
| SMYD2 | 56950 | SET and MYND domain containing 2 | -1.15 | 0.0006797 | 0.163 |
| KLHDC5 | 57542 | kelch domain containing 5 | -1.15 | 0.0014674 | 0.232 |
| TMEM9B | 56674 | TMEM9 domain family, member B | -1.15 | 0.0017569 | 0.247 |
| ZNF304 | 57343 | zinc finger protein 304 | -1.15 | 0.0018168 | 0.248 |
| GK5 | 256356 | glycerol kinase 5 (putative) | -1.15 | 0.0025517 | 0.265 |
| SOCS2 | 8835 | suppressor of cytokine signaling 2 | -1.15 | 0.0026346 | 0.265 |
| LOC347292 | 347292 | ribosomal protein L36 pseudogene 14 | -1.15 | 0.0027187 | 0.267 |
| C11ORF46 | 120534 | chromosome 11 open reading frame 46 | -1.15 | 0.0033249 | 0.276 |
| GK5 | 256356 | glycerol kinase 5 (putative) | -1.15 | 0.0025517 | 0.265 |
| SOCS2 | 8835 | suppressor of cytokine signaling 2 | -1.15 | 0.0026346 | 0.265 |
| LOC347292 | 347292 | ribosomal protein L36 pseudogene 14 | -1.15 | 0.0027187 | 0.267 |
| C11ORF46 | 120534 | chromosome 11 open reading frame 46 | -1.15 | 0.0033249 | 0.276 |

Table C-2. Continued

| Gene Symbol | Entrez ID | Gene Name | Fold-Change | Parametric *P*-Value | FDR |
|---|---|---|---|---|---|
| STX16 | 8675 | syntaxin 16 | -1.15 | 0.0037438 | 0.29 |
| VAMP4 | 8674 | vesicle-associated membrane protein 4 | -1.15 | 0.0039966 | 0.295 |
| C1ORF131 | 128061 | chromosome 1 open reading frame 131 | -1.15 | 0.0040033 | 0.295 |
| LTBP2 | 4053 | latent transforming growth factor beta binding protein 2 | -1.15 | 0.0040103 | 0.295 |
| PQLC3 | 130814 | PQ loop repeat containing 3 | -1.15 | 0.0040677 | 0.295 |
| ZNF187 | 7741 | zinc finger protein 187 | -1.15 | 0.004258 | 0.3 |
| NGRN | 51335 | neugrin, neurite outgrowth associated | -1.15 | 0.0043007 | 0.302 |
| RHEB | 6009 | Ras homolog enriched in brain | -1.15 | 0.00447 | 0.305 |
| HS.133324 | | - | -1.15 | 0.0045816 | 0.305 |
| SNORA76 | 677842 | small nucleolar RNA, H/ACA box 76 | -1.15 | 0.0045932 | 0.305 |
| SERPINE2 | 5270 | serpin peptidase inhibitor, clade E (nexin, plasminogen activator inhibitor type 1), member 2 | -1.14 | 0.0012791 | 0.231 |
| ERP27 | 121506 | endoplasmic reticulum protein 27 | -1.14 | 0.0013217 | 0.231 |
| CCL3L1 | 6349 | chemokine (C-C motif) ligand 3-like 1 | -1.14 | 0.0013283 | 0.231 |
| MLLT11 | 10962 | myeloid/lymphoid or mixed-lineage leukemia (trithorax homolog, Drosophila); translocated to, 11 | -1.14 | 0.0013952 | 0.231 |
| AASDHPPT | 60496 | aminoadipate-semialdehyde dehydrogenase-phosphopantetheinyl transferase | -1.14 | 0.00153 | 0.235 |
| C20ORF30 | 29058 | chromosome 20 open reading frame 30 | -1.14 | 0.0016723 | 0.246 |
| LOC642341 | 642341 | hypothetical LOC642341 | -1.14 | 0.0019922 | 0.258 |
| VTA1 | 51534 | Vps20-associated 1 homolog (S. cerevisiae) | -1.14 | 0.0024282 | 0.265 |
| MFSD6 | 54842 | major facilitator superfamily domain containing 6 | -1.14 | 0.0024388 | 0.265 |
| KBTBD6 | 89890 | kelch repeat and BTB (POZ) domain containing 6 | -1.14 | 0.0025852 | 0.265 |
| LOC731915 | 731915 | similar to ATP-binding cassette sub-family D member 1 (Adrenoleukodystrophy protein) (ALDP) | -1.14 | 0.0026105 | 0.265 |
| CCL3L3 | 414062 | chemokine (C-C motif) ligand 3-like 3 | -1.14 | 0.002803 | 0.269 |
| LOC100130633 | 100130633 | hypothetical protein LOC100130633 | -1.14 | 0.0029335 | 0.27 |
| CCNB1IP1 | 57820 | cyclin B1 interacting protein 1, E3 ubiquitin protein ligase | -1.14 | 0.0036227 | 0.285 |
| PPIA | 5478 | peptidylprolyl isomerase A (cyclophilin A) | -1.14 | 0.0039574 | 0.295 |
| MST4 | 51765 | serine/threonine protein kinase MST4 | -1.14 | 0.0049485 | 0.314 |
| ZXDB | 158586 | zinc finger, X-linked, duplicated B | -1.12 | 0.0013386 | 0.231 |
| NUDT11 | 55190 | nudix (nucleoside diphosphate linked moiety X)-type motif 11 | -1.12 | 0.0028079 | 0.269 |
| BCL2L13 | 23786 | BCL2-like 13 (apoptosis facilitator) | -1.12 | 0.0030176 | 0.27 |
| PALB2 | 79728 | partner and localizer of BRCA2 | -1.12 | 0.0030502 | 0.272 |
| C9ORF85 | 138241 | chromosome 9 open reading frame 85 | -1.12 | 0.0030864 | 0.273 |
| MRPS36 | 92259 | mitochondrial ribosomal protein S36 | -1.12 | 0.0031178 | 0.273 |
| LYRM4 | 57128 | LYR motif containing 4 | -1.12 | 0.0031671 | 0.274 |

Table C-2. Continued

| Gene Symbol | Entrez ID | Gene Name | Fold-Change | Parametric *P*-Value | FDR |
|---|---|---|---|---|---|
| MFF | 56947 | mitochondrial fission factor | -1.12 | 0.0034594 | 0.278 |
| MRPS17 | 51373 | mitochondrial ribosomal protein S17 | -1.12 | 0.0038929 | 0.295 |
| HS.581615 | | - | -1.12 | 0.004807 | 0.309 |
| DNAJA4 | 55466 | DnaJ (Hsp40) homolog, subfamily A, member 4 | -1.12 | 0.004935 | 0.314 |
| FBXO3 | 26273 | F-box protein 3 | -1.11 | 0.004473 | 0.305 |

[1] Determined by paired t-test at $P < 0.005$ and a permutation of 10,000 (n = 9). FDR, false discovery rate.

APPENDIX D
EFFECTS OF DIETARY ZINC RESTRICTION ON MT AND ZINC TRANSPORTER TRANSCRIPTS IN TONGUE EPITHELIAL CELLS OF MOUSE

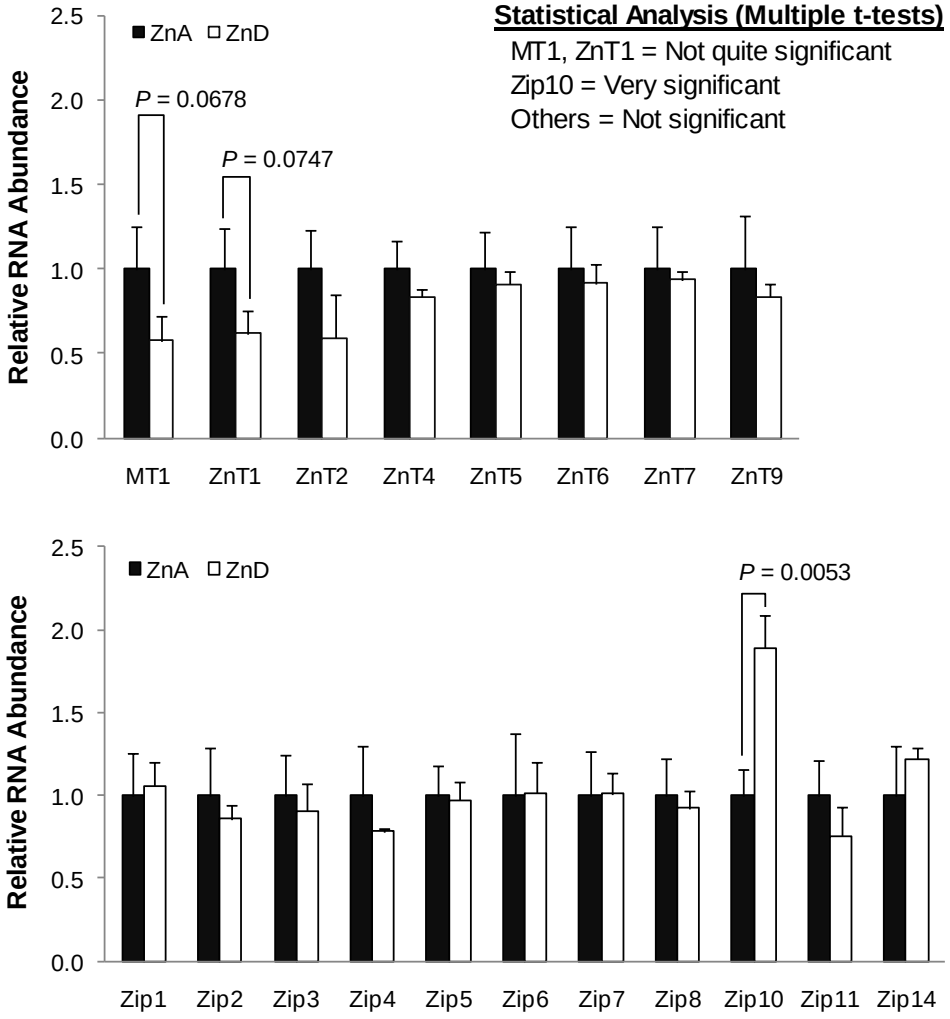


Figure D-1. Effects of dietary zinc deprivation on zinc transporter mRNA levels in the tongue epithelium of mouse. Mice were fed a zinc-adequate or low zinc diet for 21 d. The whole tongue was collected and washed with calcium-free medium. Mixture of collagenase (2 mg/mL), dispase (1.5 units/mL) and trypsin inhibitor (0.5 mg/mL) was injected between the epithelium and muscle layers with a 27G needle. After incubation for 15 min, the epithelium was peeled off from the cut end of the tongue with a fine forceps. The epithelial sheet was stored in RNAlater, 4°C before treated with TRI reagent for total RNA isolation. Relative mRNA abundance was quantified by qPCR and normalized to 18S rRNA levels. Data are expressed as mean ± SD (n=3 animals).

LIST OF REFERENCES


1. Cousins RJ (2006) Zinc. *Present Knowledge in Nutrition*, eds Bowman BA, Russel RM (Int. Life Sci. Inst.-Nutr. Foundation, Washington, DC), 9th Ed, pp 445–457.

2. King J, Cousins RJ (2005) Zinc. *Modern Nutrition in Health and Disease*, eds Shils ME, Shike M, Ross AC, Caballero B, Cousins RJ (Lippincott Williams and Wilkins, Baltimore), 10th Ed, pp 271-285.

3. Radtke F*, et al.* (1993) Cloned transcription factor MTF-1 activates the mouse metallothionein I promoter. *Embo J* 12(4):1355-1362.

4. Langmade SJ, Ravindra R, Daniels PJ, Andrews GK (2000) The transcription factor MTF-1 mediates metal regulation of the mouse ZnT1 gene. *J Biol Chem* 275(44):34803-34809.

5. Zheng D, Feeney GP, Kille P, Hogstrand C (2008) Regulation of ZIP and ZnT zinc transporters in zebrafish gill: zinc repression of ZIP10 transcription by an intronic MRE cluster. *Physiol Genomics* 34(2):205-214.

6. Lichten LA, Ryu MS, Guo L, Embury JE, Cousins RJ (2011) MTF-1-mediated repression of the zinc transporter Zip10 is alleviated by zinc restriction. *PLoS One* (in press).

7. Guo L*, et al.* (2010) STAT5-glucocorticoid receptor interaction and MTF-1 regulate the expression of ZnT2 (Slc30a2) in pancreatic acinar cells. *Proc Natl Acad Sci U S A* 107(7):2818-2823.

8. Lichten LA, Cousins RJ (2009) Mammalian zinc transporters: nutritional and physiologic regulation. *Annu Rev Nutr* 29:153-176.

9. Cousins RJ, Liuzzi JP, Lichten LA (2006) Mammalian zinc transport, trafficking, and signals. *J Biol Chem* 281(34):24085-24089.

10. Liuzzi JP, Guo L, Chang SM, Cousins RJ (2009) Kruppel-like factor 4 regulates adaptive expression of the zinc transporter Zip4 in mouse small intestine. *Am J Physiol Gastrointest Liver Physiol* 296(3):G517-523.

11. Dufner-Beattie J, Kuo YM, Gitschier J, Andrews GK (2004) The adaptive response to dietary zinc in mice involves the differential cellular localization and zinc regulation of the zinc transporters ZIP4 and ZIP5. *J Biol Chem* 279(47):49082-49090.

12. Liuzzi JP, Bobo JA, Lichten LA, Samuelson DA, Cousins RJ (2004) Responsive transporter genes within the murine intestinal-pancreatic axis form a basis of zinc homeostasis. *Proc Natl Acad Sci U S A* 101(40):14355-14360.

13. Wang F, Kim BE, Petris MJ, Eide DJ (2004) The mammalian Zip5 protein is a zinc transporter that localizes to the basolateral surface of polarized cells. *J Biol Chem* 279(49):51433-51441.

14. Ryu MS, Lichten LA, Liuzzi JP, Cousins RJ (2008) Zinc transporters ZnT1 (Slc30a1), Zip8 (Slc39a8), and Zip10 (Slc39a10) in mouse red blood cells are differentially regulated during erythroid development and by dietary zinc deficiency. *J Nutr* 138(11):2076-2083.

15. McMahon RJ, Cousins RJ (1998) Regulation of the zinc transporter ZnT-1 by dietary zinc. *Proc Natl Acad Sci U S A* 95(9):4841-4846.

16. Prasad AS (1985) Clinical manifestations of zinc deficiency. *Annu Rev Nutr* 5:341-363.

17. Hambidge M (2000) Human zinc deficiency. *J Nutr* 130(5S Suppl):1344S-1349S.

18. Prasad AS (2001) Recognition of zinc-deficiency syndrome. *Nutrition* 17(1):67-69.

19. Jansen J, Karges W, Rink L (2009) Zinc and diabetes--clinical links and molecular mechanisms. *J Nutr Biochem* 20(6):399-417.

20. Sun Q, van Dam RM, Willett WC, Hu FB (2009) Prospective study of zinc intake and risk of type 2 diabetes in women. *Diabetes Care* 32(4):629-634.

21. Haase H, Rink L (2009) Functional significance of zinc-related signaling pathways in immune cells. *Annu Rev Nutr* 29:133-152.

22. Rink L, Haase H (2007) Zinc homeostasis and immunity. *Trends Immunol* 28(1):1-4.

23. Caulfield LE, Black RE (2004) Zinc deficiency. *Comparative quantification of health risks*, eds Ezzati M, Lopez AD, Rodgers A, Murray CJ (World Health Organization, Geneva, Switzerland), Vol 1, pp 257-280.

24. Dufner-Beattie J*, et al.* (2003) The acrodermatitis enteropathica gene ZIP4 encodes a tissue-specific, zinc-regulated zinc transporter in mice. *J Biol Chem* 278(35):33474-33481.

25. Kury S*, et al.* (2002) Identification of SLC39A4, a gene involved in acrodermatitis enteropathica. *Nat Genet* 31(3):239-240.

26. Moynahan EJ (1974) Letter: Acrodermatitis enteropathica: a lethal inherited human zinc-deficiency disorder. *Lancet* 2(7877):399-400.

27. Chandra RK (1980) Acrodermatitis enteropathica: zinc levels and cell-mediated immunity. *Pediatrics* 66(5):789-791.

28. Neldner KH, Hambidge KM (1975) Zinc therapy of acrodermatitis enteropathica. *N Engl J Med* 292(17):879-882.

29. Turnlund JR, King JC, Keyes WR, Gong B, Michel MC (1984) A stable isotope study of zinc absorption in young men: effects of phytate and alpha-cellulose. *Am J Clin Nutr* 40(5):1071-1077.

30. Davies NT, Olpin SE (1979) Studies on the phytate: zinc molar contents in diets as a determinant of Zn availability to young rats. *Br J Nutr* 41(3):590-603.

31. Miller LV, Krebs NF, Hambidge KM (2007) A mathematical model of zinc absorption in humans as a function of dietary zinc and phytate. *J Nutr* 137(1):135-141.

32. Hambidge KM, Miller LV, Westcott JE, Krebs NF (2008) Dietary reference intakes for zinc may require adjustment for phytate intake based upon model predictions. *J Nutr* 138(12):2363-2366.

33. Gibson RS, Hess SY, Hotz C, Brown KH (2008) Indicators of zinc status at the population level: a review of the evidence. *Br J Nutr* 99 Suppl 3:S14-23.

34. Ruz M*, et al.* (1991) Development of a dietary model for the study of mild zinc deficiency in humans and evaluation of some biochemical and functional indices of zinc status. *Am J Clin Nutr* 53(5):1295-1303.

35. Wessells KR*, et al.* (2010) Plasma zinc concentration responds rapidly to the initiation and discontinuation of short-term zinc supplementation in healthy men. *J Nutr* 140(12):2128-2133.

36. Chung CS*, et al.* (2008) Current dietary zinc intake has a greater effect on fractional zinc absorption than does longer term zinc consumption in healthy adult men. *Am J Clin Nutr* 87(5):1224-1229.

37. Gordon PR, Woodruff CW, Anderson HL, O'Dell BL (1982) Effect of acute zinc deprivation on plasma zinc and platelet aggregation in adult males. *Am J Clin Nutr* 35(1):113-119.

38. Hotz C, Peerson JM, Brown KH (2003) Suggested lower cutoffs of serum zinc concentrations for assessing zinc status: reanalysis of the second National Health and Nutrition Examination Survey data (1976-1980). *Am J Clin Nutr* 78(4):756-764.

39. Allan AK*, et al.* (2000) Lymphocyte metallothionein mRNA responds to marginal zinc intake in human volunteers. *Br J Nutr* 84(5):747-756.

40. Cao J, Cousins RJ (2000) Metallothionein mRNA in monocytes and peripheral blood mononuclear cells and in cells from dried blood spots increases after zinc supplementation of men. *J Nutr* 130(9):2180-2187.

41. Aydemir TB, Blanchard RK, Cousins RJ (2006) Zinc supplementation of young men alters metallothionein, zinc transporter, and cytokine gene expression in leukocyte populations. *Proc Natl Acad Sci U S A* 103(6):1699-1704.

42. Grider A, Bailey LB, Cousins RJ (1990) Erythrocyte metallothionein as an index of zinc status in humans. *Proc Natl Acad Sci U S A* 87(4):1259-1262.

43. Thomas EA, Bailey LB, Kauwell GA, Lee DY, Cousins RJ (1992) Erythrocyte metallothionein response to dietary zinc in humans. *J Nutr* 122(12):2408-2414.

44. Andree KB*, et al.* (2004) Investigation of lymphocyte gene expression for use as biomarkers for zinc status in humans. *J Nutr* 134(7):1716-1723.

45. Ruz M, Cavan KR, Bettger WJ, Gibson RS (1992) Erythrocytes, erythrocyte membranes, neutrophils and platelets as biopsy materials for the assessment of zinc status in humans. *Br J Nutr* 68(2):515-527.

46. Smith JC, Jr., Lewis S, Holbrook J, Seidel K, Rose A (1987) Effect of heparin and citrate on measured concentrations of various analytes in plasma. *Clin Chem* 33(6):814-816.

47. Mocchegiani E*, et al.* (2008) Zinc deficiency and IL-6 -174G/C polymorphism in old people from different European countries: effect of zinc supplementation. ZINCAGE study. *Exp Gerontol* 43(5):433-444.

48. Prasad AS*, et al.* (1999) Effect of zinc supplementation on incidence of infections and hospital admissions in sickle cell disease (SCD). *Am J Hematol* 61(3):194-202.

49. Prasad AS, Mantzoros CS, Beck FW, Hess JW, Brewer GJ (1996) Zinc status and serum testosterone levels of healthy adults. *Nutrition* 12(5):344-348.

50. Milne DB, Canfield WK, Gallagher SK, Hunt JR, Klevay LM (1987) Ethanol metabolism in postmenopausal women fed a diet marginal in zinc. *Am J Clin Nutr* 46(4):688-693.

51. Aydemir TB, Liuzzi JP, McClellan S, Cousins RJ (2009) Zinc transporter ZIP8 (SLC39A8) and zinc influence IFN-gamma expression in activated human T cells. *J Leukoc Biol* 86(2):337-348.

52. Kitamura H*, et al.* (2006) Toll-like receptor-mediated regulation of zinc homeostasis influences dendritic cell function. *Nat Immunol* 7(9):971-977.

53. Adeniyi FA, Heaton FW (1980) The effect of zinc deficiency on alkaline phosphatase (EC 3.1.3.1) and its isoenzymes. *Br J Nutr* 43(3):561-569.

54. Luecke RW, Olman ME, Baltzer BV (1968) Zinc deficiency in the rat: effect on serum and intestinal alkaline phosphatase activities. *J Nutr* 94(3):344-350.

55. Kasarskis EJ, Schuna A (1980) Serum alkaline phosphatase after treatment of zinc deficiency in humans. *Am J Clin Nutr* 33(12):2609-2612.

56. Weismann K, Hoyer H (1985) Serum alkaline phosphatase and serum zinc levels in the diagnosis and exclusion of zinc deficiency in man. *Am J Clin Nutr* 41(6):1214-1219.

57. Naber TH, Baadenhuysen H, Jansen JB, van den Hamer CJ, van den Broek W (1996) Serum alkaline phosphatase activity during zinc deficiency and long-term inflammatory stress. *Clin Chim Acta* 249(1-2):109-127.

58. Blostein-Fujii A, DiSilvestro RA, Frid D, Katz C, Malarkey W (1997) Short-term zinc supplementation in women with non-insulin-dependent diabetes mellitus: effects on plasma 5'-nucleotidase activities, insulin-like growth factor I concentrations, and lipoprotein oxidation rates in vitro. *Am J Clin Nutr* 66(3):639-642.

59. Davis CD, Milne DB, Nielsen FH (2000) Changes in dietary zinc and copper affect zinc-status indicators of postmenopausal women, notably, extracellular superoxide dismutase and amyloid precursor proteins. *Am J Clin Nutr* 71(3):781-788.

60. Paik HY*, et al.* (1999) Serum extracellular superoxide dismutase activity as an indicator of zinc status in humans. *Biol Trace Elem Res* 69(1):45-57.

61. Driessen C, Hirv K, Kirchner H, Rink L (1995) Zinc regulates cytokine induction by superantigens and lipopolysaccharide. *Immunology* 84(2):272-277.

62. Wellinghausen N, Driessen C, Rink L (1996) Stimulation of human peripheral blood mononuclear cells by zinc and related cations. *Cytokine* 8(10):767-771.

63. Prasad AS (2000) Effects of zinc deficiency on Th1 and Th2 cytokine shifts. *J Infect Dis* 182 Suppl 1:S62-68.

64. Prasad AS, Bao B, Beck FW, Sarkar FH (2006) Correction of interleukin-2 gene expression by in vitro zinc addition to mononuclear cells from zinc-deficient human subjects: a specific test for zinc deficiency in humans. *Transl Res* 148(6):325-333.

65. Prasad AS*, et al.* (2007) Zinc supplementation decreases incidence of infections in the elderly: effect of zinc on generation of cytokines and oxidative stress. *Am J Clin Nutr* 85(3):837-844.

66. Song Y, Leonard SW, Traber MG, Ho E (2009) Zinc deficiency affects DNA damage, oxidative stress, antioxidant defenses, and DNA repair in rats. *J Nutr* 139(9):1626-1631.

67. Yan M, Song Y, Wong CP, Hardin K, Ho E (2008) Zinc deficiency alters DNA damage response genes in normal human prostate epithelial cells. *J Nutr* 138(4):667-673.

68. Song Y*, et al.* (2009) Dietary zinc restriction and repletion affects DNA integrity in healthy men. *Am J Clin Nutr* 90(2):321-328.

69. Sunde RA (2010) mRNA transcripts as molecular biomarkers in medicine and nutrition. *J Nutr Biochem* 21(8):665-670.

70. Shi L*, et al.* (2006) The MicroArray Quality Control (MAQC) project shows inter- and intraplatform reproducibility of gene expression measurements. *Nat Biotechnol* 24(9):1151-1161.

71. Tian Z*, et al.* (2009) A practical platform for blood biomarker study by using global gene expression profiling of peripheral whole blood. *PLoS One* 4(4):e5157.

72. Debey S*, et al.* (2006) A highly standardized, robust, and cost-effective method for genome-wide transcriptome analysis of peripheral blood applicable to large-scale clinical trials. *Genomics* 87(5):653-664.

73. Debey-Pascher S, Eggle D, Schultze JL (2009) RNA stabilization of peripheral blood and profiling by bead chip analysis. *Methods Mol Biol* 496:175-210.

74. Wang Z, Gerstein M, Snyder M (2009) RNA-Seq: a revolutionary tool for transcriptomics. *Nat Rev Genet* 10(1):57-63.

75. Holland NT, Smith MT, Eskenazi B, Bastaki M (2003) Biological sample collection and processing for molecular epidemiological studies. *Mutat Res* 543(3):217-234.

76. Rainen L*, et al.* (2002) Stabilization of mRNA expression in whole blood samples. *Clin Chem* 48(11):1883-1890.

77. Debey S*, et al.* (2004) Comparison of different isolation techniques prior gene expression profiling of blood derived cells: impact on physiological responses, on overall expression and the role of different cell types. *Pharmacogenomics J* 4(3):193-207.

78. Spira A*, et al.* (2004) Noninvasive method for obtaining RNA from buccal mucosa epithelial cells for gene expression profiling. *Biotechniques* 36(3):484-487.

79. Sridhar S*, et al.* (2008) Smoking-induced gene expression changes in the bronchial airway are reflected in nasal and buccal epithelium. *BMC Genomics* 9:259.

80. Natarajan P, Trinh T, Mertz L, Goldsborough M, Fox DK (2000) Paper-based archiving of mammalian and plant samples for RNA analysis. *Biotechniques* 29(6):1328-1333.

81. Field LA*, et al.* (2007) Functional identity of genes detectable in expression profiling assays following globin mRNA reduction of peripheral blood samples. *Clin Biochem* 40(7):499-502.

82. Liu J, Walter E, Stenger D, Thach D (2006) Effects of globin mRNA reduction methods on gene expression profiles from whole blood. *J Mol Diagn* 8(5):551-558.

83. King JC*, et al.* (2001) Effect of acute zinc depletion on zinc homeostasis and plasma zinc kinetics in men. *Am J Clin Nutr* 74(1):116-124.

84. Bonafoux B, Commes T (2009) Serial analysis of gene expression adapted for downsized extracts (SAGE/SADE) analysis in reticulocytes. *Methods Mol Biol* 496:299-311.

85. Jung R, Lubcke C, Wagener C, Neumaier M (1997) Reversal of RT-PCR inhibition observed in heparinized clinical specimens. *Biotechniques* 23(1):24, 26, 28.

86. Ulitsky I*, et al.* (2010) Expander: from expression microarrays to networks and functions. *Nat Protoc* 5(2):303-322.

87. Kroh EM, Parkin RK, Mitchell PS, Tewari M (2010) Analysis of circulating microRNA biomarkers in plasma and serum using quantitative reverse transcription-PCR (qRT-PCR). *Methods* 50(4):298-301.

88. Black RE*, et al.* (2008) Maternal and child undernutrition: global and regional exposures and health consequences. *Lancet* 371(9608):243-260.

89. Cousins RJ*, et al.* (2003) A global view of the selectivity of zinc deprivation and excess on genes expressed in human THP-1 mononuclear cells. *Proc Natl Acad Sci U S A* 100(12):6952-6957.

90. Haase H*, et al.* (2007) Differential gene expression after zinc supplementation and deprivation in human leukocyte subsets. *Mol Med* 13(7-8):362-370.

91. Foster M, Hancock D, Petocz P, Samman S (2011) Zinc transporter genes are coordinately expressed in men and women independently of dietary or plasma zinc. *J Nutr* 141(6):1195-1201.

92. Seo YA, Lopez V, Kelleher SL (2011) A histidine-rich motif mediates mitochondrial localization of ZnT2 to modulate mitochondrial function. *Am J Physiol Cell Physiol* 300(6):C1479-1489.

93. Bloomer JR, Reuter RJ, Morton KO, Wehner JM (1983) Enzymatic formation of zinc-protoporphyrin by rat liver and its potential effect on hepatic heme metabolism. *Gastroenterology* 85(3):663-668.

94. Fiske DN, McCoy HE, 3rd, Kitchens CS (1994) Zinc-induced sideroblastic anemia: report of a case, review of the literature, and description of the hematologic syndrome. *Am J Hematol* 46(2):147-150.

95. Keen CL, Gershwin ME (1990) Zinc deficiency and immune function. *Annu Rev Nutr* 10:415-431.

96. Rink L, Kirchner H (2000) Zinc-altered immune function and cytokine production. *J Nutr* 130(5S Suppl):1407S-1411S.

97. Fraker PJ, King LE (2004) Reprogramming of the immune system during zinc deficiency. *Annu Rev Nutr* 24:277-298.

98. Ho E (2004) Zinc deficiency, DNA damage and cancer risk. *J Nutr Biochem* 15(10):572-578.

99. Fong LY (2010) Zinc in Cancer Development and Prevention. *Bioactive Compounds and Cancer,* Nutrition and Health, eds Milner JA, Romagnolo DF (Humana Press, New York), 1st Ed, pp 497-531.

100. Hasan MR, Ho SH, Owen D, Tai IT (2011) VEGF inhibitors induce cellular senescence in colorectal cancer cells. *Int J Cancer* .

101. Wu W, Shu X, Hovsepyan H, Mosteller RD, Broek D (2003) VEGF receptor expression and signaling in human bladder tumors. *Oncogene* 22(22):3361-3370.

102. Golovine K*, et al.* (2008) Depletion of intracellular zinc increases expression of tumorigenic cytokines VEGF, IL-6 and IL-8 in prostate cancer cells via NF-kappaB-dependent pathway. *Prostate* 68(13):1443-1449.

103. Issell BF*, et al.* (1981) Serum zinc levels in lung cancer patients. *Cancer* 47(7):1845-1848.

104. Buntzel J*, et al.* (2007) Zinc concentrations in serum during head and neck cancer progression. *Anticancer Res* 27(4A):1941-1943.

105. Martin-Lagos F, Navarro-Alarcon M, Terres-Martos C, Lopez GdlSH, Lopez-Martinez MC (1997) Serum copper and zinc concentrations in serum from patients with cancer and cardiovascular disease. *Sci Total Environ* 204(1):27-35.

106. Prasad AS, Bao B, Beck FW, Sarkar FH (2001) Zinc activates NF-kappaB in HUT-78 cells. *J Lab Clin Med* 138(4):250-256.

107. Mackenzie GG, Zago MP, Keen CL, Oteiza PI (2002) Low intracellular zinc impairs the translocation of activated NF-kappa B to the nuclei in human neuroblastoma IMR-32 cells. *J Biol Chem* 277(37):34610-34617.

108. Oteiza PI, Clegg MS, Keen CL (2001) Short-term zinc deficiency affects nuclear factor-kappab nuclear binding activity in rat testes. *J Nutr* 131(1):21-26.

109. Yamamoto Y, Gaynor RB (2001) Therapeutic potential of inhibition of the NF-kappaB pathway in the treatment of inflammation and cancer. *J Clin Invest* 107(2):135-142.

110. DePasquale-Jardieu P, Fraker PJ (1979) The role of corticosterone in the loss in immune function in the zinc-deficient A/J mouse. *J Nutr* 109(11):1847-1855.

111. DePasquale-Jardieu P, Fraker PJ (1980) Further characterization of the role of corticosterone in the loss of humoral immunity in zinc-deficient A/J mice as determined by adrenalectomy. *J Immunol* 124(6):2650-2655.

112. Lee J, Li Z, Brower-Sinning R, John B (2007) Regulatory circuit of human microRNA biogenesis. *PLoS Comput Biol* 3(4):e67.

113. Remick DG, Newcomb DE, Friedland JS (2000) Whole-blood assays for cytokine production. *Methods Mol Med* 36:101-112.

114. Hussain R*, et al.* (2002) Cytokine profiles using whole-blood assays can discriminate between tuberculosis patients and healthy endemic controls in a BCG-vaccinated population. *J Immunol Methods* 264(1-2):95-108.

115. Giamarellos-Bourboulis EJ*, et al.* (2010) Ex-vivo effect of dexamethasone on cytokine production from whole blood of septic patients: correlation with disease severity. *Cytokine* 49(1):89-94.

116. Schluep M*, et al.* (1998) In vitro cytokine profiles as indicators of relapse activity and clinical course in multiple sclerosis. *Mult Scler* 4(3):198-202.

117. Wallis RS*, et al.* (1998) Measurement of induced cytokines in AIDS clinical trials using whole blood: a preliminary report. ACTG Inducible Cytokines Focus Group. AIDS Clinical Trials Group. *Clin Diagn Lab Immunol* 5(4):556-560.

118. Ahmad SM, Haskell MJ, Raqib R, Stephensen CB (2009) Markers of innate immune function are associated with vitamin a stores in men. *J Nutr* 139(2):377-385.

119. Eggesbo JB, Hjermann I, Hostmark AT, Kierulf P (1996) LPS induced release of IL-1 beta, IL-6, IL-8 and TNF-alpha in EDTA or heparin anticoagulated whole blood from persons with high or low levels of serum HDL. *Cytokine* 8(2):152-160.

120. Bai X, Fischer S, Keshavjee S, Liu M (2000) Heparin interference with reverse transcriptase polymerase chain reaction of RNA extracted from lungs after ischemia-reperfusion. *Transpl Int* 13(2):146-150.

121. Beutler E, Gelbart T, Kuhl W (1990) Interference of heparin with the polymerase chain reaction. *Biotechniques* 9(2):166.

122. Wellinghausen N, Kirchner H, Rink L (1997) The immunobiology of zinc. *Immunol Today* 18(11):519-521.

123. Gilmore TD (2006) Introduction to NF-kappaB: players, pathways, perspectives. *Oncogene* 25(51):6680-6684.

124. Frederickson CJ*, et al.* (2002) Depletion of intracellular zinc from neurons by use of an extracellular chelator in vivo and in vitro. *J Histochem Cytochem* 50(12):1659-1662.

125. Brautigan DL, Bornstein P, Gallis B (1981) Phosphotyrosyl-protein phosphatase. Specific inhibition by Zn. *J Biol Chem* 256(13):6519-6522.

126. Ho Y*, et al.* (2008) Selective inhibition of mitogen-activated protein kinase phosphatases by zinc accounts for extracellular signal-regulated kinase 1/2-dependent oxidative neuronal cell death. *Mol Pharmacol* 74(4):1141-1151.

127. Yamasaki S*, et al.* (2007) Zinc is a novel intracellular second messenger. *J Cell Biol* 177(4):637-645.

128. Csermely P, Szamel M, Resch K, Somogyi J (1988) Zinc can increase the activity of protein kinase C and contributes to its binding to plasma membranes in T lymphocytes. *J Biol Chem* 263(14):6487-6490.

129. von Bulow V*, et al.* (2007) Zinc-dependent suppression of TNF-alpha production is mediated by protein kinase A-induced inhibition of Raf-1, I kappa B kinase beta, and NF-kappa B. *J Immunol* 179(6):4180-4186.

130. Besecker B*, et al.* (2008) The human zinc transporter SLC39A8 (Zip8) is critical in zinc-mediated cytoprotection in lung epithelia. *Am J Physiol Lung Cell Mol Physiol* 294(6):L1127-1136.

131. Bartel DP (2009) MicroRNAs: target recognition and regulatory functions. *Cell* 136(2):215-233.

132. Bartel DP (2004) MicroRNAs: genomics, biogenesis, mechanism, and function. *Cell* 116(2):281-297.

133. Siomi H, Siomi MC (2010) Posttranscriptional regulation of microRNA biogenesis in animals. *Mol Cell* 38(3):323-332.

134. Wittmann J, Jack HM (2010) Serum microRNAs as powerful cancer biomarkers. *Biochim Biophys Acta* 1806(2):200-207.

135. Chen X*, et al.* (2008) Characterization of microRNAs in serum: a novel class of biomarkers for diagnosis of cancer and other diseases. *Cell Res* 18(10):997-1006.

136. Mitchell PS*, et al.* (2008) Circulating microRNAs as stable blood-based markers for cancer detection. *Proc Natl Acad Sci U S A* 105(30):10513-10518.

137. Gilad S*, et al.* (2008) Serum microRNAs are promising novel biomarkers. *PLoS One* 3(9):e3148.

138. Hunter MP*, et al.* (2008) Detection of microRNA expression in human peripheral blood microvesicles. *PLoS One* 3(11):e3694.

139. Valadi H*, et al.* (2007) Exosome-mediated transfer of mRNAs and microRNAs is a novel mechanism of genetic exchange between cells. *Nat Cell Biol* 9(6):654-659.

140. Wang K, Zhang S, Weber J, Baxter D, Galas DJ (2010) Export of microRNAs and microRNA-protective protein by mammalian cells. *Nucleic Acids Res* 38(20):7248-7259.

141. Bentwich I*, et al.* (2005) Identification of hundreds of conserved and nonconserved human microRNAs. *Nat Genet* 37(7):766-770.

142. Kozomara A, Griffiths-Jones S (2011) miRBase: integrating microRNA annotation and deep-sequencing data. *Nucleic Acids Res* 39(Database issue):D152-157.

143. Friedman RC, Farh KK, Burge CB, Bartel DP (2009) Most mammalian mRNAs are conserved targets of microRNAs. *Genome Res* 19(1):92-105.

144. Najafi-Shoushtari SH*, et al.* (2010) MicroRNA-33 and the SREBP host genes cooperate to control cholesterol homeostasis. *Science* 328(5985):1566-1569.

145. Rayner KJ*, et al.* (2010) MiR-33 contributes to the regulation of cholesterol homeostasis. *Science* 328(5985):1570-1573.

146. Castoldi M*, et al.* (2011) The liver-specific microRNA miR-122 controls systemic iron homeostasis in mice. *J Clin Invest* 121(4):1386-1396.

147. Liuzzi JP, Valencia K, Cao J, Gonzalez A (2011) Zinc deficiency increases miR-34a expression in mice. *Faseb J* 25:977.971.

148. Hershfinkel M, Aizenman E, Andrews G, Sekler I (2010) Zinc bells rang in Jerusalem! *Sci Signal* 3(129):mr2.

149. Esquela-Kerscher A, Slack FJ (2006) Oncomirs - microRNAs with a role in cancer. *Nat Rev Cancer* 6(4):259-269.

150. Chin LJ, Slack FJ (2008) A truth serum for cancer--microRNAs have major potential as cancer biomarkers. *Cell Res* 18(10):983-984.

151. Lee Y*, et al.* (2010) Network modeling identifies molecular functions targeted by miR-204 to suppress head and neck tumor metastasis. *PLoS Comput Biol* 6(4):e1000730.

152. Wei JJ*, et al.* (2011) Regulation of HMGA1 expression by microRNA-296 affects prostate cancer growth and invasion. *Clin Cancer Res* 17(6):1297-1305.

153. Ohno H*, et al.* (1985) A study of zinc distribution in erythrocytes of normal humans. *Blut* 50(2):113-116.

154. Hodge D*, et al.* (2006) A global role for EKLF in definitive and primitive erythropoiesis. *Blood* 107(8):3359-3370.

155. Ferreira R, Ohneda K, Yamamoto M, Philipsen S (2005) GATA1 function, a paradigm for transcription factors in hematopoiesis. *Mol Cell Biol* 25(4):1215-1227.

156. O'Dell BL, Browning JD, Reeves PG (1987) Zinc deficiency increases the osmotic fragility of rat erythrocytes. *J Nutr* 117(11):1883-1889.

157. Naber TH, van den Hamer CJ, van den Broek WJ, van Tongeren JH (1992) Zinc uptake by blood cells of rats in zinc deficiency and inflammation. *Biol Trace Elem Res* 35(2):137-152.

158. Van Wouwe JP, Veldhuizen M, De Goeij JJ, Van den Hamer CJ (1991) Laboratory assessment of early dietary, subclinical zinc deficiency: a model study on weaning rats. *Pediatr Res* 29(4 Pt 1):391-395.

159. Chesters JK, Will M (1978) The assessment of zinc status of an animal from the uptake of 65Zn by the cells of whole blood in vitro. *Br J Nutr* 39(2):297-306.

160. Glader B (2008) Destruction of Erythrocyte. *Wintrobe's Clinical Hematology*, eds Greer JP, Foerster J, Rodgers GM, Paraskevas F, Glader B (Lippincott Williams and Wilkins, Philadelphia), 12th Ed, pp 156-169.

161. Siegel DL, Branton D (1985) Partial purification and characterization of an actin-bundling protein, band 4.9, from human erythrocytes. *J Cell Biol* 100(3):775-785.

162. Rana AP, Ruff P, Maalouf GJ, Speicher DW, Chishti AH (1993) Cloning of human erythroid dematin reveals another member of the villin family. *Proc Natl Acad Sci U S A* 90(14):6651-6655.

163. Salomao M*, et al.* (2008) Protein 4.1R-dependent multiprotein complex: new insights into the structural organization of the red blood cell membrane. *Proc Natl Acad Sci U S A* 105(23):8026-8031.

164. Anong WA*, et al.* (2009) Adducin forms a bridge between the erythrocyte membrane and its cytoskeleton and regulates membrane cohesion. *Blood* 114(9):1904-1912.

165. Khanna R*, et al.* (2002) Headpiece domain of dematin is required for the stability of the erythrocyte membrane. *Proc Natl Acad Sci U S A* 99(10):6637-6642.

166. Chen H*, et al.* (2007) Combined deletion of mouse dematin-headpiece and beta-adducin exerts a novel effect on the spectrin-actin junctions leading to erythrocyte fragility and hemolytic anemia. *J Biol Chem* 282(6):4124-4135.

167. Husain-Chishti A, Levin A, Branton D (1988) Abolition of actin-bundling by phosphorylation of human erythrocyte protein 4.9. *Nature* 334(6184):718-721.

168. Tsukamoto T, Suyama K, Germann P, Sonenberg M (1980) Adenosine cyclic 3',5'-monophosphate uptake and regulation of membrane protein kinase in intact human erythrocytes. *Biochemistry* 19(5):918-924.

169. Husain-Chishti A, Faquin W, Wu CC, Branton D (1989) Purification of erythrocyte dematin (protein 4.9) reveals an endogenous protein kinase that modulates actin-bundling activity. *J Biol Chem* 264(15):8985-8991.

170. Frank BS, Vardar D, Chishti AH, McKnight CJ (2004) The NMR structure of dematin headpiece reveals a dynamic loop that is conformationally altered upon phosphorylation at a distal site. *J Biol Chem* 279(9):7909-7916.

171. Vugmeyster L, McKnight CJ (2009) Phosphorylation-induced changes in backbone dynamics of the dematin headpiece C-terminal domain. *J Biomol NMR* 43(1):39-50.

172. Donnelly TE, Jr. (1978) Effects of zinc chloride on the hydrolysis of cyclic GMP and cyclic AMP by the activator-dependent cyclic nucleotide phosphodiesterase from bovine heart. *Biochim Biophys Acta* 522(1):151-160.

173. Larsson C (2006) Protein kinase C and the regulation of the actin cytoskeleton. *Cell Signal* 18(3):276-284.

174. Matsuoka Y, Li X, Bennett V (1998) Adducin is an in vivo substrate for protein kinase C: phosphorylation in the MARCKS-related domain inhibits activity in promoting spectrin-actin complexes and occurs in many cells, including dendritic spines of neurons. *J Cell Biol* 142(2):485-497.

175. Lutchman M*, et al.* (1999) Loss of heterozygosity on 8p in prostate cancer implicates a role for dematin in tumor progression. *Cancer Genet Cytogenet* 115(1):65-69.

# BIOGRAPHICAL SKETCH

Moon-Suhn Ryu was born in Seoul, South Korea. He received his Bachelor of Science degree in biotechnology from Yonsei University in 2001. Moon-Suhn joined the Republic of Korea Air Force for his military service from 2001 to 2003. In 2004, Moon-Suhn started his career as an assistant manager of the overseas business unit of Lotte Chilsung Beverage Company Limited, in South Korea. He came to the United States in the fall of 2005 to start his master's studies with Dr. Cousins at the University of Florida. After receiving his Master of Science degree in 2005, Moon-Suhn continued his graduate studies by entering the doctorate program for nutritional sciences at the University of Florida.